GRADUATE SCHOOL OF NATURAL AND APPLIED SCIENCES

MASTER'S THESIS

MAY, 2015

REPUBLIC OF TURKEY
YILDIZ TECHNICAL UNIVERSITY
GRADUATE SCHOOL OF NATURAL AND APPLIED SCIENCES

CLIMATE AND LAND USE CHANGE IMPACT ON URBAN FLOODING

EMMANUEL RUKUNDO

MASTER'STHESIS
DEPARTMENT OF CIVIL ENGINEERING
PROGRAM OF HYDRAULICS ENGINEERING

ADVISER
ASSOC. PROF. DR. AHMETDOĞAN

İSTANBUL, 2015

REPUBLIC OF TURKEY
YILDIZ TECHNICAL UNIVERSITY
GRADUATE SCHOOL OF NATURAL AND APPLIED SCIENCES

CLIMATE AND LAND USE CHANGE IMPACT ON URBAN FLOODING

A thesis submitted byEmmanuel RUKUNDOin partial fulfillment of the requirements for the degree of **MASTER OF SCIENCE** is approved by the committee on 12.06.2015 in Department of Civil Engineering, Hydraulics Engineering Program.

Thesis Adviser

Assoc. Prof. Dr. AhmetDOĞAN

Yıldız Technical University

Approved By the Examining Committee

Assoc. Prof. Dr. AhmetDOĞAN

Yıldız Technical University ______________________

Prof.Dr.Hayrullah AĞAÇCIOĞLU

Yıldız Technical University ______________________

Assoc. Prof. Dr. Mehmet ÖZGER

Istanbul Technical University ______________________

ACKNOWLEDGEMENTS

First of all I thank the Almighty God for His endless Grace and Blessing on me during all these months here at Yildiz Technical University and in all my life.

I would like to express my thanks and gratitude to the YTB (Yurtdışı Türkler ve Akraba Topluluklar Başkanlığı) for granting me this opportunity to study for a Master of Science degree in Turkey and for all their financial support.

I express my sincere gratitude to Associate Professor Dr.AHMET DOGAN for having given me an opportunity to work under his guidance and provided the necessary resources for the achievement of the objective of this research. The meteorological Center of Rwanda, METEO-Rwanda and other stakeholders in the field of water and environment in Rwanda are acknowledged as providers of data used in this work.
My thanks are also addressed to all Lecturers of the Hydraulic department in Yildiz technical University for their intellectual training.
I'm grateful to my classmates for their help and encouragement during the research.
I would like to thank MohsenMahmoody Vanolya for his support during the research.
I would like to thank also Miss BAGWANEZA Rosette for her valuable moral and love she showed me during this academic Journey.
I wish to express special thanks to the family of NGIRUMPATSE Straton, to the family of KARANGWA Vedaste and to the family of KAYIRANGA Vivens for their moral and financial support during my studies. It is here to express my thanks for theirs special understanding.
We say thanks, although neither the words nor the pages are enough to express our gratitude to everyone who, near or far, participated in our building and contributed to the achievement of this work.

May, 2015

Emmanuel RUKUNDO

TABLE OF CONTENT

Page

LIST OF SYMBOLS

Q_o	Initial discharge
r_i	A stochastic output from a linear random-number generator
α_j	The estimated regression coefficient
β_j	The estimated regression coefficients
ω_i	The candidate in random process generator
g	The apparent gravitational acceleration
$I_{t,\ t-1}$	Inflow discharge at times t and t-1
k	recession constant
L	longest flow path
$Q_{t,t-1}$	Outflow discharge at times t and t-1
S	Maximum possible retention
$S_{t,\ t-1}$	Storage at time t and t-1
t	time
u_i	The normalized predictor on day i
V	The velocity relative to the rotating earth
Y	T Basin slope (%)
Δt	simulation time step
ρ	The atmosphere density
Ω	The angular velocity vector of the earth
ε	The distributed stochastic error term
ϕ	The normal cumulative distribution function

LIST OF ABBREVIATIONS

CN	Curve Number
DEM	Digital Elevation Model
FAO	Food and Agriculture Organisation
GCM	Global Climate Model
GHG	Green House Gases
HadCM3	Hadley Center Coupled Model version3
HEC-GeoHMS	Hydrologic Engineering Center – Geospatial Hydrologic Modeling System
HEC-HMS	Hydrologic Engineering Center – the Hydrologic Modeling System
IPCC	Intergovernmental Panel on Climate Change
IS92	The 1992 IPCC Scenarios
LAMS	Limited-Area Models
MININFRA	Ministry of Infrastructures
MININENA	Ministry of Natural Resources
NCEP	National Centers for Environmental Prediction
RCMs	Regional Climate Models
RCP	Representative Concentration Pathways
REMA	Rwanda Environmental Management Authority
SA90	The 1990 IPCC Scenario A
SDSM	Statistical Downscaling Model
SRES	Special Report on Emissions Scenarios
WMO	World Meteorological Organisation

LIST OF FIGURES

Page

LIST OF TABLES

Page

ABSTRACT

CLIMATE AND LAND USE CHANGE IMPACT ON URBAN FLOODING

Emmanuel RUKUNDO

Department of Civil Engineering

Msc.Thesis

Adviser: Assoc.Prof.Ahmet DOĞAN

Urban floods can cause damage to properties, disruption to business and traffic, discomfort to community and in some worse cases human loss. Floods occur due to meteorological, hydrological and human factors, which can be categorized as climate change, the most significant challenges facing human beings in 21st century, and land use change (urbanization). The specific objectives of this study were to develop future climate scenarios on extremes temperature and rainfall based on downscaling the output of Global Climate Models (GCMs) and to estimate flood volumes from climate and land use change scenarios at Nyabugogo catchment in Rwanda. GCMs have been used to project climate change in next 100 years based on different development trends and global greenhouse gas emission scenarios. As the outputs of GCMs are at low resolutions and cannot be used for any local area directly, in this study, we have adpted Statistical Downscaling Model (SDSM), a hybrid of stochastic weather generator and regression based methods to generate climate variable at high resolution. The meteorological variables downscaled from SDSM and land use projection data were used as input to the hydrological model (HEC-HMS) to estimate the flood discharge peak and volume in order to analyze the impact of climate and land use change in Nyabugogo watershed.

The results of SDSM predict an increase trend in extreme temperature for the future periods for both A2 and B2 SRES emissions which are respectively comparable to high emissions RCP 8.5, and intermediate emission RCP 6 used in 5th Assessment report of IPCC. The average annual minimum temperature will be increased by 1.4 °C and 1.2 °C under A2, B2 scenario respectively and the average maximum temperature will be increased by 2.84 °C under A2 and 2.4 °C under B2 towards the end of century. The results of downscaled rainfall do not manifest a systematic increase or decrease in all future time horizons for both A2 and B2 scenarios. However the total annual rainfall decrease of 0.2% and 5.9 % are expectable for 2020s under A2 and B2 respectively. A decrease of 4.4% and increase of 1.08% are likely to happen for 2050s under A2 and B2 respectively. In 2080s the Annual rainfall will be increased by 4.51% and 7% underA2 and B2. The hydrological modeling(HEC-HMS) results show that the climate change has a considerable impact in decreasing the expected peak discharge whereas the land use change pronounce an increasing of discharge volume for different return periods of storm.

Key words: Climate Change, Land Use Change, GCM, SDSM, HEC-HMS.

ÖZET

İKLİM VE ARAZİ DEĞİŞİKLİĞİNİN KENTSEL SELDEKİ ETKİSİ

Emmanuel RUKUNDO

İnşaat Mühendisliği Anabilim Dalı
Yüksek Lisans Tezi

Tez Danışmanı: Doç. Dr. Ahmet DOĞAN

Şehirlerde meydana gelen seller çok yüksek oranda can ve mal kaybına yol açmakta , sosyal hayatı , çevreyi ve ülkenin ekonomi durumunu felç etmektedir. Bu sellerin neden olduğu taşkınlar ise meteorolojik, hidrolojik ve insan faktörlerine bağlı olarak iklim ve arazı kullanım değişikliği (Kentleşme) olarak adlandırılabilir.Bu çalışmada farklı gelişim eğilimleri ve küresel sera gaz emisyonu senaryolarına dayanarak gelecek yılların küresel iklim değişikliğini yansıtabilmek için genel sirkülasyon modelleri (GCMs) metodu kullanılmıştır.Bu metoda göre elde edilen sonuçların yüksek çözünürlükte olmamasıyla birlikte herhangi bir yerel alan için doğrudan kullanılamaz.Bu çalışma kapsamında verilerin yüksek çözünürlükte elde edilmesi için Stokastik hava tahmin üreteci ve regresyonunun bir birleşimiolan istatistiksel ölçek küçültme metodolojisi (SDSM) kullanılmıştır. Ruanda'nın Nyabugogo havzası için iklim ve arazi kullanım değişikliği etkilerini analiz sonucu taşkın deşarj pik noktası ve hacmini daha yakın ve doğru tahmin edebilmek için meteorolojik değişkenler olarak SDSM ve arazi kullanım değişiklik değerleri hidrolojik modelde (HEC-HMS) veri olarak kullanılmıştır.

SDSM'inin sonuçlarına göre A2 ve B2 SRES emisyon değerleri açısından gelecekteki süre zarfında aşırı sıcaklık dolayısıyla bir artış eğilimi göstermiştir. Bu sonuçlar IPCC'inin 5. Değerlendirme raporunda kullanılan değerlerle sırasıyla yüksek emisyon RCP 8.5 ve orta emisyon RCP 6 ile karşılaştırılabilir.A2 ve B2 senaryosu için minimum yıllık ortalama sıcaklık sırasıyla 1.4°C ve 1.2°C artırılacaktır. Maksimum ortalama sıcaklık için A2'yi 2.84°C ve B2'yi ise 2.4°C yüzyılın sonunda artışı olacaktır.Küçültme metodolojisiyle elde edilen yağış sonuçları A2 ve B2 için gelecekteki tüm zaman ufuklarında herhangi bir artış veya azalma tezahür etmediğini ortaya koymaktadır.Ancak toplam yıllık yağışın 2020 yılında A2 ve B2 değerleri için sırasıyla 0.2% ve 5.9% bir azalma beklenebilir. Ayrıca 2050 yılı için A2 ve B2 değerleri sırasıyla 4.4% oranda azalma ve 1.08% oranda ise bir artış gerçekleşme ihtimalı olabilir. Hem de 2080'li yılları için de yıllık yağışta A2 ve B2'ler için sırasıyla 4.51% ve 7%'lik bir artışı olabilir.Hidrolojik modelleme sonuçlarına göre iklim değişikliği pik debilerin azalmasın nedene olurken, arazi kullanım değişikliğinden dolayı oluşacak pik debilerdeki artış Nyabugogo havzasının farklı dönüş aralıklarına sahip olan fırtınalarında fark edilir şekilde fazla olmaktadır.

Anahtar Kelimeler: İklim Değişikliği, Arazi Kullanımı Değişikliği, GCM, SDSM, HEC-HMS.

CHAPTER 1

INTRODUCTION

1.1 Literature Review

1.1.1 Background

Climate change refers to long-term changes in temperature, precipitation, discharge and other elements of the earth´s climate system. It may be due to some external influences, such as changes in solar radiation and volcanism, and other human related influence such as greenhouse gases emission in atmosphere. Anthropogenic greenhouse gas (GHG) emissions have increased since the pre-industrial era, driven largely byeconomic and population growth, and are now higher than ever [1]. This has led to atmosphericconcentrations of carbon dioxide (CO_2), methane (CH_4) and nitrous oxide (N_2O). Their effects, together with those of other anthropogenic drivers, have been detectedthroughout the climate system and are extremely likelyto have been the dominant cause of theobserved warming since the mid-20th century [1].

Temperature of the Earth is determined by the balance between the incoming solar radiation and outgoing terrestrial radiation energy. The energy coming from the sun can pass through atmosphere and therefore heats the surface of the earth. But the radiation emitted from the surface of the earth is partly absorbed by some gases in the atmosphere and some of it re-emitted downwards. This effects warm the surface of the earth and lower part of the atmosphere. Warming of the climate system is unequivocal, and since the 1950s, many of the observed changes areunprecedented over decades to millennia [1]. The atmosphere and ocean have warmed, the amounts ofsnow and ice have diminished, and sea level has risen [1].

Observations that delineate how global temperature has increased in the past show that the global average surface temperature has increased by 0.85 [0.65 to 1.06] °C over the period

1880 to 2012[1]. This has led to more vigorous hydrological cycle, with changes in precipitation rate regionally variable. These changes had in turn affected water availability, runoff and thus affected the discharge regime of rivers and increases the flooding especially in urban areas where the percentage of impervious surface is high. The climate variability and change have shown direct consequences on global flood hazard [2]. The increased frequency of occurrence of flood events in the world is partially attributed to climate change-driven increase of extreme precipitation[1][3][4]. Due to global warming, the global water cycle is likely to be accelerated, resulting in many regions with increased flood magnitude, as well as flood frequency. Climate change is making weather less predictable, rains more uncertain and heavy storm rainfalls more likely [3].

The Intergovernmental Panel on Climate Change (IPCC), Fifth Assessment Report, in its summary projections of climate change impacts for Africa, deemed the continent of the most vulnerable in the world due to its high exposure and low adaptive capacity[1]. Poor urban planning in Africa cities are experiencing the negative impacts of changing weather patterns associated with climate change and climate variability with future projections suggesting that these impacts will get worse.

At the other hand, since the appearance of humans on Earth, natural landscapes have routinely been converted to human dominated areas for cultivation, occupation and other economic activity that alters the land on Earth. Increasing of urbanization is enhancing the risk from river flooding in urban areas due to local changes in hydrological and hydro meteorological conditions that increase flood hazard, as well as to urban concentrations that increase the vulnerability.

The relationship between the increasing of urban runoff and flooding due to increased imperviousness is better perceived than that between the cyclic impact of urban growth and the urban rainfall via microclimatic changes [5]. Recent studies show that land use is a local phenomenon, so the impact of any disturbance is likely to strongly decrease with catchment size. The position in the landscape will modulate the scale effects. In contrast, climate impacts may occur at larger scales(Figure1.1) so one would expect them to be apparent in both small and large catchments and be consistent in a region[6]. The schematic of Figure 1.1 visualizes hypothesized relative roles of climate and land use changes.

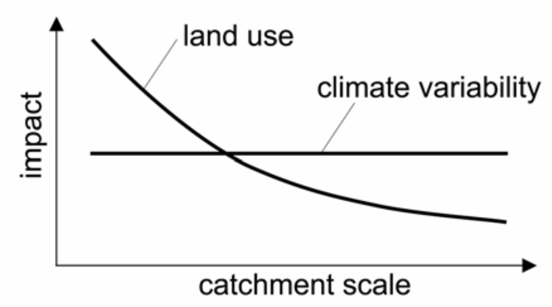

Figure1.1Hypothesized impact of land use and climate variability on hydrological response as a function of scale[6]

There is a need of assessing the risk of urban flooding to get a proper proactive preparedness. This research will combine the effect of climate and land use change to study theirs impacts on flooding in Kigali city located in Nyabugogo catchment.

1.1.2 Problem Statement

Flooding in urban areas can cause damage to properties, disruption to business and traffic, discomfort to community and in some worse cases human lives loss. Floods occur due to meteorological, hydrological and human factors, which can be categorized as climate change and urbanization. Climate and land use change threaten the achievement of the millennium development goals and has a significant impact on urban water resources.Climate change is expected to alter in intensity and frequency of extreme rainfall events [7]. In urban areas, because of the anthropogenic activities, like increasing of impervious surface and lack of adequate drainage system and disposal of sediments and solid wastes, the risk of flash flooding will likely to be increased [8].

Observation done in Rwanda from existing data shows that over the last 3 decades, some parts of country have experienced visible irregularities to hydro-climatic data such as the variation of atmospheric water vapor content; variation in temperature; changes in evapo- transpiration; changing of precipitation patterns, intensity and extremes; and changes in soil moisture and runoff [9].The increased precipitation intensity and variability are the main cause of the risks of flooding and drought in many parts of Rwandan catchments.

Many cities in the developing countries are growing rapidly due to population growth, but to a much larger extent due to migration from rural areas to the cities, and transformation of rural settlements into cities. This results in ncontrolled urban sprawl with increasing human settlements, industrial growth and infrastructure development [10]. İt has demonstrated that flood hazards can be increased by hydrological and hydro-climatological changes brought by the land use and microclimatic changes driven by urbanization [5]. The increase in artificial surfaces due to urbanization causes an increase in flooding frequency due to poor infiltration and reduction of flow resistance (due to faster concentration times)[5].

Kigali city faces typical challenge of urbanization. One of its most serious problems is flash floodsmainly caused by a Nyabarongo River breaking out through its banks due to the heavy rainfall happens in this catchment [11].Recently flood have been affecting Nyabugogo wetland and causedmany negatives consequences(Figure 1.2).

(a)

(b)

Figure1.2(a) A skeleton of car transported by floods (b) Disruption of transport caused by Nyabugogo flooding

The immediate impacts of Nyabarongo flooding include loss of human life, damage to property, destruction of crops, loss of livestock, and deterioration of health conditions owing to waterborne diseases. As communication links and infrastructure such as power plants, roads and bridges are damaged and disrupted, some economic activities may come to a standstill, people are forced to leave their homes and normal life is disrupted.

1.2 Objective of the Thesis

The main objective of this research is to assess the potential impact of climate and land use change on flooding of Kigali city.

1.2.1 Specific objectives

In order to accomplish the main objective, the following specific objectives should also have been met:

- ✓ To develop future climate scenarios on extremes temperature and rainfall based on a general circulation Model and Statistical Downscaling Model.
- ✓ To estimate peak discharge and volumes of floodunder climate and land use scenarios by using HEC-HMS model (latest version 4.0).
- ✓ To assess and quantify a combined climate and land use change impacts on flooding of Kigali city.

1.3 Methodology of the Thesis

A research of climate and land use change impact on the flooding of urban city consists of:

(1) the development and use of general circulation models (GCMs) to provide future global climate scenarios under the effect of increasing greenhouse gases;

(2) the development and use of downscaling techniques for downscaling the GCMs outputs to the scales compatible with hydrological models and

(3) the development and use of hydrological model (HEC-HMS)to simulate the effects of climate and land use change on Kigali city flooding.

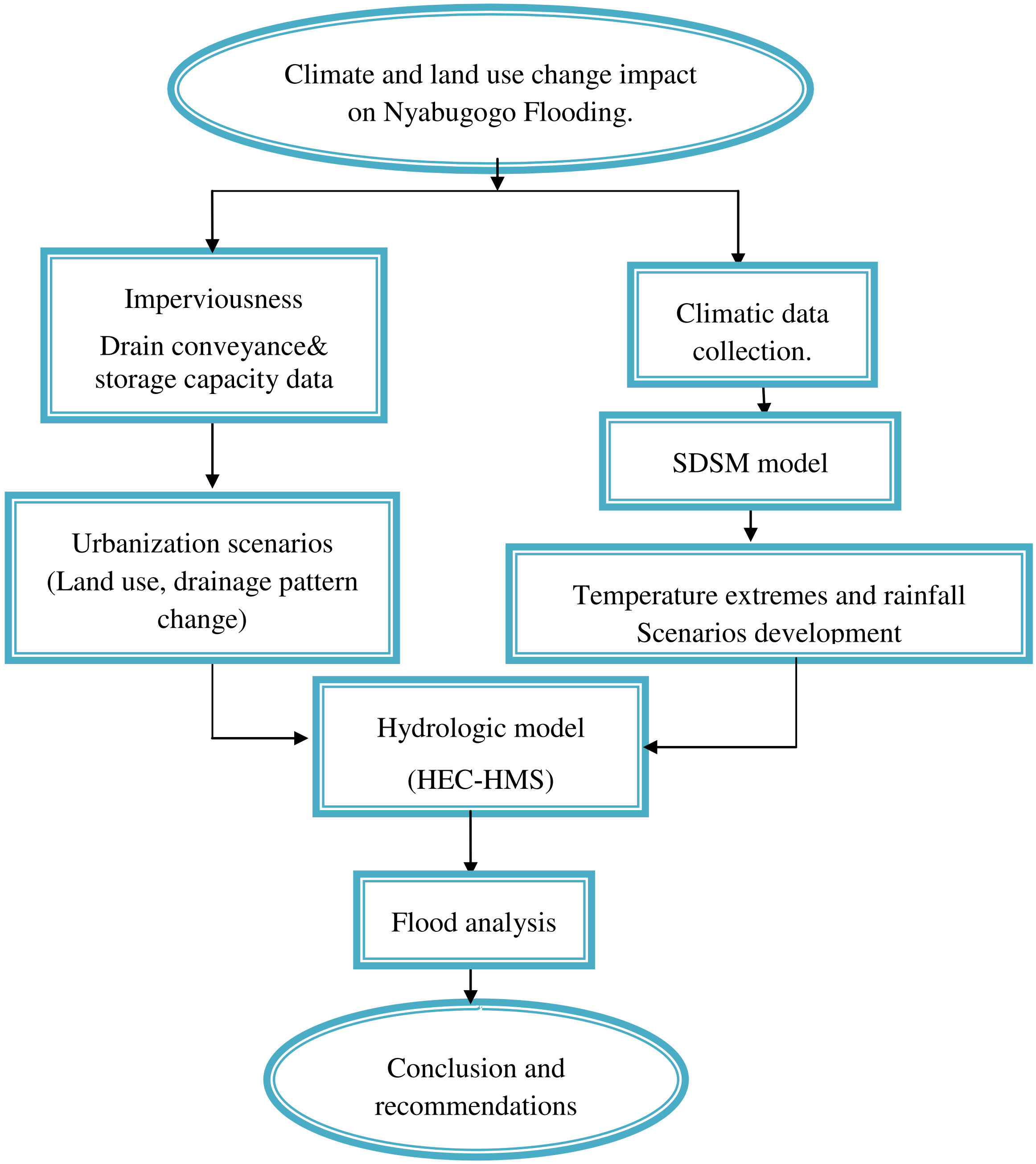

Figure1.3 Flowchart of research methodology process

CHAPTER 2

GENERAL INFORMATION

2.1 Climate Change

Climate change in IPCC usage refers to a change in the state of the climate that can be identified by changes in the mean and/or the variability of its properties and that persists for an extended period, typically decades or longer [4]. Climate change is considered a dynamic phenomenon [12]. Humans' activities such as use of fossil fuels, deforestation, intensified land use change, have contributed to enhancement of natural greenhouse effect and results from an increase in the atmospheric concentration of the so-called greenhouse gases [13]. Typically human activities in cities such as polluting industries, commercial businesses, and heavy traffic as well as dependency on cars contribute to emission of greenhouse gases and therefore to climate change. According to the 5th AssessmentReport (AR5) of the Intergovernmental Panel on Climate Change (IPCC), global (land and ocean) average temperature has shown a 0.85 1C (0.65–1.06 °C) increase over the period of 1800–2012 (IPCC, 2013), and a 0.747 to 0.18 °C increase during the last hundred years (1906–2005) [4]. This trend in global warming is predicted to likely increase during the 21st century under all the Representative Concentration Pathways (RCPs). The projected values of increase are 0.3–1.7 °C (RCP2.6), 1.1–2.6 °C (RCP4.5), 1.4–3.1 °C (RCP6.0), 2.6–4.8 °C (RCP8.5) for 2081–2100, relative to 1986–2005 [1]. Such changes in global mean temperature can radically disturb human society and the natural environment [14].

2.1.1 Climate Models

Climate models are the primary tools available for investigating the response of the climate system to various forcings, for making climate predictions on seasonal to decadal time scales and for making projections of future climate over the coming century and beyond [1]. They refer as mathematical representations of the climate system based on physical, biological and chemical principles [8]. Computer models have been developed for trying to mathematically simulate the climate system, including the interaction between the system component[15]. Climate models have continued to be developed and improved since the AR4, and many models have been extended into Earth System models by including the representation of biogeochemical cycles important to climate change [16].

For climate simulation, the major components of the climate system that must be represented in sub-models are atmosphere, ocean, land surface, cryosphere and biosphere, along with the processes that go on with and between them[3]. Climate models require some inputs derived from observations or other model studies as shown in Figure 2.1.

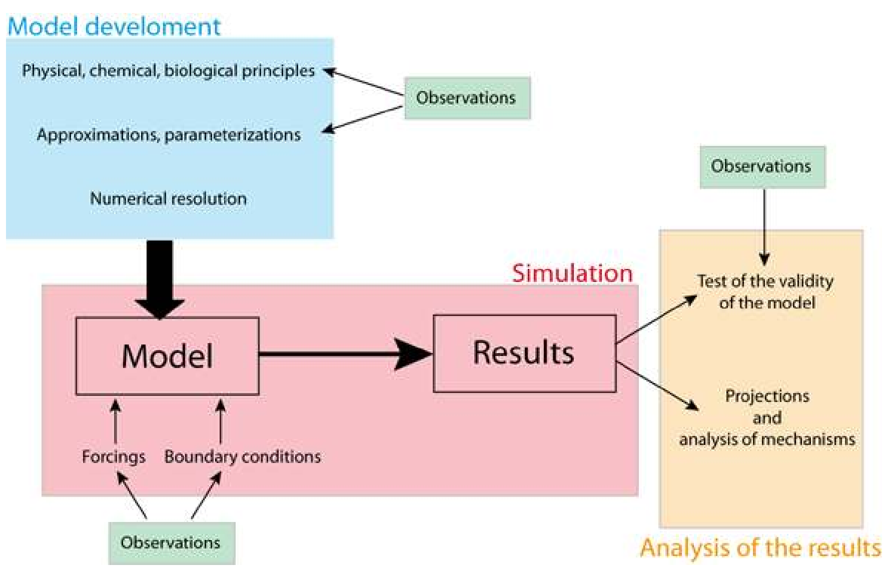

Figure 2.1 Schematic Representation of the Development and Use of Climate Model [17]

Large numbers of observations are needed to test the validity of the models in order to gain confidence in the conclusions derived from their results [17]. Many climate models have been developed to perform climate projections, i.e. to simulate and understand climate changes in response to the emission of greenhouse gases and aerosols. In addition, models can be formidable tools to improve our knowledge of the most important characteristics of the climate system and of the causes of climate variations [17].

2.1.1.1 General Circulation Model (GCMs)

GCM's are the most appropriate tools for addressing future climate changes[18]. General Circulation Models represents physical processes in the atmosphere, ocean, cryosphere and land surface and are the most advanced tools currently available for simulating the response of the global climate system to increasing greenhouse gas concentrations [1]. These models divide the earth, ocean and atmosphere into a grid(Figure 2.2)[18]. The values of the predicted variables, such as surface pressure, wind, temperature, humidity and rainfall are calculated at each grid point over time, to predict their future values [19]. According to IPCC (1994) only GCMs in conjunction with nested regional models or other downscaling methods such as Regional Circulation Models (RCM) have the potential to provide geographically and physically consistent estimates of regional climate change which are needed in flood analysis. GCMs depict the climate using a three dimensional grid over the globe, typically having a horizontal resolution of between 250 and 600 km, 10 to 20 vertical layers in the atmosphere and sometimes as many as 30 layers in the oceans[4]. These models solve a series of equations in the atmosphere describing the movement of energy and momentum and conservation of mass and water vapor.

1. Momentum equation:

$$\frac{D\bar{v}}{Dt} = -2\bar{\Omega}\wedge\bar{v} - (\rho^{-1})\nabla.p + \bar{g} + \bar{F} \quad (2.1)$$

2. Mass conservation equation

$$\frac{Dr}{Dt} = -\rho(\nabla.\bar{v}) + C - E \quad (2.2)$$

3. Energy conservation equation:

$$\frac{DI}{Dt} = -p\frac{d\rho^{-1}}{dt} + Q \quad (2.3)$$

4. Gas law:

$$p = \rho RT \quad (2.4)$$

Where v is the velocity relative to the rotating earth , t is the time ,Ω is the angular velocity vector of the earth, ρ is the atmosphere density, g is the apparent gravitational acceleration, F is the force per unit of mass, R is the density, C and E are the rate of creation and destruction of atmosphere constitutions, I is the internal energy per unit of mass ($I = c_v.T$), Q is the heating rate per init mass, R is gas constant, T is the temperature, c_v is the specific heat of air at constant volume, and p is the atmospheric pressure. These equations are solved with defined values of divergence terms at each grid points, and defined input and output for the upper and lower surfaces of the array for each defined elements of the atmosphere [18]

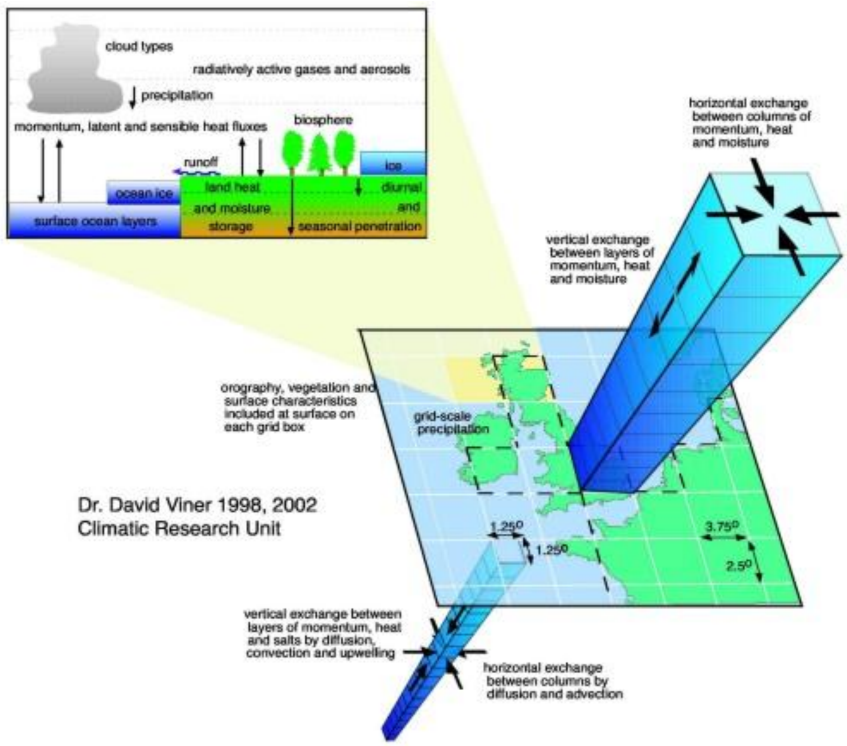

Figure 2.2 Schematic Description of Atmosphere for Utilizing GCMs [4]

The major advantage of using GCMs as the basis for creating climate change scenarios is that they are only tool that estimates changes in climate due to increased GHGs for a large number of climate variables in physically consistent manner[18]. A major disadvantage of using GCMs is that, although they accurately represent global climate their simulations of current regional climate are often inaccurate [18],[20]. In many regions, GCMs may significantly underestimate or overestimate current temperatures and precipitation.

2.1.1.2 Regional Climate Models

RCMs help simulating climate change at the regional and national levels [21]. It helps again to assess the real impact that will be on different countries and its outputs are used to justify difficult social and economic policies to avert a dangerous deterioration in the global climate. Furthermore, RCMs give understanding processes on the regional scale which is a crucial part of global research. Regional Climate Models (RCMs) work by increasing the resolution of the GCM in a small(Figure 2.3), limited area of interest [22].RCMs can then resolve the local impacts given small scale information about orography (land height) and land use, giving weather and climate information at resolutions as fine as 50 or 25km.

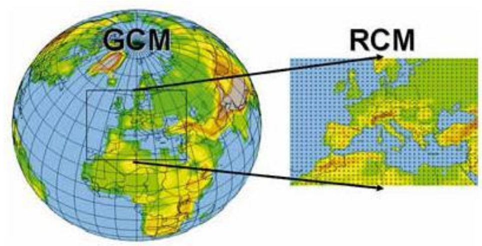

Figure2.3 Regional Climate Model Nesting Approach [22]

One technique used to overcome the coarse spatial resolution of coupled GCMs is that of nested modeling [21]. This involves the linking of models of different scales within a global model to provide increasingly detailed analysis of local conditions while using the general analysis of the global output as a driving force for the higher resolution model. Results for a particular region from a coupled GCM are used as initial and boundary conditions for the RCM, which operates at much higher resolution and often, with more detailed topography and physical parameterizations [23]. This enables the RCM to be used to enhance the detailed regional model climatology and this downscaling can be extended to even finer detail in local models [19].

2.1.1.3 Downscaling Models

Downscaling is a method for obtaining high-resolution climate or climate change information from relatively coarse-resolution global climate models (GCMs) [24]. There is a need to convert GCM outputs into a least reliable daily rainfall series at the scale of the watershed to which the hydrological impact is going to be investigated [25]. The methods used to convert GCM outputs into local variables required for reliable hydrological modeling are usually referred to as´´ downscaling`` techniques [18]. There are two categories of climatic downscaling, namely dynamic downscaling and statistical downscaling.

- ✓ **Dynamic Downscaling**

Dynamic downscaling is method of extracting local scale information by developing and using limited-area models (LAMs) or regional climate models (RCMs) with the coarse GCM data used as boundary condition [26]. The basic steps are then to use the GCMs to simulate the response of the global circulation to large scale forcing and RCM to account for sub-GCM grid scale forcing such as complex topographical features and land cover heterogeneity in physically based away, and thus enhance the simulation of atmospheric circulations and climate variables at the fine spatial scales[27].

- ✓ **Statistical Downscaling**

Statistical downscaling involves developing a quantitative relationship between large scale atmospheric variables (predictors) and local surface variables (predictants)[28]. From this perspective, regional or local climate information is derived by first determining a statistical model which relates large-scale climate variables (or predictor) to regional and local variables (or predictands) then the large –scale output of a GCM simulation is fed into the statistical model to estimate the corresponding local and regional climate characteristics [28]. The most common form has the predictand as a function of the predictors. The concept of regional climate being conditioned by the large scale state may be written:

$$R = F(L) \qquad (2.5)$$

Where, R represents the predictand (a regional or local climate variables), L is the predictor (a set of large-scale climate variables), and F is deterministic/stochastic function conditioned by L and has to be found empirically from observation or modeled data sets.

- ✓ **Statistical Downscaling Model**

The models that are used in climatic studies to simulate the weather parameters with the same variability as observed values are called weather generator [29]. The statistical downscaling model (SDSM) is a hybrid between a multilinear regression method and a stochastic weather generator [30].

In the application of SDSM, the first step is to determine whether in each day variable (e.g rainfall) occurs or not, as follows:

$\omega_i = \alpha_o + \sum_{j=1}^{n} \alpha_j \hat{u}_i^{(j)}$ (2.6)

Where ω_i is the candidate in random process generator that indicates a state of rainfall occurring or not occurring on day i, u_i is the normalized predictor on day i, andα_j is the estimated regression coefficient. Precipitation on day i occurs if $\omega_i \leq r_i$, where r_i is a stochastic output from a linear random-number generator.

The value of rainfall in each rainy day is estimated in the second step using z-score as follows:

$Z_i = \beta_o + \sum_{j=1}^{n} \beta_j \hat{u}_i(j) + \varepsilon$ (2.7)

Where Z_i is the Z-score for day, i, β_j are the estimated regression coefficients for each month,ε is a normally distributed stochastic error term, and the amount of rainfall at day i can be simulate as:

$y_i = F^{-1}[\phi(Z_i)]$ (2.8)

Where $\phi$the normal cumulative distribution function and F is is the empirical function of y_i daily precipitation amounts. The standardized predictors used in this method are provided by subtracting the means and dividing them by standard deviations over the calibration period [30]. During downscaling with SDSM, a multiple linear regression model is developed between few selected large-scale predictors and the local-scale predictands such as rainfall.

2.1.2 Climate Scenarios

Scenarios are alternative images of how the future might unfold[1]. Also they are an appropriate tool with which to analyze how driving forces may influence future emission outcomes and to assess the associated uncertainties[3],[4]. Scenarios have long been used by planners and decision makers to analyze situations in which outcomes are uncertain [31].In climate research, emissions scenarios are used to explore how much humans could contribute to future climate change given uncertainties in factors such as population growth, economic development, and development of new technologies [4]. Projections and scenarios of future social and environmental conditions are also used to explore how much impact lesser or greater amounts of climate change would have on different possible states of the world, for example futures with greater or lesser amounts of poverty[31]. The purpose of using scenarios is not to predict the future, but to explore both the scientific and real-world implications of different plausible futures [4].

The choice of climate change scenarios is important because it can determine the outcome of a climate change impact analysis, based on which urban water resources planning and management strategies will be developed [8]. The selected climate change scenarios for impact assessment should meet the following five conditions:

Condition 1: the scenarios should be consistent with the broad range of global warming projections based on increased atmospheric concentrations of GHGs.

Condition 2: The scenarios should be physically plausible, that is, they should not violate the basic laws of physics.

Condition3: the scenarios should estimate a sufficient number of variables on a spatial and temporal scale that allows for impact assessments [32].

Condition 4: The scenarios should, to a reasonable extent, reflect the potential range of future regional climate change.

Condition 5: The scenarios should be straightforward to obtain, interpret, and apply for impact assessment. There are three generic types of climate change scenarios: scenarios based on outputs from GCMs, synthetic scenarios, and analogue scenarios [8]. Since the majority of impact studies have used the scenarios based on GCMs. Over time, a variety of approaches to scenarios in climate research have been used, from stylized representations of annual percentage increases in global average concentrations of greenhouse gases to advanced representations of emissions of many gases and particles affecting climate and derived from detailed socioeconomic and technology assumptions[8]. An overview of several of the most prominent sets of emissions scenarios is provided in Table 2.1.

Table2.1 History of scenarios

Year	Name	Used in
1990	SA90	First Assessment Report
1992	IS92	Second Assessment Report
2000	SRES-Special Report on Emissions and Scenarios	Third and Fourth Assessment Report
2009	RCP- Representative Concentration Pathways	Fifth Assessment Report

2.1.2.1 Emission Scenario

In IPCC special report on emission scenario (SRES), four different narrative storylines were developed to describe consistently the relationships between the forces driving emission and their evolution and to add context for scenario quantification. The storylines describe developments in many different social, economic, technological, environmental and policy dimensions. The titles of the storylines have been kept simple: A1, A2, B1 and B2. There is no particular order among the storylines; they are listed in the alphabetic and numeric order[3], [4].

- ✓ The A1 storyline and scenario family describes a future world of very rapid economic growth, low population growth, and the rapid introduction of new and more efficient technologies. Major underlying themes are convergence among regions, capacity building and increased cultural and social interactions, with a substantial reduction in regional differences in per capita income. The A1 scenario family develops into four groups that describe alternative directions of technological change in the energy system[3], [4].
- ✓ The A2 storyline and scenario family describes a very heterogeneous world. The underlying theme is self-reliance and preservation of local identities. Fertility patterns across regions converge very slowly, which results in high population growth. Economic development is primarily regionally oriented and per capita economic growth and technological change is more fragmented and slower than in other storylines[3], [4].
- ✓ The B1 storyline and scenario family describes a convergent world with the same low population growth as in the A1 storyline, but with rapid changes in economic structures toward a service and information economy, with reductions in material intensity, and the

introduction of clean and resource-efficient technologies. The emphasis is on global solutions to economic, social, and environmental sustainability, including improved equity, but without additional climate initiatives[3], [4].

- ✓ The B2 storyline and scenario family describes a world in which the emphasis is on local solutions to economic, social, and environmental sustainability. It is a world with moderate population growth, intermediate levels of economic development, and less rapid and more diverse technological change than in the B1 and A1 storylines. While the scenario is also oriented toward environmental protection and social equity, it focuses on local and regional levels[3], [4].

The four scenario "families" are illustrated, very simplistically, as branches of a two-dimensional tree(Figure 2.4). In reality, the four scenario families share a space of a much higher dimensionality given the numerous assumptions needed to define any given scenario in a particular modeling approach. The schematic diagram illustrates that the scenarios build on the main driving forces of GHG emissions. Each scenario family is based on a common specification of some of the main driving forces.

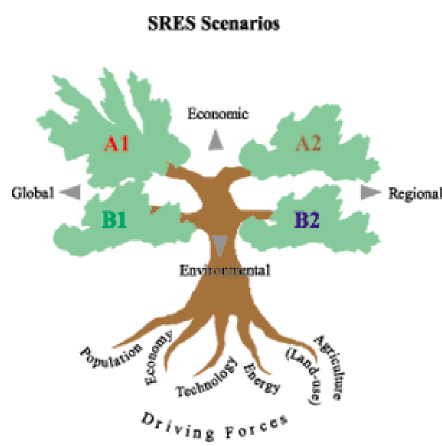

Figure2.4 Schematic illustration of SRES scenarios[4].

2.1.2.2 Scenarios Based on output from Climate Model

Climate models at different spatial scales and levels of complexity provide the major source of information for constructing scenarios [4]. The most common method of developing climate scenarios for quantitative impact assessment is to use result from General climate models (GCMs)(Figure 2.5)[30]. The evolving (transient) pattern of climate response to gradual changes in atmosphere composition was introduced into climate scenarios using the outputs from coupled Atmosphere-Ocean Models from early 1990s onwards. Recent AOGCM simulations begin by modeling historical forcing by greenhouse gases and aerosols from 19th or early 20th century onwards. Climate scenarios based on these simulations are being increasingly adopted in impact studies. However, there are several limitations that restrict the use fullness of AOGCM outputs for impact assessment [20]:

I. The large resources required to undertake GCM simulations and store their outputs, which have restricted the range of experiments that can be conducted;
II. Their course spatial resolution compared to the scale of many impact assessments;
III. The difficult of distinguishing an anthropogenic signal from noise of natural internal model variability;
IV. The difference in climate sensitivity between the models.

The source of scenario and their mutual linkages discussed above is demonstrated in figure below

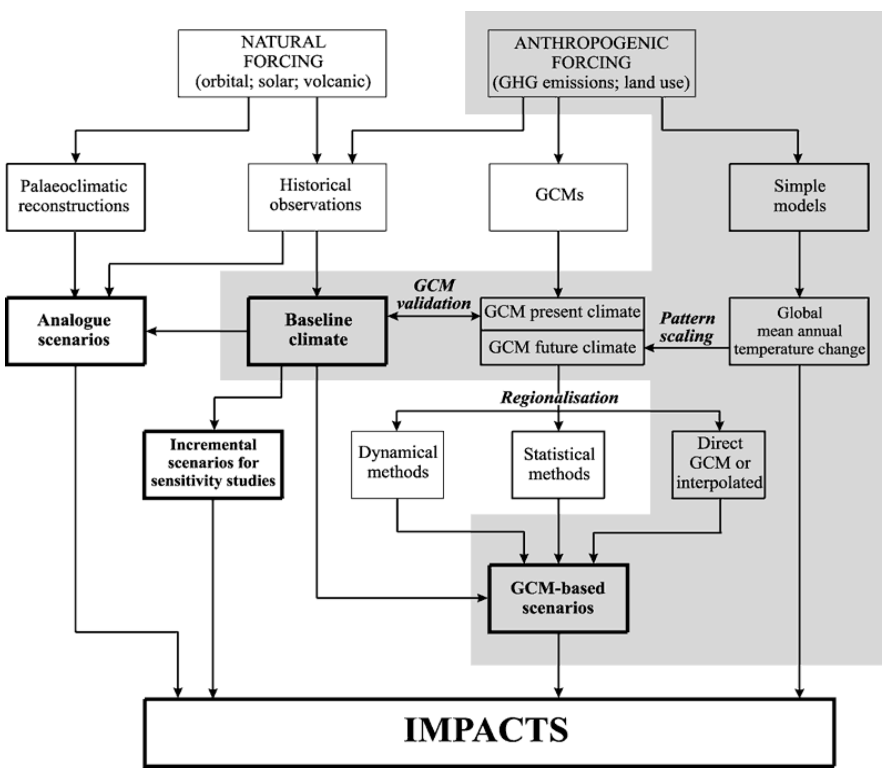

Figure2.5 Some alternative data sources and procedures for constructing climate scenarios for use in impact assessment.

Highlighted boxes indicate the baseline climate and common types of scenario (see text for details). Grey shading encloses the typical components of climate scenario generators [3].

2.1.2.3 Representative concentration pathways

The Representative Concentration Pathways (RCP) is the latest generation of scenarios that provide input to climate models [33]. They are identified by their approximate total radiative forcing in year 2100 relative to 1750(Figure 2.6 and Table 2.2): 2.6 W m-2 for RCP2.6, 4.5 W m-2 for RCP4.5, 6.0 W m-2 for RCP6.0, and 8.5 W m-2 for RCP8.5. These four RCPs include one mitigation scenario leading to a very low forcing level (RCP2.6), two stabilization scenarios (RCP4.5 and RCP6), and one scenario with very high greenhouse gas emissions (RCP8.5).

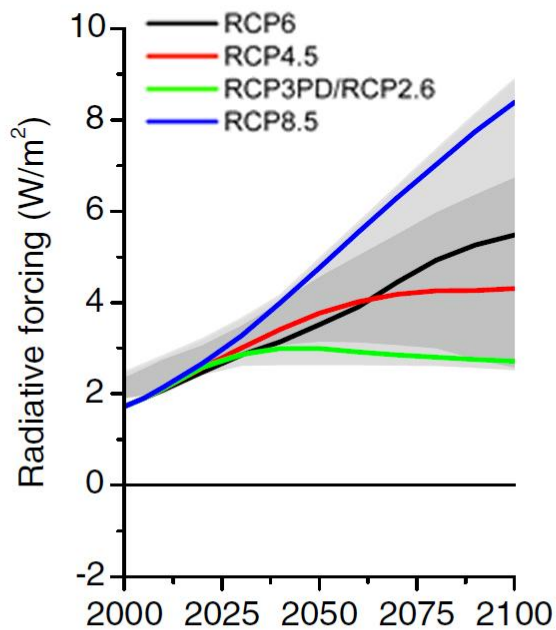

Figure2.6Radiative forcing of the representative concentration pathways

Table2.2RCPS description and comparison to SRES scenario

RCPs	Description	Radiative forcing	Publication	Comparable SRES scenario
RCP8.5	High range emission scenario (possible development for high population numbers, high fossil/coal use)	8.5 W/m2	Riahi et al. 2007	A2 / A1FI
RCP6.0	Medium range emission scenario (low-medium baseline scenario or high mitigation scenario)	6.0 W/m2	Fujino et al. 2006; Hijioka et al. 2008	B2 / A1B
RCP4.5	Medium range emission scenario (high mitigation scenario)	4.5 W/m2	Clarke et al. 2007; Smith and Wigley 2006; Wise et al. 2009.	B1
RCP2.6	Low range mitigation scenario.	2.6 W/m2	Van Vuuren et al. 2007a; van Vuuren et al. 2006	-

Each RCP provides spatially resolved data sets of land use change and sector-based emissions of air pollutants, and it specifies annual greenhouse gas concentrations and anthropogenic emissions up to 2100. RCPs are based on a combination of integrated assessment models, simple climate models, atmospheric chemistry and global carbon cycle models.

2.2 Hydrological Model and Software Description

2.2.1 Modeling Definition and Types

Model is basically a representation of reality. Modeling of phenomenon is always a 'miniature' or the functions of a group of mathematical equations[34]. These equations are not sufficient to represent the total complexity of real world rather than the simplification. Though models give more generalized view of basin hydraulics of the real world, (a) these are more advanced, capable, functional scope, multi activities, efficient models are coming continuously and are improving their work status as per requirement; (b) these can handle huge amount of data sets for large drainage networks with a limited time and cost. The effective modeling depends upon experience; selection of appropriate model and it is not a replacement of fieldwork which may help to make a better outcome. All models cannot operate or give appropriate result in various spatiotemporal environments though they are made for same purpose. Models for physical process are open and accepted by scientific community[34].

Types of Hydrological and Hydraulic Models:

- ✓ Based on types:
  - **a)** Physical vs. Mathematical vs. Numerical,
  - **b)** Empirical vs. Mathematical,
  - **c)** Deterministic vs. Stochastic vs. Conceptual,
  - **d)** Steady vs. Unsteady,
  - **e)** Based on Hydrologic assumptions.

2.2.2 Hydrologic Modeling Module

The hydrologic modeling module is referred to as Tree Module, is the center for hydrologic modeling input, execution and output review. The model interfaces allow you to view and edit model input parameters quickly and easily. Nowadays many models are used for the hydrologic purposes and the section below show different models used for hydrological watershed(table2.3)

.

Table2.3Watershed models and theirs descriptions

Model name	**descriptions**
HEC-1 (HMS)	Developed by hydrologic Engineering center, HEC-1 is the most commonly used lumped parameter available. HEC-1 is designed to simulate surface runoff from a single precipitation event.
TR-20	Developed by the NRCS, TR-20 is designed to compute surface runoff from natural or synthetic rainstorm events.
TR-55	Was developed by the NRCS as a simplified method to compute storm runoff in small, urbanized watersheds.
StormDrain	The stormDrain model does complete storm sewer network analysis for steady state or transient flow conditions. It is based on the HYDRAIN analysis code from FHWA.
Rational Method	One of the simplest and best-known methods of hydrology, the rational method computes peak discharge from area based on rainfall intensity and a runoff coefficient.
NFF	The national Flood Frequency program, developed by USGS in cooperation with FHWA and FEMA, evaluates regional regression equations for estimating flood peak discharges.
HEC-RAS	HEC-RAS is 1D hydraulic model for computing water surface profiles for steady state or gradually varied flow.
HSPF	The hydrological simulation Program FORTRAN simulates hydrologic and water quality processes on land surfaces, streams, and impoundments.
GSSHA	Developed by USACE ERDC, a distributed (2D) hydrologic model developed for analysis of surface runoff, channel hydraulics and groundwater interaction.

2.2.3 HEC-1 (HEC-HMS)

The HEC-HMS is a reliable model developed by the US Army Corps of Engineers that could be used for many hydrological simulations[35]. The hydrologic modeling system is popular model employed for rainfall-runoff analysis in dendrite water systems. It is designed to be applicable in wide range of geographic areas for solving the widest possible range of problems. This range includes large basin water supply and flood hydrology, and small urban or natural watershed runoff. Hydrographs produced by the program are used directly or in conjunction with other software for studies of water availability, urban drainage, flow forecasting, future urbanization impact, reservoir spillways design, flood damage reduction, floodplain regulation, and system operation. Computations in HEC-HMS include loss calculations, conversion of extreme rainfall to runoff, baseflow estimation, and routing in reaches and reservoirs [36]. HEC-HMS has been successfully applied in many catchments worldwide. For example: Christopher and Yung (2001) used HEC-HMS to perform a grid-based hydrologic analysis of a catchment [37].

They compared distributed, semi-distributed and lumped models and reasonable contribution of flood observation and runoff volume. Fleming and Neary (2004) successfully used HEC-HMS as a tool for continuous hydrologic simulation in the Cumberland River basin [38]. Neary et al. (2004) applied the HEC-HMS model to continuous simulation by comparing streamflow simulations using basin-average gauge and basin-average radar estimates[39]. Cunderlik and Simonovic (2005) also used the continuous simulation version of the HEC-HMS model to describe the main hydroclimatic processes in the Ontario River basin [40]. Chu and Steinman (2009) carried out continuous hydrologic simulations by applying HEC-HMS to the Mona Lake watershed in west Michigan [41]. Bouabid and Elalaoui (2010) used HEC-HMS for assessing the impact of climate change on water resources in the Sebou Basin in Morocco [42]. Boyogueno et al. (2012) applied HEC-HMS for the prediction of flow rate in Sanaga Basin in Cameroon [43].

The program features a completely integrated work environment including a database, data entry utilities, computation engine, and results reporting tools. The figure 2.7 show the process of rainfall-runoff is done in HEC.HMS.

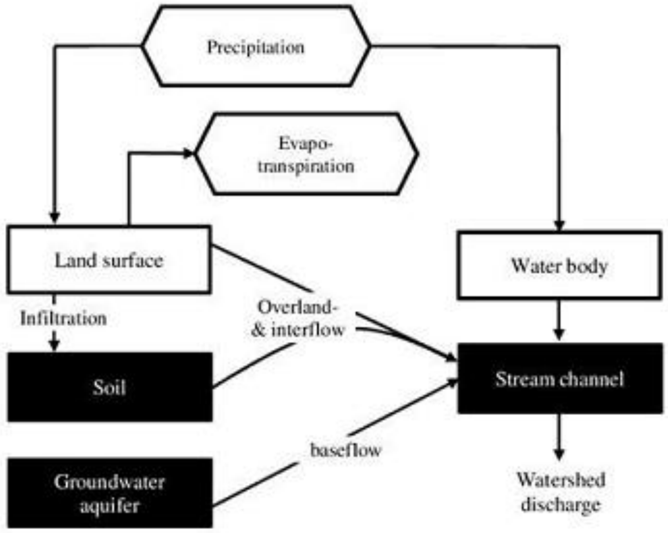

Figure2.7 Schematic rainfall-runoff process in HEC-HMS[44]

The HEC-HMS is composed of several different modeling components that make up the entire watershed model, including(Figure2.8): (a) a meteorological model that handles precipitation inputs, (b) a loss method (infiltration model) that calculates runoff, and (c) a transform function that routes runoff to subbasin outlets, and (d) a routing function that accumulates modeled flow from each of the distributed subbasins, creating a streamflow hydrograph.

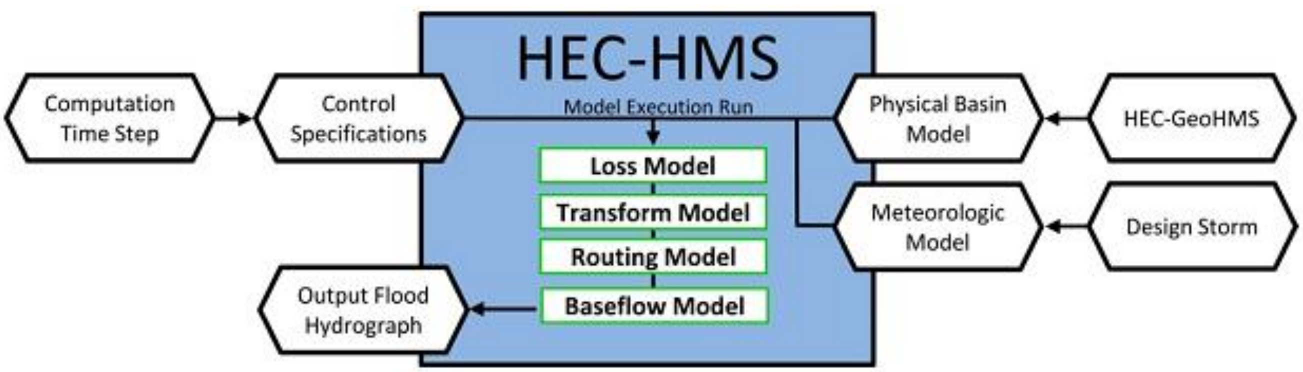

Figure2.8 HEC-HMS software components [45]

CHAPTER 3

DESCRIPTION OF THE STUDY AREA AND METHODOLOGY

3.1 General Description

3.1.1 Geographical Description

The case study is located in country of Africa named Rwanda. It is a mountainous country with relatively high rainfall, and is situated in Central Africa, bordered by Burundi in the South, the Democratic Republic of Congo in the West, Uganda in the North and Tanzania in the East. The total area of Rwanda is about 26 338 km^2 out where 24,948 km^2 is the land and 1,390 km^2 is covered by water (5.3%). The country extends between 1º02'40'' and 2º50'16'' south and between 28º51'39'' and 30º53'56'' East of Greenwich.

The flooded part of Kigali city is located in Nyabugogo watershed in the central eastern part of Rwanda(Figure 3.1). The catchment drains a total area of about 1,647 km^2. The upper part of the basin is drained by Muhazi Lake. The major land use activity in the catchment is agriculture, which occupies about 897 km^2 (about 54%) of the catchment. The Nyabugogo River traverses the City of Kigali and has many tributaries such as the Mwange River, Rusine River and Marenge River on its upstream portion. It is later fed by other rivers from the urbanized part of Kigali such as the Rwanzekuma River, the Mpazi River and the Yanze River.

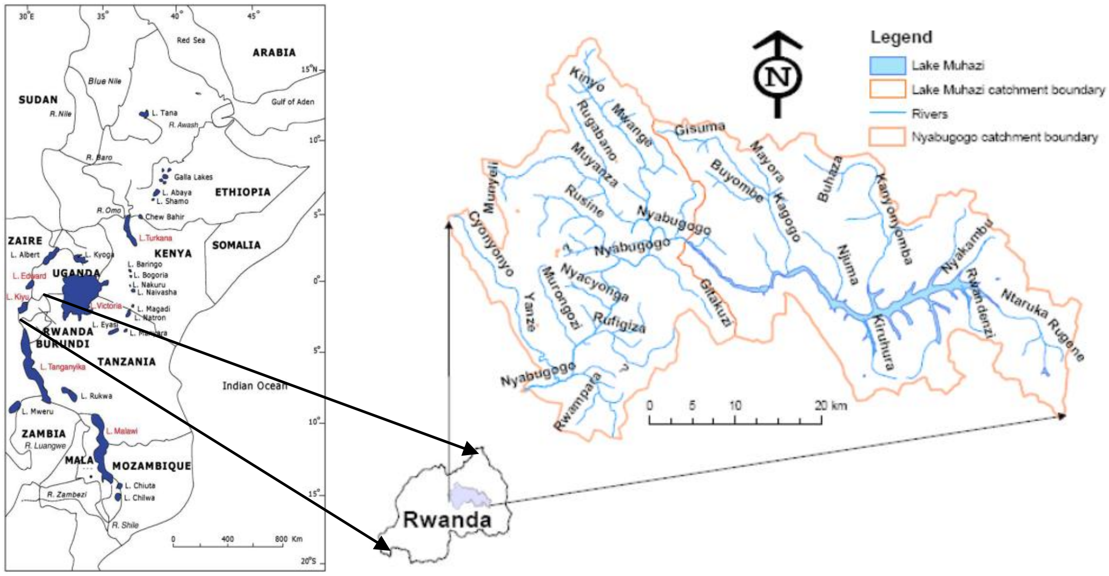

Figure3.1 The case study location

3.1.2 Climate Description

The mean annual rainfall in Rwanda is about 1100 mm and varies from 700 mm in the South-West to about 1600 mm/year in the North-West(Figure3.2)[46]. Rwanda is divided into three agro-climatic zones: i) high-altitude region, ii) central plateau, and iii) plateau of eastern lowlands and the west [47].

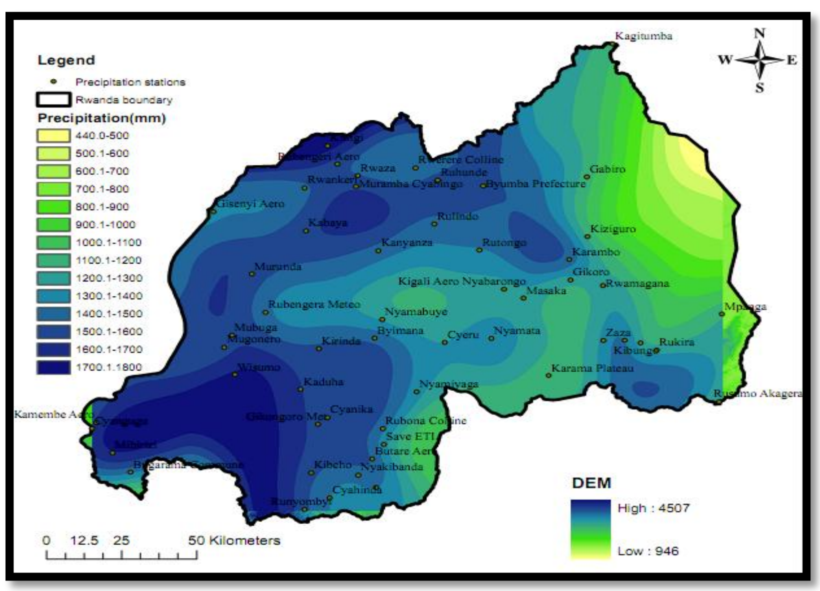

Figure3.2 Rwanda Precipitation Distribution

The Rwanda has a moderate climate with an annual average temperature of 19^{0}C. Low temperatures are observed in the regions of high altitude with average temperatures ranging between 13°C and 17°C. Moderate temperatures are found in areas with intermediary altitude where average temperatures vary between 19°C and 21°C. In the lowlands (east and southwest), temperatures are higher and the extreme can go beyond 30°C in February and July-August(Figure 3.3)[9].

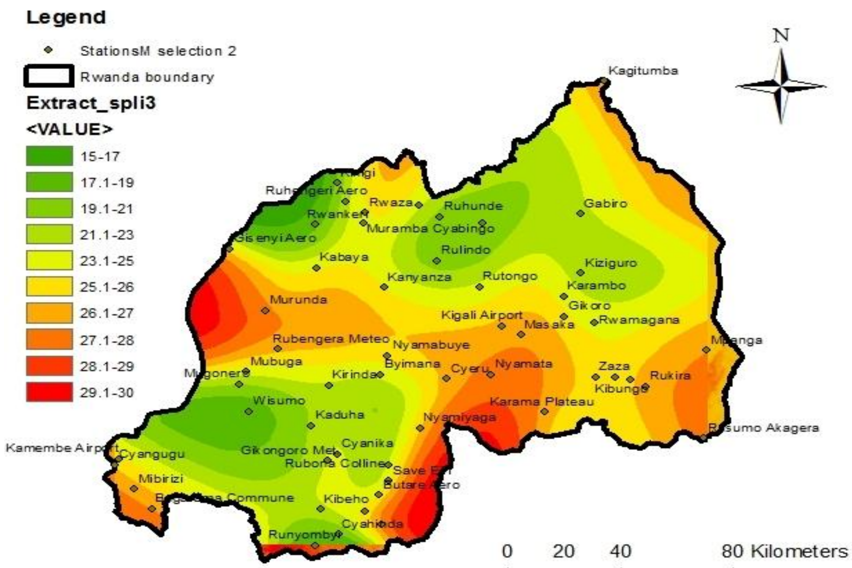

Figure3.3Rwanda temperature distribution

The climate of the Nyabugogo catchment is mostly of temperate and equatorial type with average temperature ranging between 16°C and 23°C, depending on the altitude of the area. The annual rainfall in Rwanda varies from about 800 mm to 1,600 mm in this catchment. There are normally four seasons in Rwanda. The first is a long dry season that spans from June to September, followed by a short rainy season spanning from October to December. This season receives 30% to 40% of the annual rainfall with the highest rains falling in November. The third is a short dry season starting in December and ending in January. The fourth is a rainy season spanning from February to end of May. This season receives around 60% of annual rainfall [48].

The mean rainfall at the station near the flooded area is represented in figure 3.4 since 1970 to 2014(Figure3.4) it varies between 1356.6 mm (max) in 1979 and 687.2 mm (min) in 1992. The average rainfall for this period reaches 995.57 mm/ year.

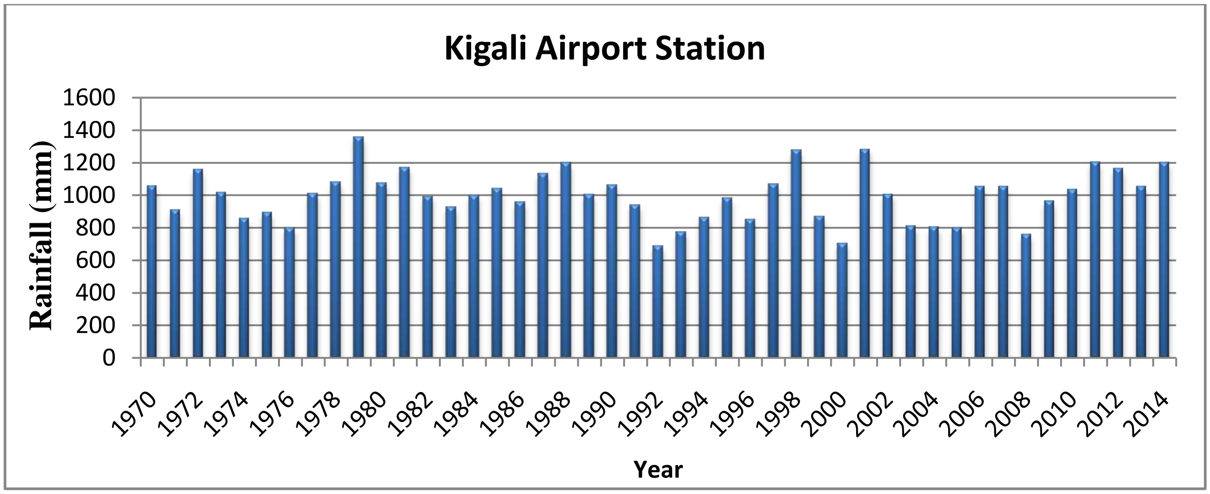

Figure3.4 Precipitation at station near flooded area

The mean temperature at the station near the flooded area is represented in figure since 1971 to 2014(Figure3.5) it varies between 22.40 °C (max) in 2011 and 19.97°C (min) in 1971 with the average temperature of 21.19°C for the period of 1971to 2014.

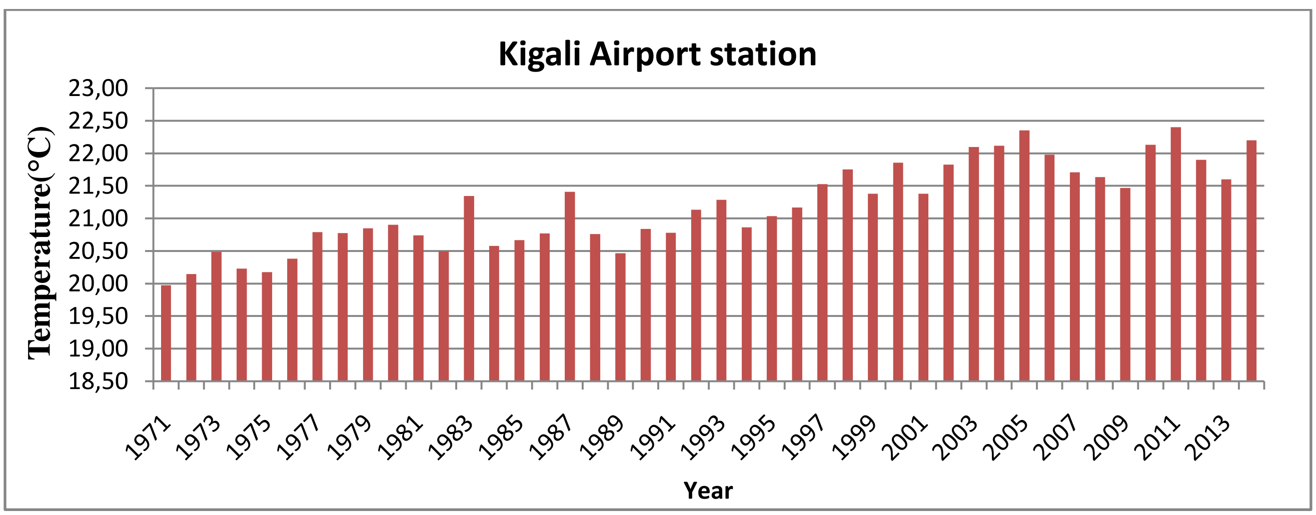

Figure3.5Temperature at station near flooded area

3.1.3 Kigali City Topography

Kigali city is built on a rolling landscape of hills, ridges and valleys(Figure3.6). The surrounding region ranges in altitude from 787 m to over 4000m, but Kigali has a lower mid-altitudinal range of 1300 m in the wetlands, to the peak of Mount Kigali at 1850 m. The slopes of the city´s hills vary in steepness from inclines of up to 45 or 50 percent, to those in Valley wetland areas with slopes of less than 2 per cent [49].

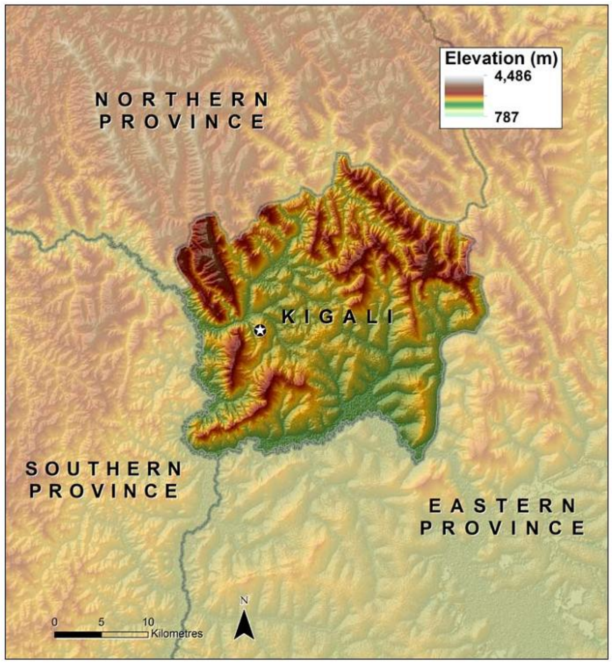

Figure3.6 Elevation map of Kigali and surrounding region[49]

3.1.4 Flooding Situation

The Nyabugogo flood plain area(Figure3.7) collects the flow from the Nyabugogo River as it winds down its way from Muhazi Lake which buffers about half of the catchment area and from some smaller but heavily urbanized catchments such as the Rugunga (Gikondo and Kigarama neighborhoods) and the Mpazi (Nyamirambo). The floodplain drains into the Nyabarongo River through a narrow valley where several small tributaries (including the Yanzi River with a catchment of just about 10 km^2) increase peak discharges from about $15m^3/s$ to about 25 m^3/s. Because of this available evidence of increased peak discharges from small catchments it was immediately clear that the cause of the flooding problem might have been related to one or several of those small catchments.

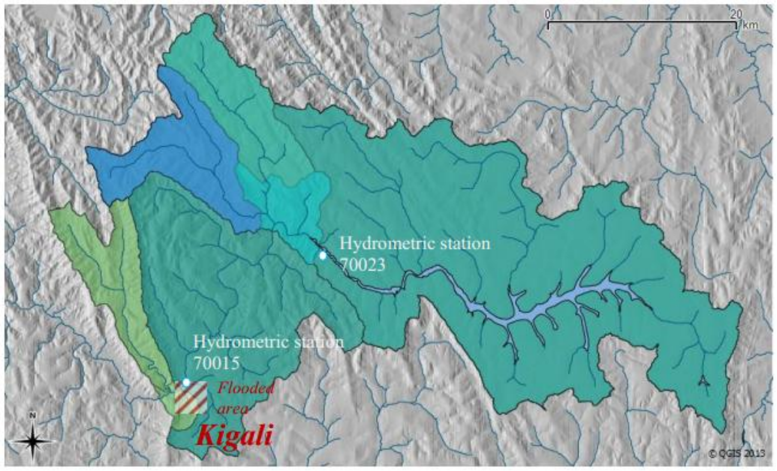

Figure3.7 The Nyabugogo basin Including lake muhazi and flooded zone in kigali city[50].

As indicated by Figure, the flooded area is located in the hydrological basin of the Nyabugogo River. The inundation zone is located directly at Muhima market. Just below this location the Rugunga tributary joins the Nyabugogo through the Muhima wetland in the East. At this same location the Mpazi basin releases its flow from Mt Kigali in the South [50].

The Nyabugogo catchment is partly protected from extreme discharges by the buffer function from Lake Muhazi which effectively stabilizes the runoff from more than half of the Nyabugogo catchment. The typical peak values of the subsequent hydrometric stations 70015, at the outflow of the Nyabugogo floodplain, and 70016 after the confluence of the Nyabugogo with the Yanzi river (about 110 km^2) increase from about 15 m^3/s to about 25 m^3/s indicating peak discharge values of the order of 10 m^3/s for the Yanzi river. These discharges are conveyed without undue damage through confined valleys leading to the confluence with the Nyabarongo[50].

The flooding damage at the Nyabugogo market area starts upstream of the bus station and extends to the confluence with the Nyabugogo. The bus station and market area is intersected by a steep channel which drains the Mpazi basin. This tiny basin of 8.7 km^2 has very steep slopes in the upper part and has elevations of more than 1800 m at Mt. Kigali. Most of the basin is very densely urbanized and slopes are very steep (some > 30 degrees). Urban drainage structures have been developed to drain runoff quickly during rain storms. The damage observed and the accounts of residents indicated that this basin is related if not the root cause of the flooding[50].

3.1.5 Land Use

Kigali city land was before covered by forest but now forests cover only an area of 10.6% [49]. Time by time urban development and farming activities including commercial daily and subsidence farming systems, have left only small, scattered patches of forest and other areas of natural vegetation(Figure 3.8).

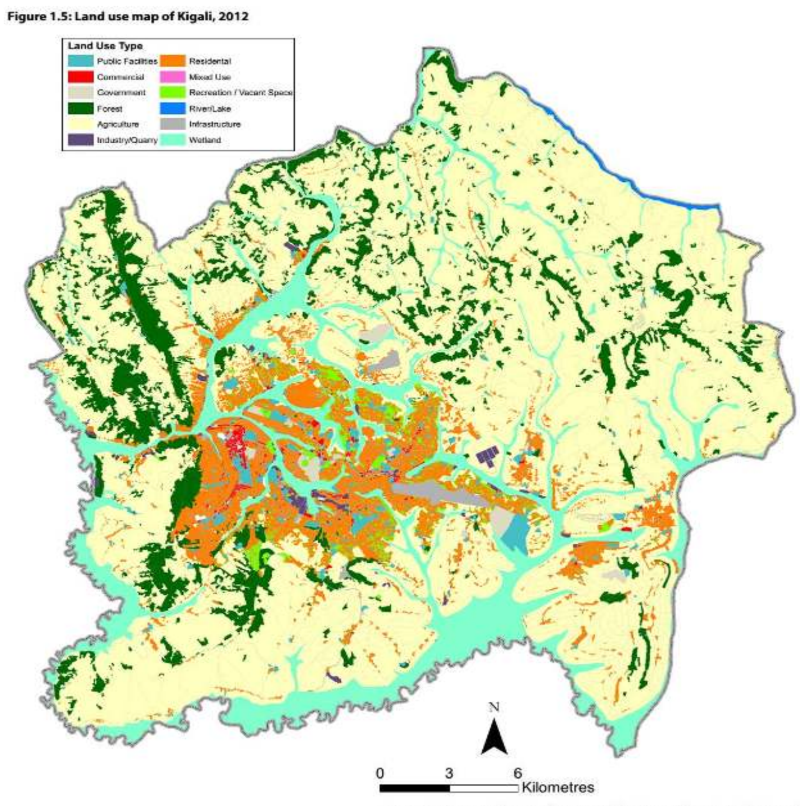

Figure 3.8 Land use map of kigali city[49]

Urban land use include residential, Commercial, and industrial, social and government infrastructure.The teable 3.1 shows the Kigali land use types by proportion.

Table 3.1Land use types by proportion in Kigali [49]

Land use type	Area (sq.km)	Percent (%)
Public Facilities	12.2	1.7
Commercial	2.7	0.4
Government	4.2	0.6
Forest	77.2	10.6
Agriculture	442	60.5
Industry/Quarry	2.9	0.4
Residential	66	9.2
Mixed use	0.2	0.03
Recreation/ Vacant space	10	1.4
River/ lake	1.6	0.2
Infrastructure	20.5	2.8
Wetland	91.6	12.5
Total	730	100

3.2 Methodology

3.2.1 Data Collection

3.2.1.1 Meteorological Data Collection

Meteorological data was required for downscaling the GCM data using Statistical Downscaling model development. Based on this objective, meteorological data was collected from many stakeholders in the field of water and environment in Rwanda, such as Ministry of Natural

Resources (MINIRENA), Ministry of Infrastructures (MININFRA), Rwanda Environmental Management Authority (REMA), and the METEO-RWANDA which has the responsibility of measuring, analyzing and storing hydro meteorological data and forecasting the weather in Rwanda. The data used, for downscaling GCM consist of daily rainfall data for near station of flooded zone over a period of 40 years (1975-2001)(Table 3.2).This period of data collection was selected according to the method that has been used during this research of statistical downscaling model which uses data baseline of 1961-1990.

Table3.2 Kigali airport station

variable	Latitude	Longitude	Altitude (m)	(Period)
Rainfall	01° 58 S	30° 08 E	1,490.0	1975-2001
Tmax	01° 58 S	30° 08 E	1,490.0	1971-2001
Tmin	01° 58 S	30° 08 E	1,490.0	1971-2001

3.2.1.2 Climate Scenario Data Collection

Climate scenario data is required to quantify the relative change of climate variables between the current and future time horizon which in turn is used as input to hydrological model for assessment of hydrological impacts caused by climate change. The climate scenario data for statistical downscaling model (SDSM) was obtained from Canadian Institute for climate studies website (http://www.cics.uvic.ca/scenarios/sdsm/select.cgi). This link contains predictors prepared to be used in SDSM (Statistical downscaling model). The predictor variables are supplies on grid by grid basis so that the data was downloaded from the nearest grid box to the study area.

Coordinates of case study (Kigali Airport station) was applied in the website to extract associated predictors variable. For each coordinates, predictor variables that already normalized could be obtained in a zip format. Each file consisted of three specific data namely National Centers for Environmental Prediction (NCEP) for current predictors and GCMs from Hadley Center Coupled Model Version 3 (HadCM3) A2 and B2 emission scenarios for projection. A brief description of each component is found below:

- **NCEP_1961-2014:** This directory contains 54 years of daily observed predictor data, derived from the NCEP re-analyses, normalized over the complete 1961-1990 period. These data were interpolated to the same grid as HadCM3 (2.5° latitude x 3.75° longitude) before the normalization was implemented.
- **H3A2a_1961-2099:** This directory contains 139 years of daily GCM predictor data, derived from the HadCM3 A2 (a) experiment, normalized over the 1961-1990 period.
- **H3B2a_1961-2099:** This directory contains 139 years of daily GCM predictor data, derived from the HadCM3 B2 (a) experiment, normalized over the 1961-1990 period.

Predictor variables explain a physical regional scale climate characteristic that would be used to predict and derive local weather variables (e.g. rainfall and temperature).

3.2.1.3 Land Use Data Collection

The land use data was collected from Kigali master plan conception as it shows clearly how Kigali city is developing in terms of built-up and water bodies (impervious area) and also agriculture(pervious area).Kigali master plan 2013 is the final product of long journey started in 2017. It includes the details of land use plans for Nyarugenge, Gasabo and Kicukiro Districts. This plan was developed to incorporate, harmonize and update all previously elaborated plans. Kigali city master plan provides a long-term vision for the city. It sets up fundamental pillars of sustainable urban development, such as protection of wet land, slopes, and forest areas. In additional it contains detailed land use and zoning plans that will guide the city´s urban development.The Figure 3.9 illustrates the kigali city proposed land use zoning. These detailed plans can now be referred to the estimation of impervious land for future years in Kigali city.

Land use change prediction is mostly perfomed through Sleuth Model.SLEUTH is a well established approach to land use change modeling based on cellular automata. The SLEUTH model was developed by Dr. Keith C. Clarke at UC-Santa Barbara and integrates 2 sub-models, the Urban Growth Model (UGM) and the Deltatron Land Use/Land Cover Model (DLM). SLEUTH has become one of the most popular simulation models of urban growth and land use change in last decades[59].SLEUTH simulates four types of urban land use changes: spontaneous growth, new spreading center growth, edge growth, and road influenced growth.

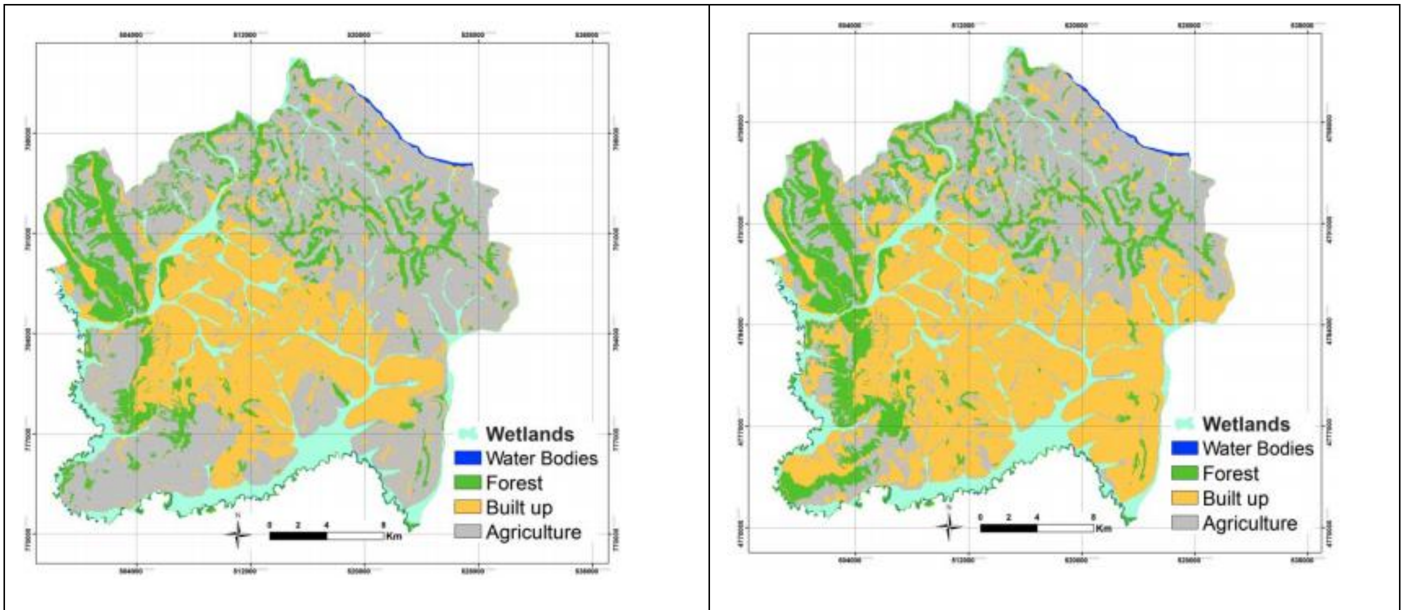

(a) (b)

Figure 3.9(a) Proposed 2025 zoning land use (b) Proposed 2040 zoning land use map

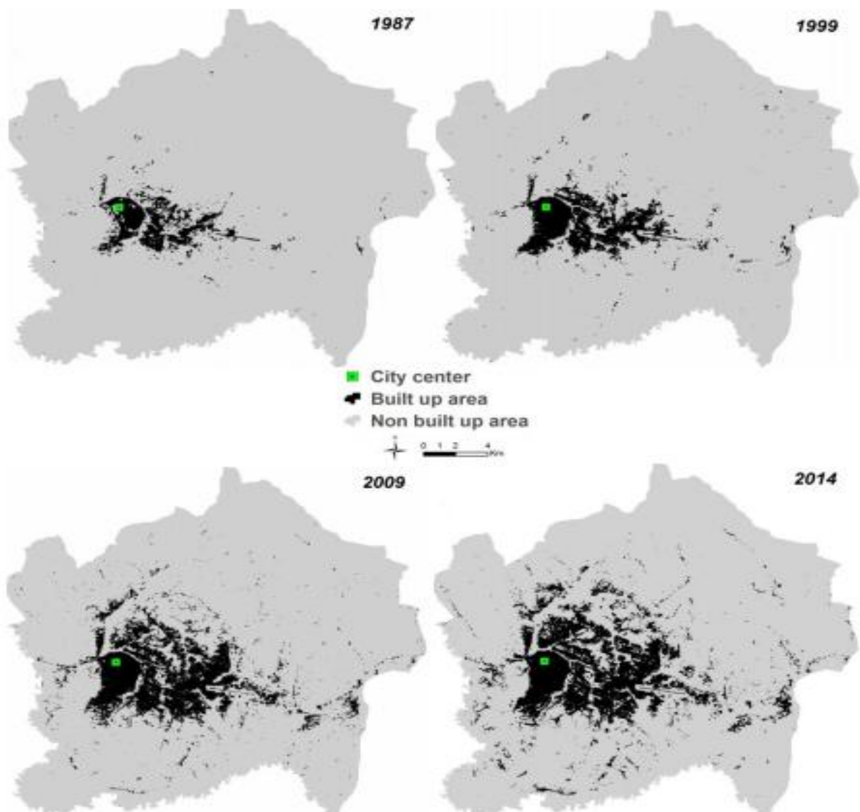

Figure3.10 Kigali built-up area change for 1987, 1999, 2009, and 2014

The figire 3.10 shows the built-up area expansion between 1987, 1999, 2009 and 2014 where 5 classes (built-up, forest, bare soil and vegetation as well as water bodies) were considered [51].

3.2.2 Models Used and their Descriptions

A research of climate and land use change effect on the hydrological regimes of urban city consists of (1) the development and use of general circulation models (GCMs) to provide future global climate scenarios under the effect of increasing greenhouse gases (2) the development and use of downscaling techniques for downscaling the GCMs outputs to the scales compatible with hydrological models and (3) the development and use of hydrological models to simulate the effects of climate and land use change on hydrological regimes at various scale.

3.2.2.1 Climatic Models

In this study climate models have been used to assess impact of climate change to the climatic data include temperature extremes and rainfall data in Nyabugogo catchment.

- **General Circulation Model (GCMS)**

For this study the Model output of HaCM3 was used for the A2 (Medium-High Emissions) and B2 (Medium-Low Emissions) scenarios. HadCM3 is a coupled atmospheric-ocean GCM developed at Hadley Center for Climate Prediction and Research, UK. The atmospheric part of HadCM3 has a horizontal resolution of 2.5 ° latitude x 3.75° longitude and has 19 vertical levels. The ocean component of model has 20 vertical levels with horizontal resolution of 1.25° latitude and 1.25° longitude. HadCM3 is applied to this research because the model provide daily predictor variables which can be used for the Statistical Downscaling model and is widely applied to many climate change impact studies.

- **Statistical Downscaling Model (SDSM)**

For this study, we have used one of the most recognized statistical downscaling tools named Statistical Downscaling Model (SDSM), widely applied to assess local climate change and its impact. This model was developed by Dawson & Wilby (in 2007)[30] supported by the Environmental Agency of England and Wales. SDSM is a hybrid of the stochastic weather generator and multi regression based methods. It uses empirical statistical techniques to establish a relationship between historical large-scale circulation patterns and atmospheric moisture variables (predictors) and locally observed temperature or precipitation (predictands) [52]

Assuming the relationship based on historical observations holds true for the future dates, the precipitation and temperature (extremes values: maximum and minimum) are then modeled through a stochastic weather generator applying the relationships with the probability of the precipitation depending on GCM predictor variables. Additionally, stochastic techniques are used to artificially inflate the variance of the downscaled daily precipitation and temperature time series to better accord with observed precipitation time series [53] because the highly variable nature of the local variable (precipitation, temperature) cannot be fully explained by the variations in large-scale predictor variables alone [54].

The downscaling procedure of the SDSM was performed through a number of steps [53] such as data quality control and data transformation, predictor screening, model calibration, weather generator, and validation of the model and generation of future precipitation and extremes temperature(maximum and minimum) projections.

a) Steps of SDSM Model

- **Quality Control and Data Transformation**

Simple Quality Control checks in SDSM enable the identification of gross data errors, specification of missing data codes and outliers prior to model calibration. In many instances it may be appropriate to transform predictors and/or the predictand prior to model calibration. The Transform facility takes chosen data files and applies selected transformations (e.g., logarithm, power, inverse, lag, binomial, etc).

- **Screening of Downscaling Predictor Variables**

Identifying empirical relationships between gridded predictors (such as mean sea level pressure) and single site predictands (such as station precipitation) is central to all statistical downscaling methods. The main purpose of the Screen Variables operation is to assist the user in the selection of appropriate downscaling predictor variables. Screen variables facilitate the examination of seasonal variations in predictor skill.

- **Calibration**

The Calibrate Model operation takes a User specified predictand along with a set of predictor variables, and computes the parameters of multiple regression equations via an optimization algorithm.

- **Weather Generation**

The Weather Generator operation generates ensembles of synthetic daily weather series given observed (or NCEP re–analysis) atmospheric predictor variables. The procedure enables the verification of calibrated models (using independent data) and the synthesis of artificial time series for present climate conditions.

- **Data Analysis**

SDSM provides means of interrogating both downscaled scenarios and observed climate data with the Summary Statistics and Frequency Analysis screens.

- **Graphic Analysis**

Three options for graphical analysis are provided by SDSM 4.2 through the Frequency Analysis, Compare Results, and the Time Series Analysis screens.

- **Scenario Generation**

The Scenario Generator operation produces ensembles of synthetic daily weather series given atmospheric predictor variables supplied by a climate model (either for present or future climate experiments), rather than observed predictors.

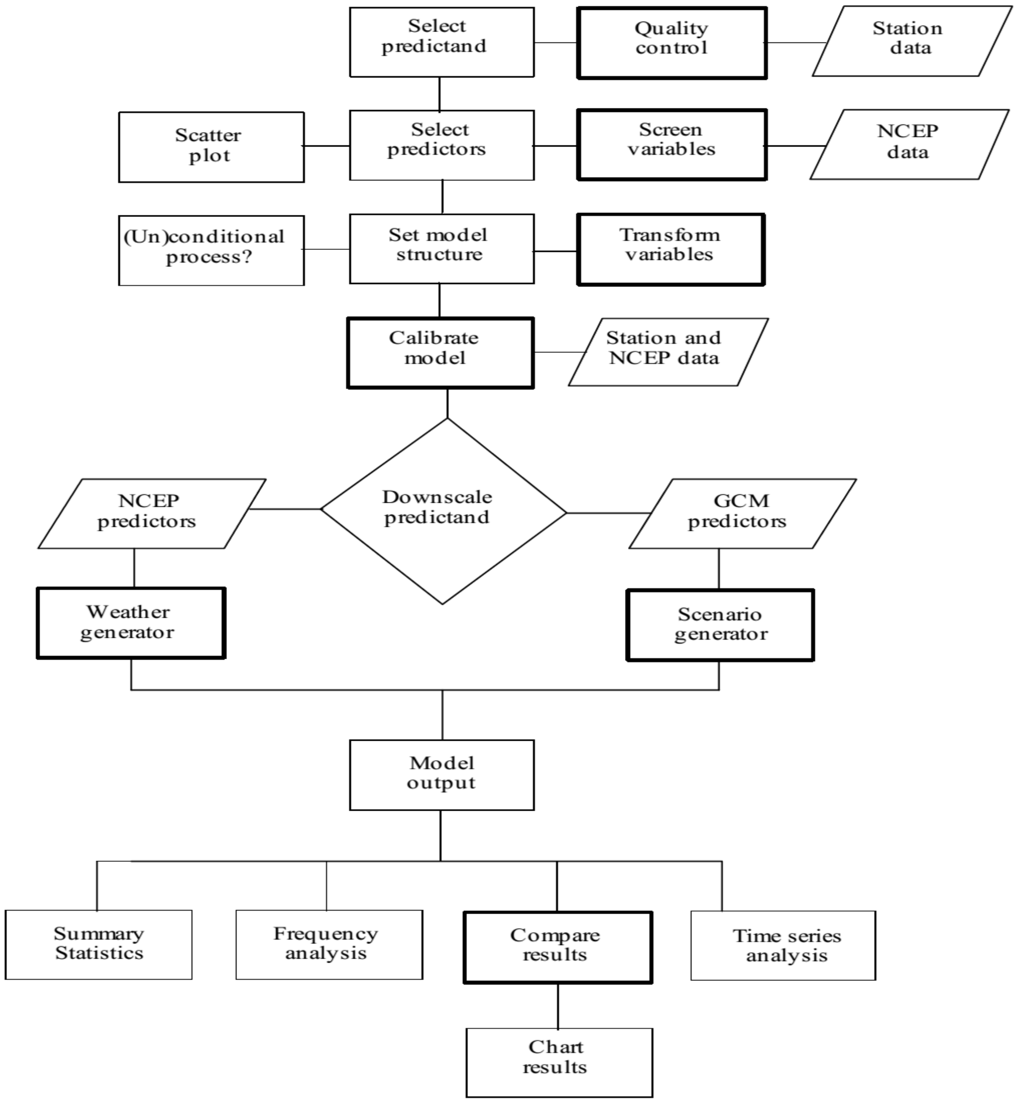

Figure3.11 SDSM climate scenario generation[53]

In Figure 3.11 bold box indicate the key function of SDSM.

3.2.2.2 Hydrological Model

In the present study, the Hydrologic Engineering Center-the Hydrologic Modeling System (HEC-HMS) was adopted as a hydrologic modeling tool for providing the flood hydrographs. The model was selected due to its capacity to analyze the spatial variation of runoff generation characteristics, simplicity in setup, limited data requirements and the free availability of the software. HEC-HMS is a modeling program developed and distributed by the United States Army Corps of Engineers (USACE) to simulate rainfall-runoff processes in watersheds. The program relies on separating the hydrologic cycle into separate pieces and constructing watershed boundaries. Each component of the water cycle is then able to be represented by a separate mathematical model [55].

Components:

The hydrologic cycle is separated into two parts; a basin model and a meteorological model. Once the basin is defined and a rainfall delivery process is chosen, a control model defines the model run time.

- **Basin Model**

The basin model provides the physical characteristics of the land surface inside of the model area. The principle purpose of Basin model is to convert atmospheric conditions into streamflow at a specific location in watershed. The components included in the basin model are infiltration, surface runoff, baseflow, and river routing. Elements that make up the basin are subbasins, reaches, reservoirs, junctions, diversions, sources, and sinks. These elements are then assembled together to create a dendritic basin. Within each element there are a series of parameters that describe how water moves through each element.

- **Meteorological Model**

The meteorological model is designed as a way to create the boundary conditions that act on a watershed [55]. This model describes how water will be generated for each subbasin element inside of a basin model. The meteorological model is also responsible for precipitation, evapotranspiration, and snowmelt processes. Precipitation may be distributed over the basin using precipitation gages, frequency storms, or gridded precipitation. Evapotranspiration can be controlled using monthly averages or the Priestley Taylor method. Snowmelt is controlled by temperature indexing.

- **Control Model**

The third component of the HEC-HMS model is the control model. This component sets the duration for a model run as well as what time step will be used during the modeling run. The time step must be set so that each element can be calculated at least once. This is most important with working with lag times, or velocities in streams.

Parameters

The following section describes the various parameters that are needed to populate the different models inside a project. In depth descriptions of the loss, transform, routing, and baseflow methods that were created within the basin model will be discussed.

- **Loss Parameters**

Determining the distribution of rainfall into infiltration and runoff is the first step in creating the final element output hydrograph. The loss is calculated at the end of each time interval by finding the difference in the volumes of each adjacent time interval [55]. There are 11 loss methods available inside of HECHMS, the SCS Curve Number method was chosen for implantation in this study. Using the SCS Curve Number, the rainfall is able to be partitioned into the two components of infiltration and runoff. The curve number is calculated in GIS using land cover and soil data. Once the curve number is calculated for each subbasin this number represents the percentage of rainfall that will be converted into direct runoff minus any initial abstractions. The initial abstraction is the amount of rainfall that must fall before any excess runoff can occur. The default value of initial abstraction is calculated from the SCS method as Ia= 0.2S. S is defined as a value of maximum potential retention which is calculated from the curve number.The last input for calculating loss is the percent of subbasin impervious. Since any areas with the potential to have impervious conditions was taken into account while creating the curve numbers this variable was left at zero for all subbasins across all model runs

$$S = \frac{25400}{CN} - 254 \tag{3.1}$$

$$\mathrm{Pe} = \frac{(\mathrm{P} - 0.2\mathrm{S})^2}{\mathrm{P} + 0.8\mathrm{S}} \tag{3.2}$$

Where CN is curve number, P is rainfall(mm),initial abstraction, Ia is the potential maximum retention after runoff begins(mm) and Pe is the cumulative rainfall excess which causes runoff.

- **Transform Parameters**

Converting the runoff that was created from the loss component into a physical hydrograph is done through the transform method in HEC-HMS. Inside of HMS there are seven transform methods to choose from, and the SCS Unit Hydrograph was selected for modeling. When using the SCS Unit Hydrograph, the runoff that was produced from the loss calculation is converted into an outflow hydrograph. The general hydrograph takes the time lag from each subbasin and scales the outflow for use in the unit hydrograph [55]. Using the standard graph type, the lag time is defined as the time between the centroid of precipitation and the peak flow of the hydrograph. This time lag is calculated in GIS using HEC-GeoHMS and uses the curve number method from the 2010 NRCS Handbook. The equation is as follows.

$$Lag = 0.6\frac{(L^{0.8}*(S+25.4)^{0.7})}{(4238*Y^{0.5})}(\text{Hour}) \quad (3.3)$$

Where L is longest flow path, Y is basin slope (%) and S is maximum possible retention.

The SCS Unit Hydrograph then transforms the lag time into a ratio to unit hydrograph peak discharge described below.

$$U_p = \frac{\Delta t}{2} + Lag \quad (3.4)$$

Where Δt is model time step.

- **Baseflow Parameters**

Once the loss method splits the rainfall into infiltration and runoff, the water that infiltrates into the soil is not represented in the model. The baseflow methods try to simulate the response of the infiltrated water back into the stream network. There are five methods of baseflow open to use in HMS. In order to match the hydrograph shape with the gage data baseflow was taken into account. This was modeled in HMS using the recession method. The recession method uses a single exponential equation that relates what baseflow will start at and at what rate it will decay. Baseflow also requires a value that will indicate when baseflow resumes the full flow in an element; this was done using the ratio to peak method. A ratio to peak of 1% was chosen for modeling in this project. The baseflow equation is shown below.

$$Q_t = Q_o k^t \quad (3.5)$$

Where Q_t is baseflow, $Q_o$is initial discharge, k is recession constant and t is time.

- **Routing Parameters**

Once the all of the basin parameters converting the rainfall into runoff have been calculated, the hydrographs need to be moved down stream through the stream network. This is done through routing methods in HEC-HMS. There are six routing methods built into HMS. Since there are no gages or historical data available to calibrate to, the best routing method available for use is the modified puls. Modified puls use a storage discharge relationship that defines how water will be attenuated through the reach using conservation of mass [55].

$$\left(\frac{S_t}{\Delta_t} + \frac{Q_t}{2}\right) = \left(\frac{I_{t-1}+I_t}{2}\right) + \left(\frac{S_{t-1}}{\Delta t} - \frac{Q_{t-1}}{2}\right) \quad (3.6)$$

Where $S_{t,\ t-1}$ isstorage at time t and t-1, $I_{t,\ t-1}$ isinflow discharge at times t and t-1, $Q_{t,t-1}$is outflow discharge at times t and t-1 and Δt is simulation time step.

- **Meteorological Parameters**

Once the basin model is set up and all of the characteristics of how the water is moved over the surface are filled, the description of how water is applied to that surface needs to be described. There are three options on how much water is generated and when it is applied. These options are precipitation and evapotranspiration. Since all of the modeling in this investigation is event based, only precipitation is considered in the meteorological model.

CHAPTER 4

SDSM AND HYDROLOGICAL MODEL DEVELOPMENT

4.1 SDSM Building

4.1.1 Predictor and Predictand File

Two types of daily predictors data required for this study were (a) the 26 predictors of National center of environmental prediction (NCEP) for the perioed of 1961-1900 and (b) the 26 predictors of HadCM3, for A2 and B2 scenarios, for the period of 1961-2099. They were downloaded from Canadian Institute for climate studies website for model output of HadCM3. (htt://www.cics.uvic.ca/scenarios/sdsm/select.cgi) and the types of predictor variables are presented in Table 4.1.

The predictants (temperature extremes and precipitation) for a specific Kigali airport station were prepared in the same format as predictor with single column text file to use as input for statistical downscaling model.

Table4.1Types of predictor variables

N°	Predictor description	Predictor description	N°	Predictor variable	Predictor description
1	mslpaf	Mean sea level pressure	14	p5zhaf	500 hpa divergence
2	p_faf	Surface air flow strength	15	p8-faf	850 hpa airflow strength
3	p_uaf	Surface zonal velocity	16	p8-uaf	850 hpa zonal velocity
4	p_vaf	Surface meridional velocity	17	p8-vaf	850 hpa meridional velocity
5	p_zaf	Surface velocity	18	p8-zaf	850 hpa vorticity
6	p_thaf	Surface wind direction	19	p850af	850 hpa geopotential height
7	p_zhaf	Surface divergence	20	p8thaf	850 hpa wind direction
8	p5_faf	500 hpa airflow strength	21	p8zhaf	850 hpa divergence
9	p5_uaf	500 hpa zonal velocity	22	p500af	Relative humidity at 500 hpa
10	p5_vaf	500 meridional velocity	23	p850af	Relative humidity at 850 hpa
11	p5_zaf	500 hpa vorticity	24	rhumaf	Near surface relative humidity
12	p500af	500 hpa geopotential height	25	shumaf	Surface specific humidity
13	p5thaf	500 hpa wind direction	26	tempaf	Mean temperature at 2 m

4.1.2 Setting of the SDSM Model

Year Length: The normal calendar uses 366 allows 29 days in February every fourth year. The alternatives allow for different numbers of days in GCM data. Whereas HadCM2 and HadCM3 have model years consisting of 360 days.

Event Threshold: was set to zero for temperature and 0.1mm/day for precipitation to treat trace rain days as dry days.

Model Transformation: Specifies the transformation applied to the predictand in conditional models. The default (None) is used whenever the predictand which is normally distributed (as is often the case for daily temperature). The alternatives (Fourth root, Natural log and Inverse Normal) are used whenever data are skewed (as in the case of daily precipitation).for this case Fourth root was used for precipitation.

Variance Inflation: Controls the magnitude of variance inflation in downscaled daily weather variables. This data can be adjusted during the calibration period to force the model replicate the observed data. The default value of 12 produces approximately normal variance inflation prior to any transformation and it is applied to temperature. For precipitation this parameter can adjusted during the calibration period and was set to 18.

Bias Correction: Compensates for any tendency to over or underestimate the mean of conditional processes by the downscaling model (e.g., mean daily rainfall totals). The default value is 1.0, indicating no bias correction and was used for temperature, 0.92 was used for precipitation to match the mean of the conditional process.

4.1.3 The downscaling Procedure

The downscaling Procedure at the station located near the flooded area in Nyabugogo River is described step by step in the following section:

Step 1: the input file was prepared; the daily precipitation data sorted based on time in two columns; first the date and second the precipitation amount (the monthly data are interpolated to develop the daily data needed as input to SDSM).

Step 2: then the process of quality control is run to test the format of prepared input file. This step is important for Handling of missing and imperfect data which is necessary for most practical situations. The quantity control information in this study shows that there are 11688 data values corresponding to daily min temperature from 1971 to 2002 with no missing data. The data range from 10.5°C to 20°C and have a mean of 15.29°C for Minimum temperature.

Step 3: After checking the quality of the input variables in SDSM, the large-scale relevant predictors from the NCEP re-analysis set of variables were selected, following the suggestions of

Khan et al.(2006a), Wilby and Dawson (2004), based on the monthly percentage of variance explaining the locally observed precipitation and temperature, physical sensitivity between predictors and local precipitation and temperature, and the predictor's ability to carry climate change information and their accurate representation by the climate models[56,][57].

Identifying empirical relationships between gridded predictors and single site predictands is essential in this step. SDSM performs three supporting tasks: seasonal correlation analysis, partial correlation analysis, and scatter plots. In this step, the 26 available weather variables are screened to find the variables that could be used as precipitation predictand. For Kigali airport station, data start from 1/01/1971 and end at 31/12/2001. The analysis is done in annual period under conditional process. At the end of this analysis, the results of explained variance and correlation matrix between precipitation and selected weather variable are given. For this study, selecting the potential predictor for temperature/ precipitation, there chosen predictors which have high explained variance among the 26 predictors are presented in table 4.2.

Table4.2Chosen predictors for each variable

Variables	**Predictors Abbreviation**	**Predictor name**
Maximum Temperature	p500af	Relative humidity at 500 hpa
	tempaf	Mean temperature at 2 m
	mslpaf	Mean sea level pressure
Minimum Temperature	p500af	Relative humidity at 500 hpa
	p850af	850 hpa geopotential height
Precipitation	p500af	500 hpa geopotential height
	p850af	Relative humidity at 850 hpa

Step 4: The model is calibrated using the observed data and the selected signals. At the end of this step, the R-squared and standard error are reported. In this step the model structure is set to unconditional for temperature and conditional for precipitation. The model type determines whether individual downscaling models will be calibrated for each calendar months,

climatological season or entire year. The model is structured as monthly model for both precipitation and temperature downscaling, in which case, twelve regression equations are derived for twelve months using different regression parameters for each month equation. Finally the data period should be set in order to specify the start and end data of the analysis. The calibration was done for a 30 years of period (1961-1990).

Step 5: Weather generator: in this step, data for considered period and selected climate change scenario (here HadCM3A2) are developed. The start date of data generating and the number choose production of one or more ensembles; here one ensemble is selected.

Step 6: Scenario Generator operation produces ensembles of synthetic daily weather series given the regression weight produced during the calibration process and the daily atmospheric predictor supplied by a GCM (either under present or future greenhouse gas forcing). Twenty ensembles of synthetic daily time series were produced for two emission scenarios (HadCM3A2a and HadCM3B2a) for a period of 139 years (1961-2099). Finally the mean of twenty ensembles for the specified period is produced for the temperature and precipitation. Precipitation downscaling is necessarily more complex than temperature because daily precipitation amounts at individual sites are relatively poorly resolved by the regional-scale predictors, and precipitation is a conditional process.

Step 7: In this step, the statistical analysis of the observed and developed data through tables are produced.

4.1.4 Downscaling the GCM for baseline period

For this study GCM was downscaled for the baseline period for two emission scenarios (A2 and B2) and the statistical properties (Mean and Variance) of the downscaled data was compared with observed data. The IPCC recommends 1961-1990 as climatological baseline period in impact assessment. Therefore this period was also used as baseline period for this study. The downscaling experiment was conducted for minimum temperature, maximum temperature and rainfall based on the data from Kigali airport station.

- **Minimum temperature**

The monthly minimum temperature downscaled for A2 and B2 scenario in the baseline period is shown in Figure 4.1.

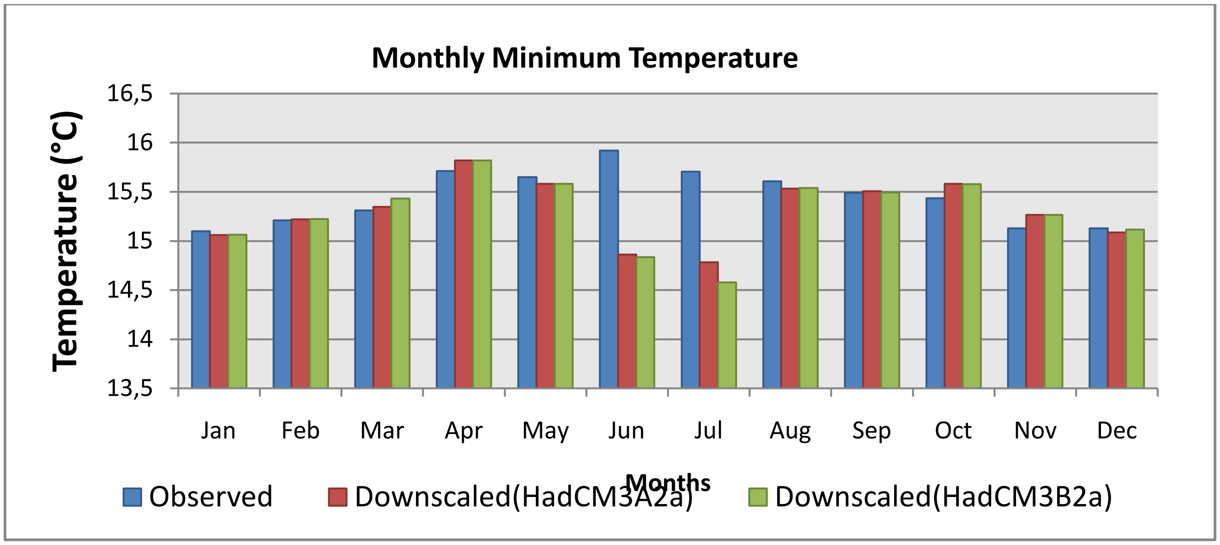

Figure4.1 Observed and downscaled monthly mean minimum temperature for baseline(1961-1990)

The result of minimum temperature downscaling shows the satisfaction agreement between observed and simulated minimum Temperature. Irregularity is shown in June and July month as the Figure 4.1 shows. The absolute error of the model in downscaling the monthly minimum temperature is very close for all HadCM3A2a and HadCM3B2a models(Figure 4.2). It becomes less than 0.2°C from January to May and becomes bigger in June and July where it reach 1.2°C but drops to around 0°C in August and September and near to 0.2 in last months of the year. The model error in each month is less than the projected temperature change in the future.

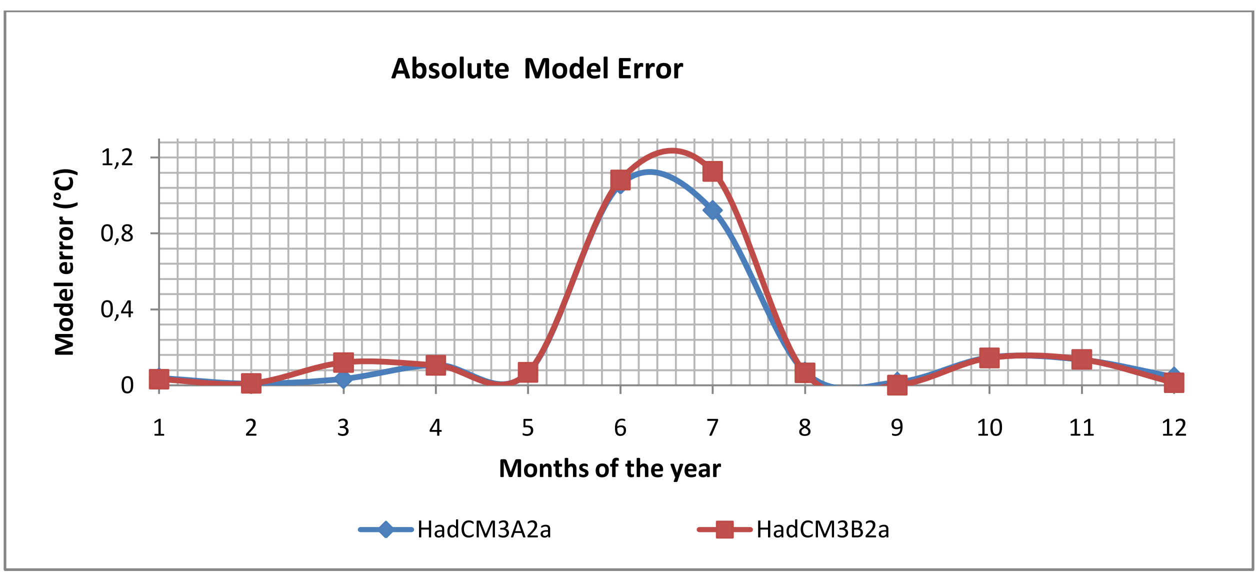

Figure4.2 Absolute model error in estimate of monthly minimum temperature

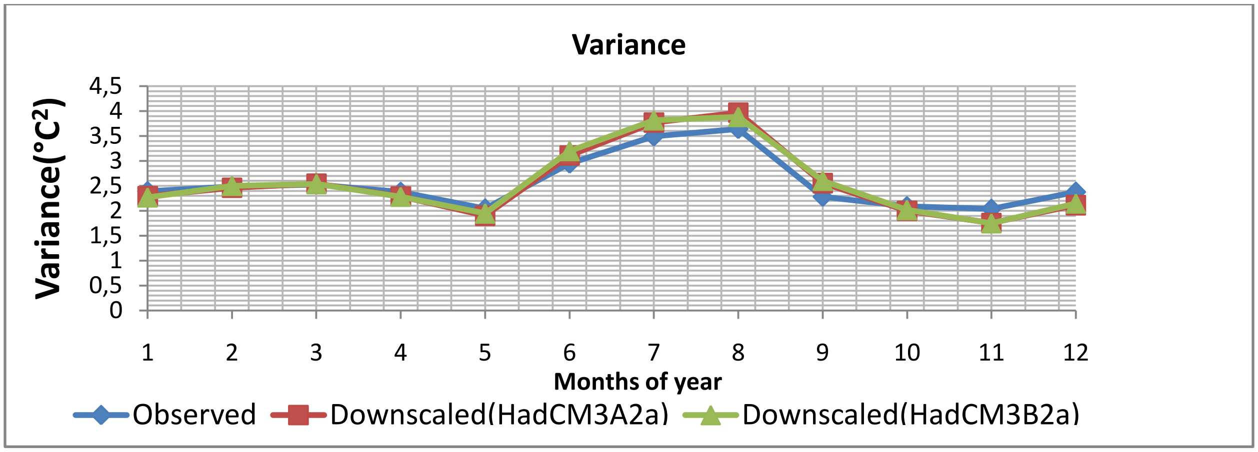

Figure4.3 Variance of observed and downscaled monthly minimum temperature

The variance indicates how far the values are identical(Figure 4.3). The small variance indicates the data tends to be very close to the mean or expected value and hence to each other while high variance indicates that the data points are very spread out around the mean and from each other. For our study in baseline period (1961-1990) the downscaled values show the close variance to the observed values for every month.

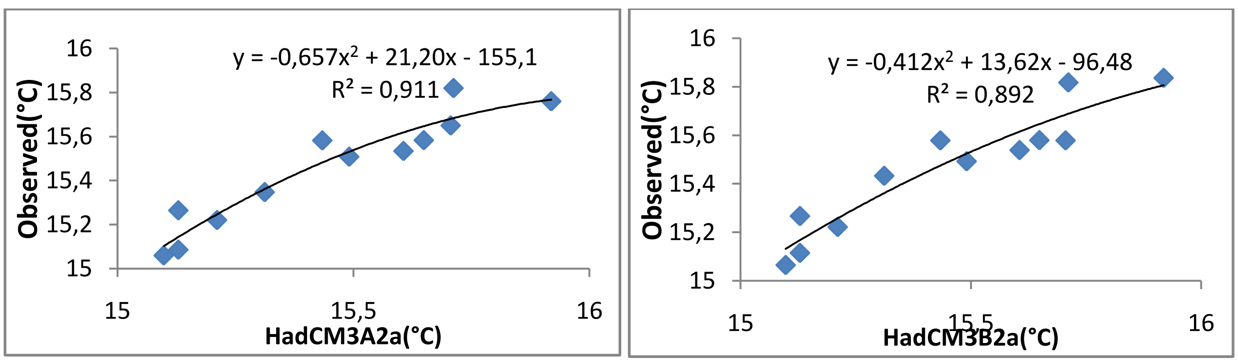

Figure 4.4 Correlation between observed and downscaled monthly minimum temperature for A2 and B2 Emission scenarios

The figure 4.4 shows high correlation between monthly minimum temperature of the Nyabugogo catchment and the downscaled values supplied by using GCMS model with correlation coefficient R of 0.9116 and 0.8924 respectively for A2 and B2 Emissions.

- **Maximum Temperature**

The monthly maximum temperature downscaled for A2 and B2 scenario in baseline periods is shown in Figure 4.5.

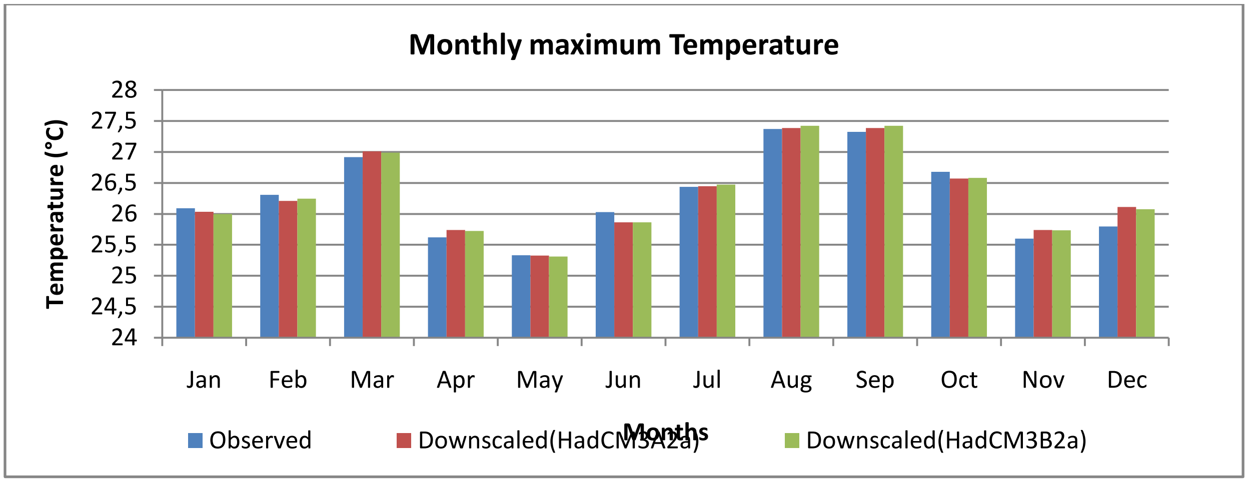

Figure4.5Observed and downscaled monthly mean maximum temperature for baseline period (1961-1990)

The result of downscaling maximum temperature indicates that there is satisfaction in agreement between observed and simulated maximum temperature.

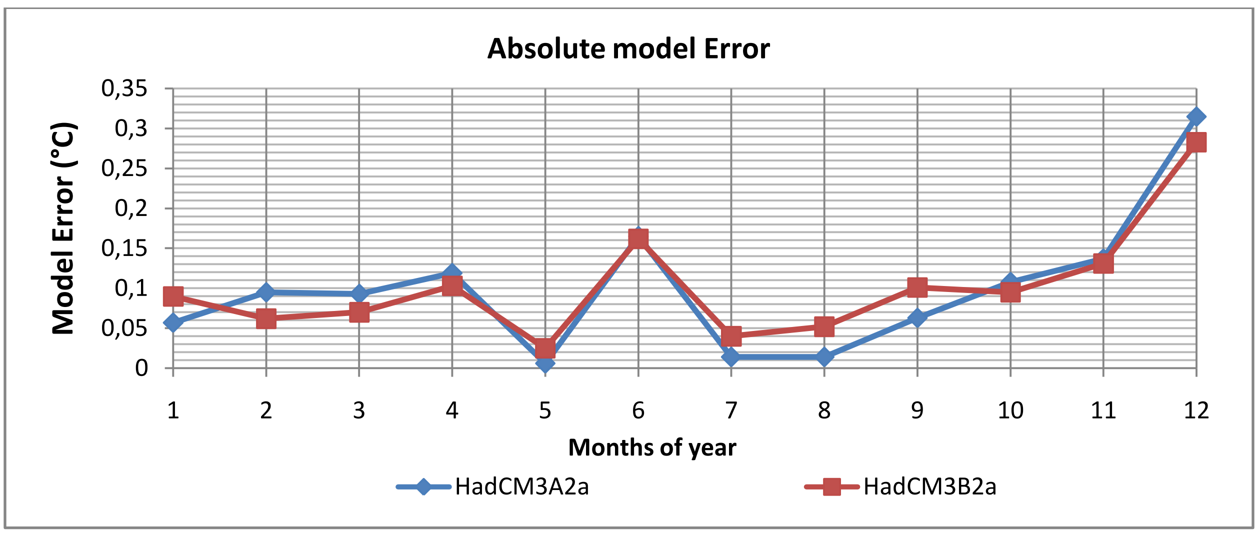

Figure4.6 Absolute model error in estimate of monthly maximum temperature

Absolute model error in downscaling of the mean maximum temperature(Figure4.6) is less than 0.35°C for the all months of the year and the maximum error occurs in December about 0.3 °C, and for all models HadCM3A2a and HadCM3B2a the model errors are quite close each other for all months.

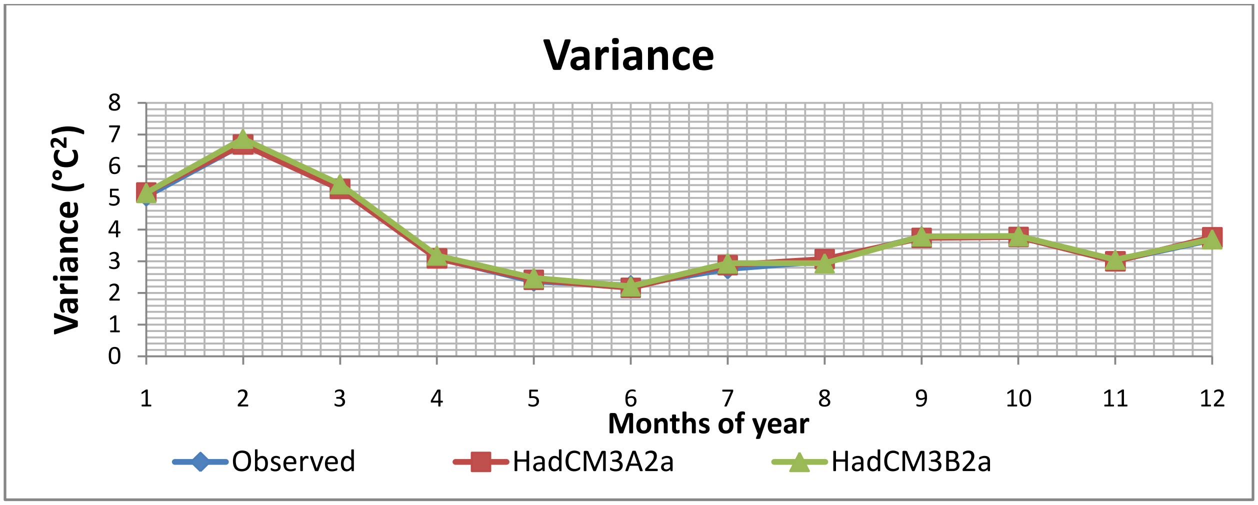

Figure4.7Variance of observed and downscaled monthly maximum temperature

The variability of observed monthly maximum temperature is well preserved in the downscaled maximum temperature for all months of year as it is shown in Figure 4.6.

The figure shows high correlation between monthly maximum temperature of the Nyabugogo catchment and the downscaled values supplied by using GCMS model with correlation coefficient R of 0.97481 and 0.9663 respectively for A2 and B2 Emissions.

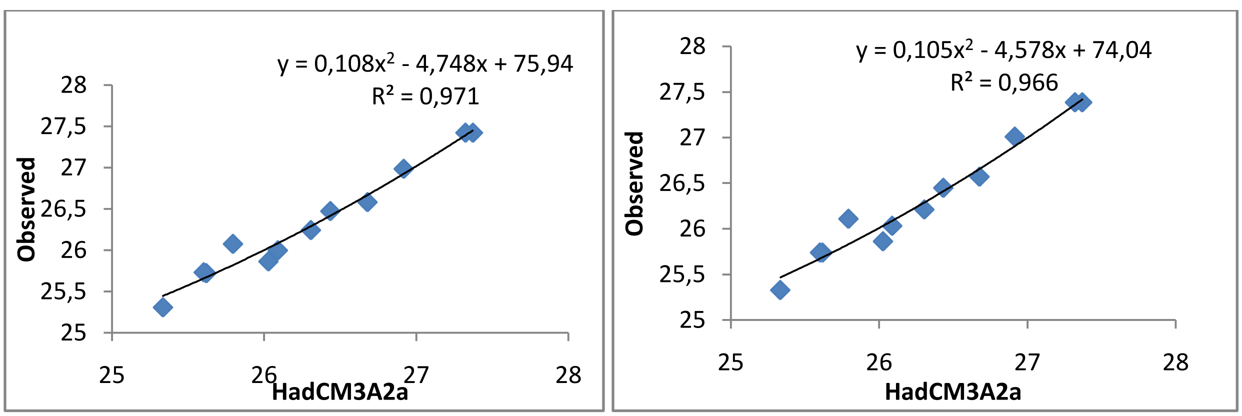

Figure 4.8 Correlation between observed and downscaled monthly maximum temperature for A2 and B2 Emission scenarios.

- **Rainfall**

The monthly rainfall downscaled for baseline period (1961-1990) is shown in Figure 4.7. The SDSM model performs reasonably the estimation of the mean monthly rainfall in many months but there is a relatively large model error in the month of April.

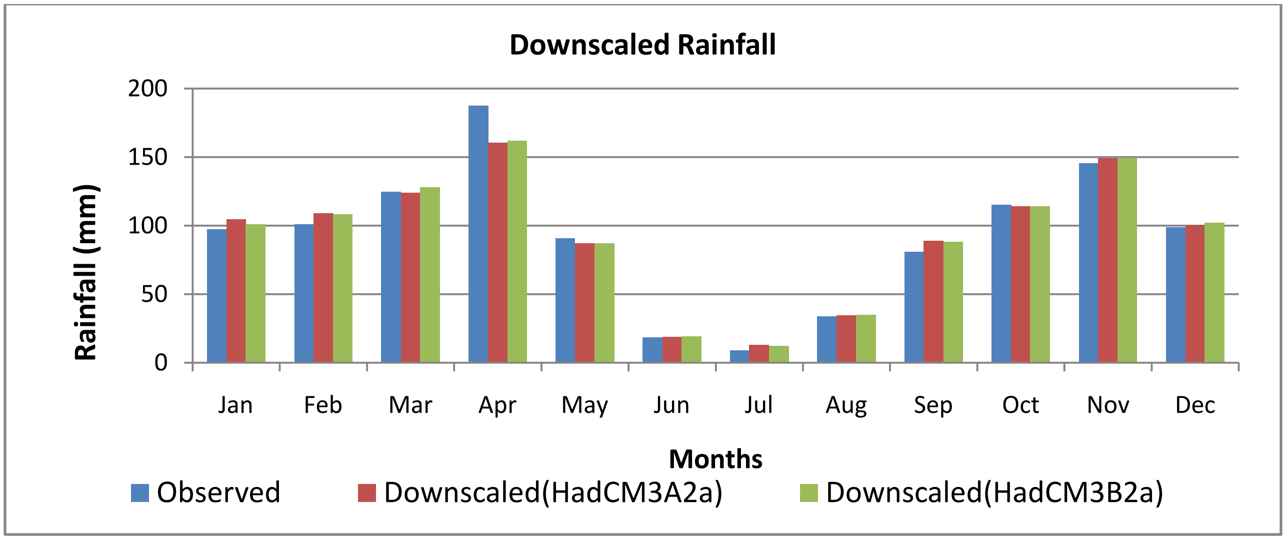

Figure4.9Mean monthly observed and downscaled rainfall for baseline period (1960-1990)

The SDSM model performs reasonably the estimation of the mean monthly rainfall in many months but there is a relatively large model error in the month of April as it is presented in Figure4.8. The total mean monthly rainfall in April is 187.589 mm whereas the downscaled value in this month is 161 mm.

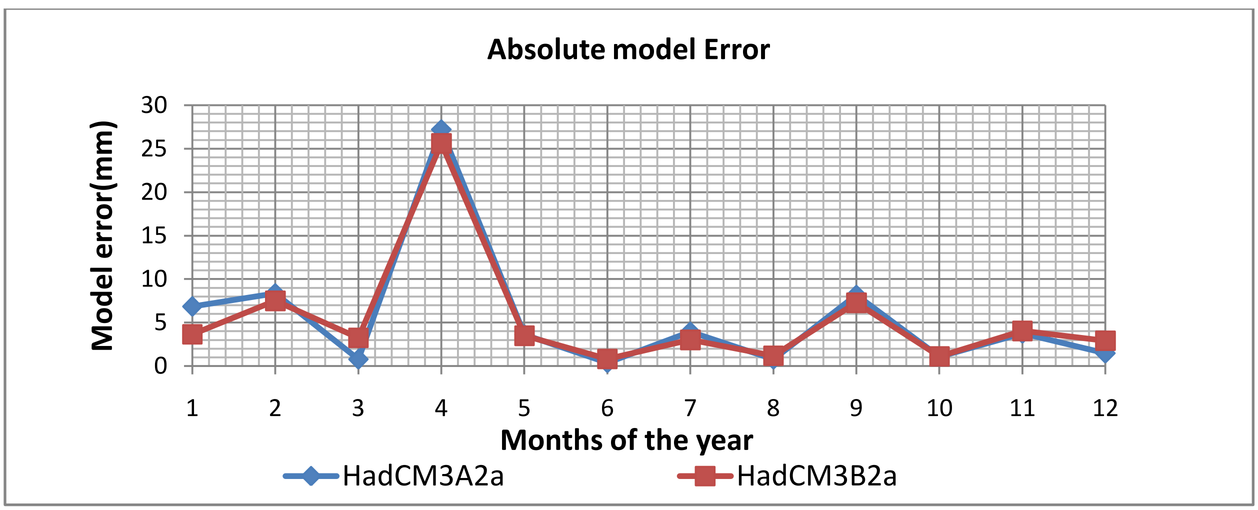

Figure4.10Absolute model error in estimating of the mean daily rainfall

The result, however, can be taken as satisfactory given the fact that precipitation downscaling is necessary more problematic than temperature, because daily precipitation amounts at individual sites, are relatively poorly resolved by regional-scale predictors.The figure 4.9 shows the variance between observed and downscaled rainfall.

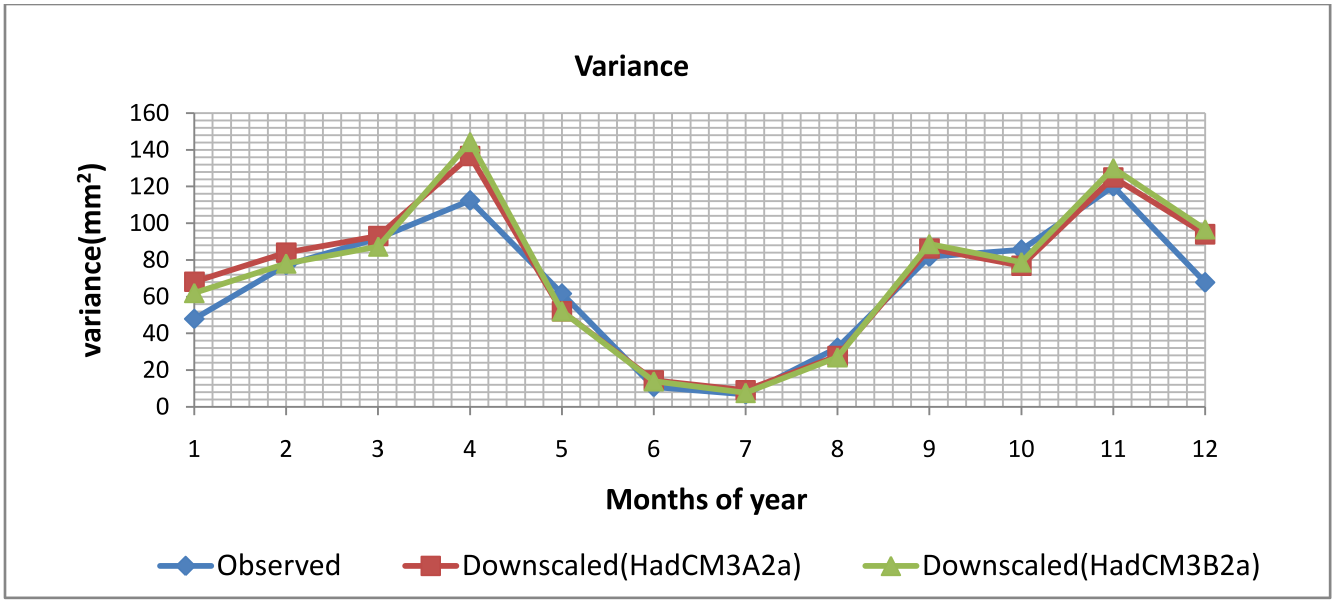

Figure4.11 The variance of observed and downscaled monthly mean rainfall

The figure shows high correlation between monthly rainfall of the Nyabugogo catchment and the downscaled rainfall supplied by using GCMS model with correlation coefficient R of 0.9161 and 0.9126 respectively for A2 and B2 Emissions.

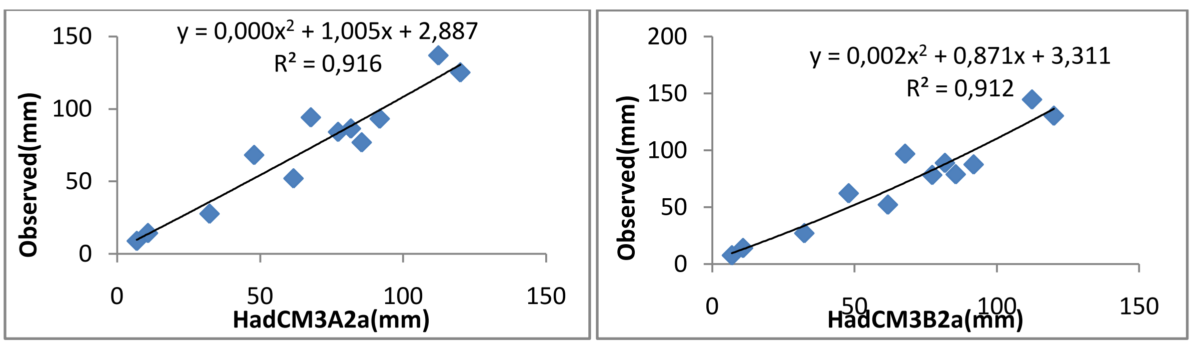

Figure 4.12 Correlation between observed and downscaled monthly rainfall temperature for A2 and B2 Emission scenarios.

4.2 HEC-HMS model building

HEC-HMS modeling is dependent on being able to supply all of the values needed to fill all the parameters inside of each component.To manipulate data sets, to create the information needed and to input into HEC-HMS, ArcGIS was used for that purpose, ArcGIS is able to create the import files that are then used in HEC-HMS.

4.2.1Arc Hydro:

4.2.1.1 DEM Reconditioning

When the new stream centerlines are created they might not line up with the lowest points in the DEM, so as a result water will not flow into the exact location of the stream. To correct this problem the DEM reconditioning tool inside of ArcHydro was used to lower the elevation of the areas that fall along the stream centerline. To make sure that the stream is the lowest point in the DEM we set the raw DEM and stream centerlines as inputs to the reconditioning pop-up window.The number of cells were also settedto be used as a buffer to create a smooth transition to the new low point, and we setted how much of a reduction in the DEM will be used. Once all of the inputs are set and the tool is run a new DEM raster was created with the default name of AgreeDEM.

4.2.1.2 Fill Sinks

After creating the reconditioned DEM there still might be areas where water will flow into local ponds instead of moving across the land into streams. Using the Fill Sinks tool, the DEM will be altered to ensure that water will flow into the stream network. The tool will take these "sinks" in the DEM and level them out with the highest elevation of the pond. In order to run all of the processes in HEC-geoHMS all sinks must be filled. For this study the resulting output was another raster file with the default name of Fil as it is presented in Figure4.10.

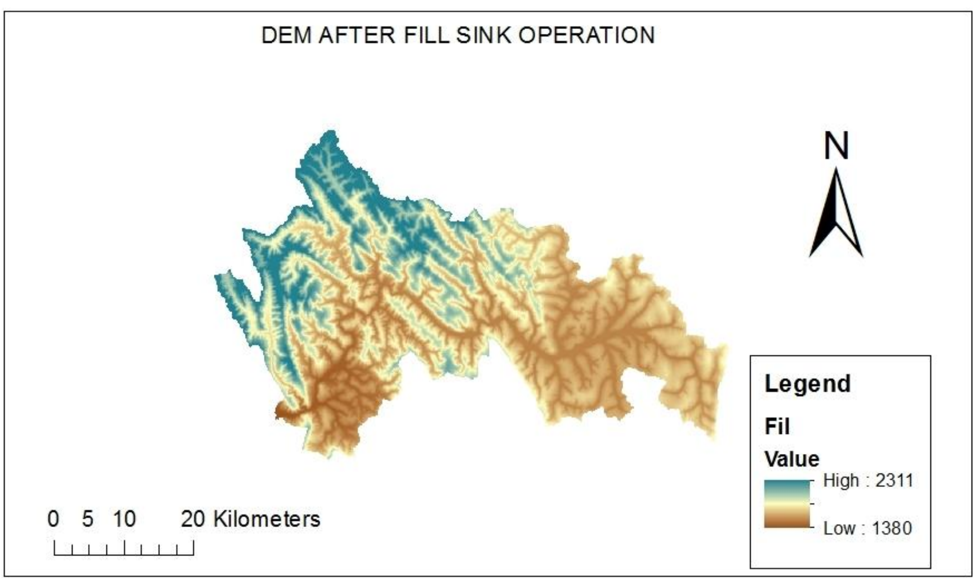

Figure4.43Thefill sinks operation

4.2.1.3 Flow Direction

Now that there is a final DEM that ensures water to flow from the land to the stream network it is time to define how the water gets to the stream network. The flow direction tool will define which direction water will flow from cell to cell using an eight point compass. For each cell the tool will find which neighboring cell has the greatest elevation change that is adjacent to the main cell [58]. Once it finds the steepest elevation it assigns the direction that water will travel away from that cell. Once this process has run the output is a new grid that is called Fdr(Figure4.11).

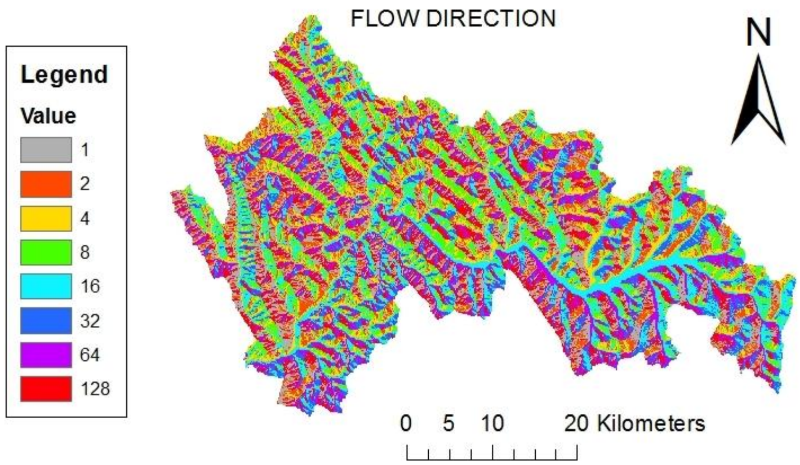

Figure4.14 Flow direction map

4.2.1.4 Flow Accumulation Grid.

Using the flow direction grid, ArcHydro can create a new layer that sums the total number of cells that drain into a given cell(Figure4.12). The Fdr grid is used to follow how water moves through the watershed at a given point. Since the Fdr grid is based on the reconditioned DEM as the program moves from the headwaters to the outlet, the places with the most cells that contribute to a point will form a rough stream network. The new layer that is created has the default name of Fac.

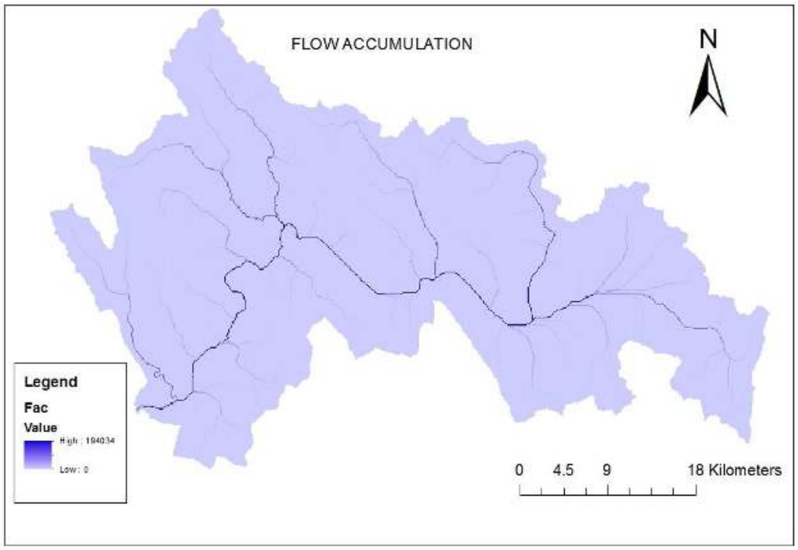

Figure4.55 Flow accumulation

4.2.1.5 Stream Definition

After generating the Fac grid the next step in the generation of the layers needed for HMS is the stream definition layer. This tool will take the Fac grid and a user defined 25 thresholds to create the stream network. The Figure 4.13 shows the nyabugogo stream definition.

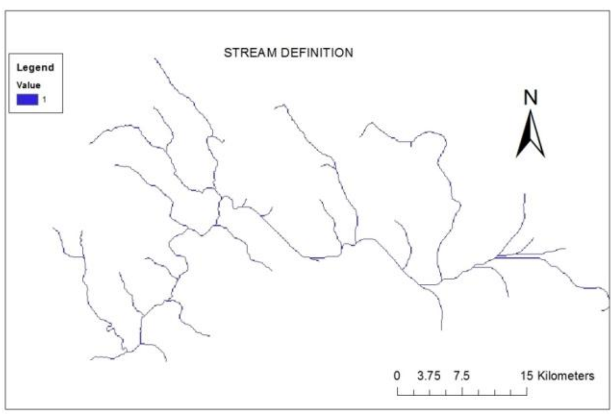

Figure4.66 Stream definition

4.2.1.6 Stream Segmentation

Once the stream network is generated the network is split into segments(Figure 4.14). These segments are sections of the stream that connect two junctions, a junction and an outlet, or a junction and the drainage divide [58]. These segments form the reaches that are used in HMS. In order to run this tool the stream definition layer and the flow direction grid are input, and will output a new shapefile called StrLnk.

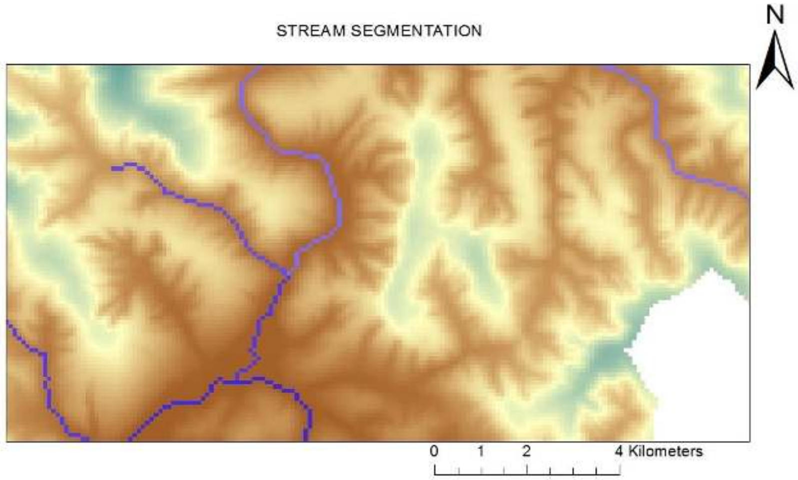

Figure4.77Stream segmentation

4.2.1.7 Catchment Grid and Polygon

The catchment grid is created by delineating a subbasin for each stream segment(Figure 4.15). The inputs needed to run this process are the stream segmentation and the flow direction layers. The output is a new layer called Cat. After creating the catchment grid, ArcHydro can create a polygon layer of the subbasins. This step is called Catchment Polygon Processing. This process takes the Cat layer that already exists and creates a vector layer of all of the subbasins. The catchment grid is input and after the tool runs the catchment polygon is output.

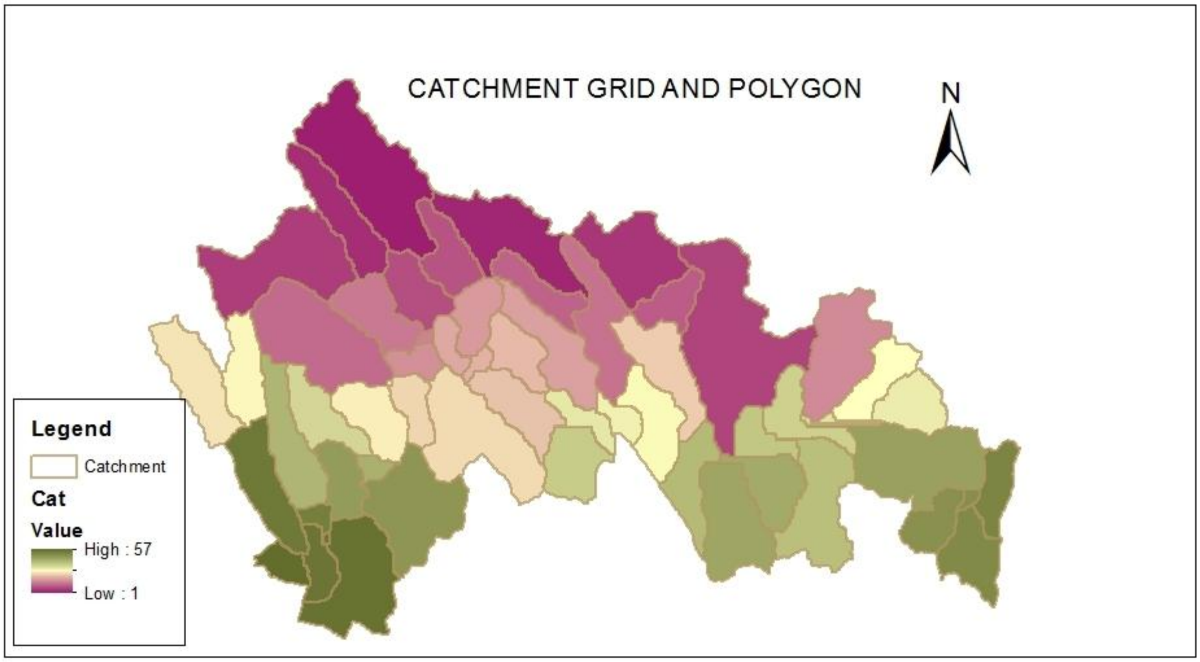

Figure4.88 Catchment grid and polygons

4.2.1.8 Drainage Line Processing

Once the subbasin layer has been turned into a vector the same step needs to be taken with the stream network(Figure 4.16). This step is done with the drainage line processing tool. The inputs for this step are the stream link grid and the flow direction grid. The output layer that is created has the default name of Drainage Line.

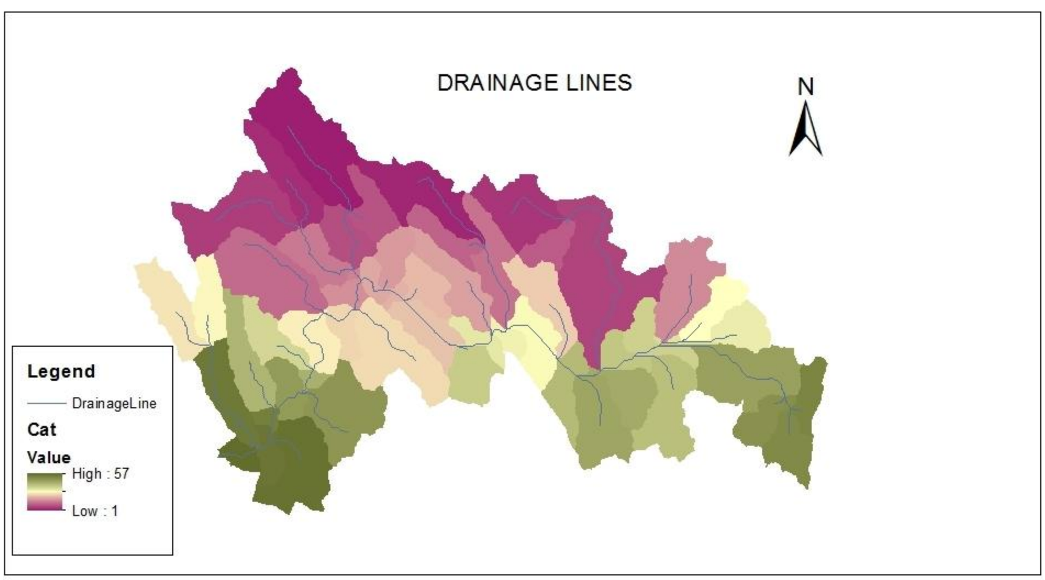

Figure4.99Drainage lines in catchment

4.2.1.9 Watershed Aggregation

This step takes the Catchment and Drainage Line layers and aggregates the upstream subbasins at every stream confluence. This step is taken to improve performance when interactively delineating sub-basins in HEC-geoHMS as well as to enhance data extraction. This outputs a new layer called Adjoint Catchment.

4.2.1.10 Watershed Slope

The slope tool will take the raw DEM and create a new raster that contains the slopes over the entire watershed. The slope is reported in units of percent(Figure 4.17). This calculation is done by extracting the vertical units from the defined projection of the raw DEM and then applying the correct factor of the elevations to create a slope.

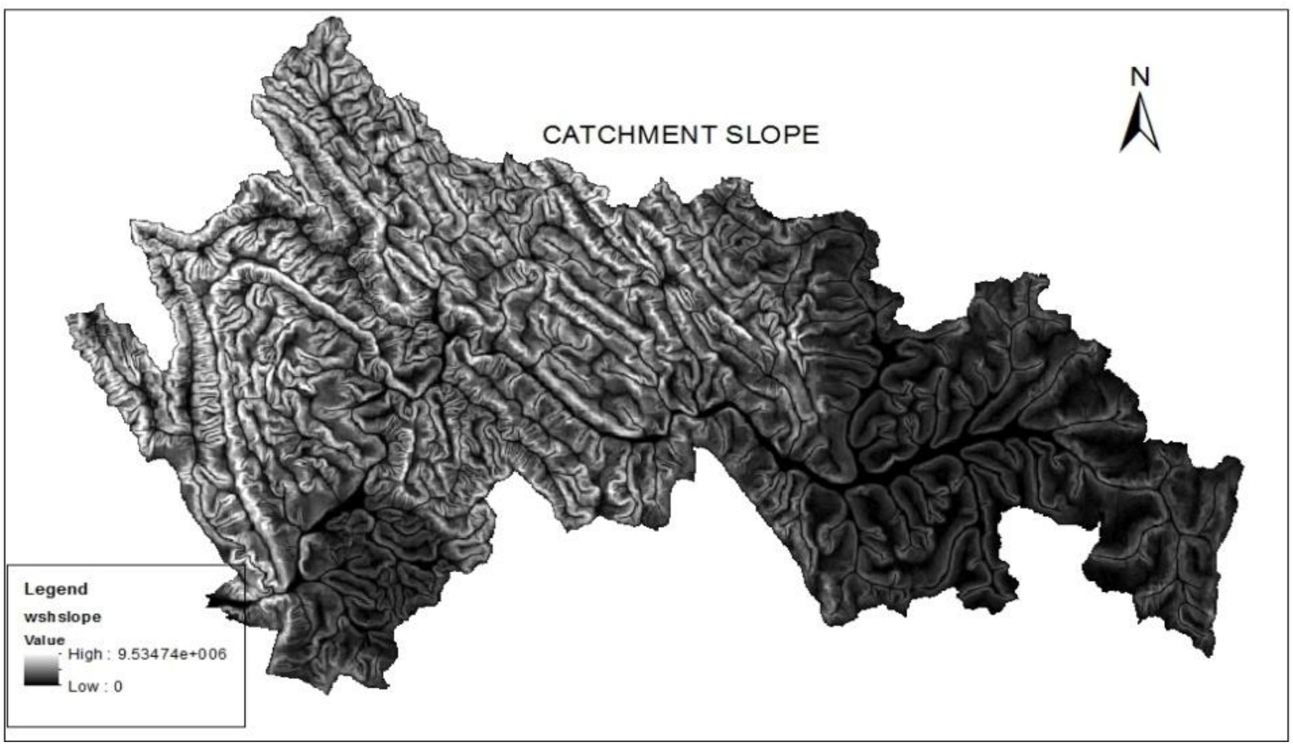

Figure4.20 Watershed slope

4.2.1.11 Curve Number Grid

The curve number is a hydrologic parameter used to describe the storm water runoff potential for drainage area. It is an index developed by the Soil Conservation Service (SCS), now called the Natural Resource Conservation Service (NRCS). SCS curve number grid was used in HEC-

GeoHms model to extract the curve number for Nyabugogo watershed. The first step was done by gathering the soil data that will be used for the creation of the curve number grid. The data were collected from the Rwanda ministry of natural resources.The soil and land use data were very useful for creating curve number for Nyabugogo watershed by using HEC-GeoHMS (in ArcGIS 10.2 version).the Figure 4.18 show the map of Nyabugogo curve number produced in ArchGIS 10.2.

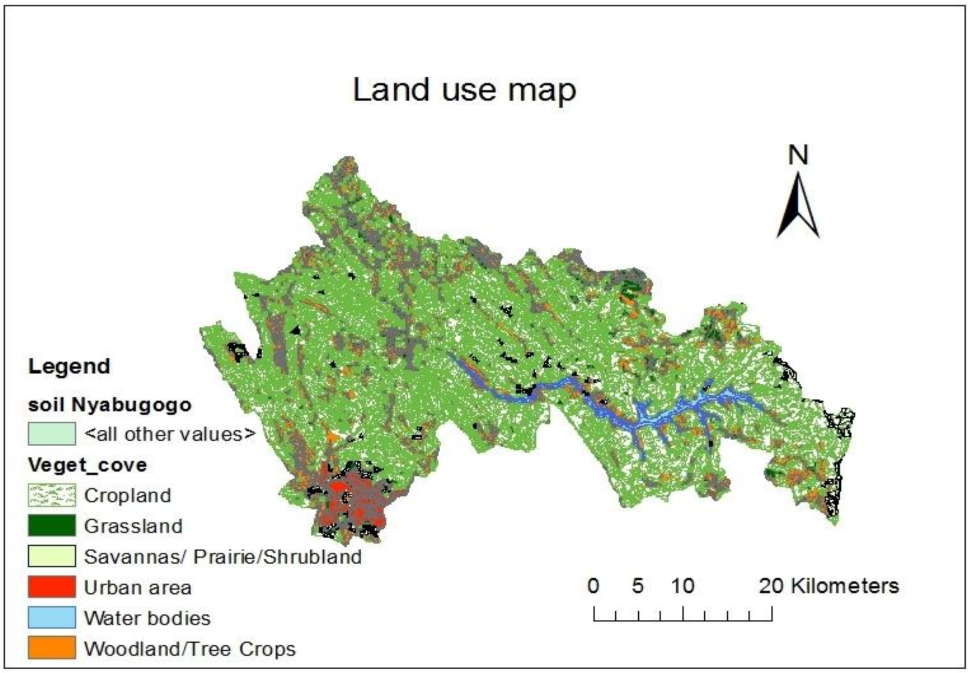

Figure 4.21 Land Use Map of Nyabugogo Watershed Used for Creation of CN

Upon startup, the user is asked to define the path and name for all required shapefiles and look-up tables. The Curve Number Generator requires three shapefiles: (1) the drainage basin boundaries for which curve number(s) will be calculated, (2) the land use map, and (3) the soil type map. The Curve Number Generator also requires user to define look-up table (table) containing the soil group table that provides the conversion from soil types to hydrologic soil groups, and the Curve Number table that defines the land use-soil group categories and curve numbers. To use the Generate CN Grid tool we created a polygon layer that merges both land use and soil type data. Before merging them, the attribute table for both layers must contain specific column headings: PctA, PctB, PctC, PctD which contain the percentage of each hydrologic soil group (A, B, C and D) in the soil layer polygons.

The Generate CN Grid tool was used after the merged land use and soil type layers and curve number lookup table(Table4.3) that had been created and the result is the map shown in figure 4.19.

Table4.3 CNLookup

OBJECTID	LUValue	A	B	C	D
1	1	67	77	83	87
2	2	67	77	83	87
3	3	67	77	83	87
4	4	30	55	70	77
5	5	43	65	76	82
6	6	43	65	76	82
7	7	90	90	90	90
8	8	77	85	90	92
9	9	100	100	100	100

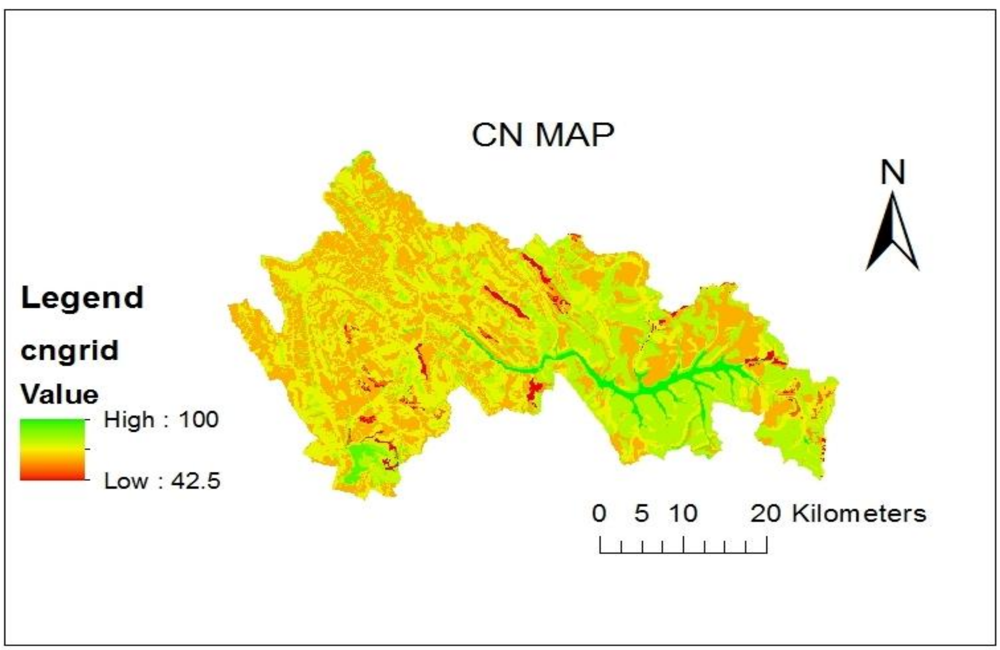

Figure4.22 Curve number generated from HEC-GeoHms

4.2.2 HEC-GeoHMS

Using the tools in the HEC-GeoHMS Project View and HEC-GeoHMS Main View toolbars, for this study, GIS was able to calculate and populate the necessary fields to create the export files needed to create the HECHMS model. For this study the following menu have been used:

4.2.2.1 Project Setup

This menu is responsible for extracting data that will be used to develop the necessary information to create an HEC-HMS project. By selecting start a new project from the Project View setup will open a new window in which the user can accept the defaults of the Project Area and Project Points layers. Project area will show the upstream area of the outlet point and the project point will show the location of the outlet. This tool was used for this project to define the outlet of the catchment. Here the user needs to name to project, give a description, choose an extraction method, and to set a location to where all new data will be stored. For this example the extraction method that was selected is original stream definition, this option uses the same stream segments and subbasins that were delineated using the terrain preprocessing tools.

4.2.2.2 Basin Processing

After the terrain processing is completed and a new project has been created, the basin processing menu was used to revise the sub-basin delineation. In this menu users can manipulate the number of subbasins by using the merge and subdivide basins tools.

4.2.2.3 Basin Characteristics

GeoHMS has the ability to calculate many of the characteristics for the streams and subbasins using the topographic information provided by the layers created during the terrain pre-processing steps. These characteristics are then stored in the attribute tables for the river and subbasin layers which can be exported for use with a spreadsheet and other programs. The river slope is calculated by the elevation at the upstream and downstream ends of each segment and then divided by the length of the segment to compute the slope. Basin slope is calculated by inputting the slope field that was generated using the slope function in ArcHydro and the subbasin layer. The slope is generated by averaging the slope values over each subbasin. Calculating the longest flow path will create a new layer and fill in a number of physical characteristics. For each flow path the length, up and down stream elevation and the slope between the points will be calculated. The longest flow path is chosen as the flow path that has the greatest length from a subbasin boundary to the subbasin outlet. The basin centroid tool creates a new layer that will contain the centroid of each subbasin. There are four ways to calculate this location, using center of gravity, longest flow path, fifty percent area, and user specified. For this application the center of gravity method was chosen.

4.2.2.4 Hydrologic Parameters

GeoHMS has the ability to calculate many of the hydrologic parameters used in HMS by way of the data in the soil and land use tables. The first step is to decide what processes are going to be used in the HMS model for the loss, transport, and routing methods. SCS Loss and SCS Unit Hydrograph Transform methods were selected for this study.

4.2.2.5 Building HMS

Once all of the basin and hydrologic characteristics have been calculated and assigned to the subbasin and river shape files, the export files need to be created. The options inside of the HMS menu in GeoHMS will assist in creating these files that will be exported to HEC-HMS. The first step is to convert the ArcMap to HMS units. After selecting the layers to match the requested data the program will ask to select the units that HMS will report in. This study was done using data that was collected in metric units so the SI reporting method was selected. Once the units have been converted, the next step is to run a script that checks for errors in the HMS layers. This script checks for unique names, river containment, centroid containment, river connectivity. Once the check runs, the user can open a file that contains the errors. Any errors that come up in the file can be fixed using GeoHMS or in HMS. When any errors have been fixed the user can then create a schematic of the HMS layout in GIS. This schematic shows the connectivity of the elements that will be exported into HMS.

4.2.2.6 Creation of Design Storms

The frequency storm method is a meteorological method used in meteorological model to produce a frequency storm from given statistical precipitation data.

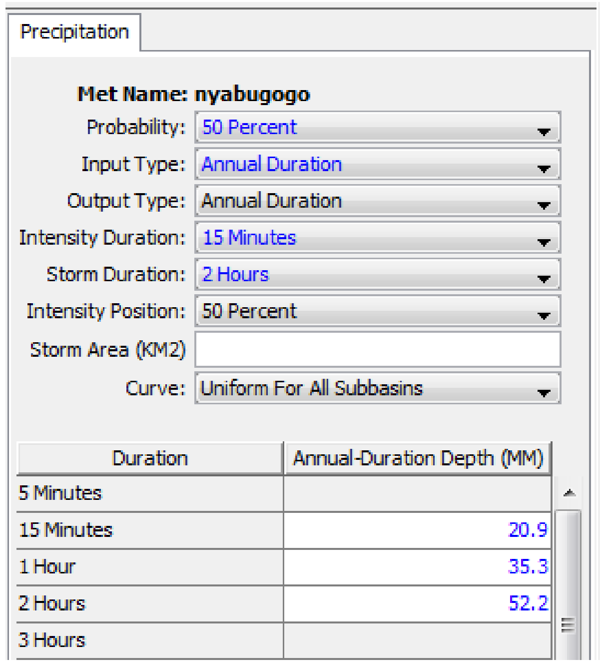

Figure4.23 Input table of the frequency storm method in HEC-HMS

Hydrologic model simulations are performed for the following return periods: 2, 10, 25, 50 and 100 years, corresponding to 50, 10, 4, 2, 1 percent exceedance probabilities, respectively.The main input data for the frequency-based design storm with a specified return period is the total storm duration, the precipitation depths for a number of given durations within the total storm duration, the position of highest intensity within the storm and the storm area(Figure 4.20). The intensity duration defines the duration of the maximum and constant intensity within the storm. Since the shortest duration that was considered in the generation of the IDF curves was 15 min, this duration was chosen as the intensity duration(Table 4.4). The intensity position defines the location of the 15 min interval with the highest intensity within the total storm duration. The storm area was chosen as 3000 km^2 which is about double the size of the analyzed watershed. Based on these input parameters, HEC-HMS uses the alternating block method to compute the design hyetograph that will be applied during the simulation. The Hydrologic Engineering Center (2000) recommends choosing the computational time step (CTS) as close as possible to the intensity duration.

Table4.4 IDF extracted data for frequency storm design (Storm duration and Return Period)

	2 Years	5 Years	10 Years	20 Years	50 years	100 Years
15Min	20.8	24	26.1	28.1	30.7	40.2
30Min	28.2	32.5	35.3	38.1	41.6	54.5
45Min	32.1	37	40.3	43.4	47.4	62.1
1 Hour	32.1	39.9	43.4	46.8	51.1	68.7
2 Hour	50.1	57.8	62.8	67.7	74	97.0
3 Hour	65.6	76.7	83.3	89.8	98.2	129.3

CHAPTER 5

RESULTS AND DISCUSSION

5.1 Climate Model Results

5.1.1 Downscaling the GCM for Future Scenario

The climate scenario for future period was developed from statistical downscaling using the GCM predictor variables for the two emission scenarios for 100 years based on the mean of 20 ensembles and the analysis was done based on three 30 year periods centered on 2020s(2011-2040), 2050s(2041-2070) and 2080s(2071-2099).

- **Minimum Temperature**

The downscaled minimum temperature indicates an increasing trend in all future time horizons for both A2 and B2 scenarios (Figure 5.1 and 5.2). The average annual minimum temperature will be increased by 0.5°C (3.25%) and 0.34°C (2.26%) in 2020s for A2 and B2 respectively. In 2050s the increment will be 0.9°C (6%) and 0.85°C (5.59%) for A2 and B2 scenario respectively. For the 2080s periods the average annual minimum temperature will be increased by 1.4°C (9.3%) and 1.2°C (8.27%) for A2 and B2 scenario respectively. The increment for A2 scenario is greater than B2 scenario because A2 scenario represents a medium high scenario which produces more CO2 concentration than B2 scenario which represents a medium low scenario. The relative change of monthly minimum temperature varies from month to month as shown in Figures for percentage difference.

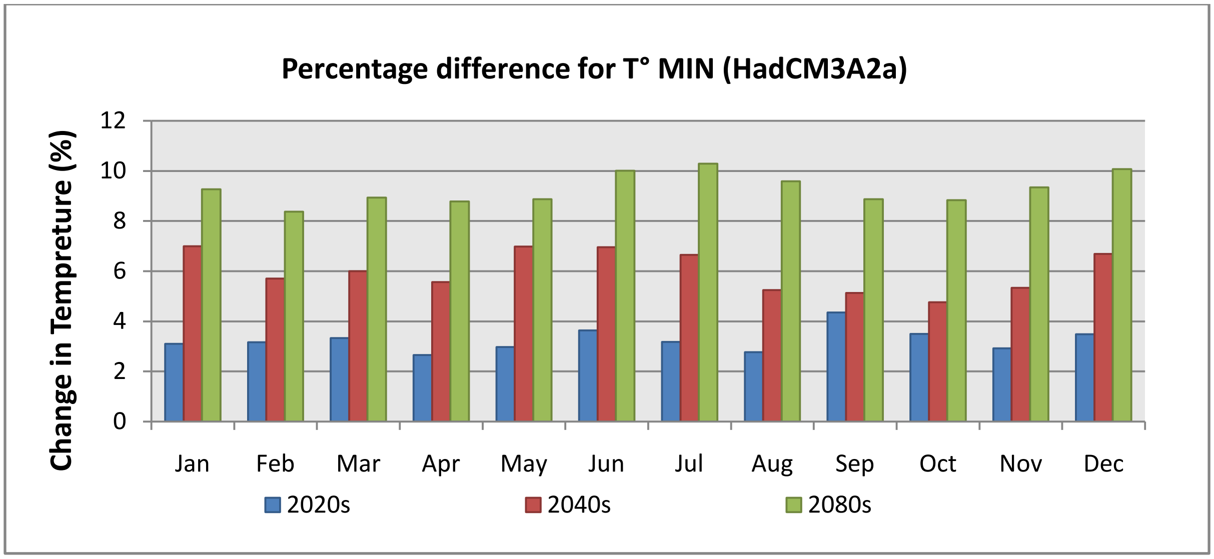

Figure5.1 Change of downscaled monthly minimum temperature from baseline period for HadCM3A2a

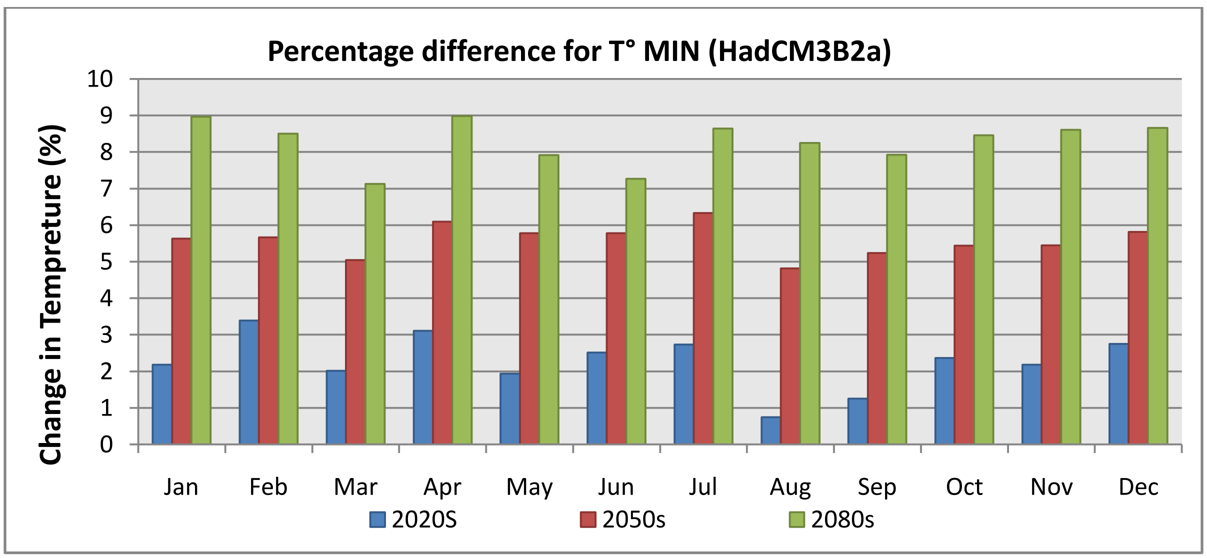

Figure 5.2 Change of Downscaled Monthly Minimum Temperature from Baseline Period for HadCM3B2a

- **Maximum Temperature**

The downscaled maximum temperature scenario also indicates that there will be an increasing trend for both A2 and B2 scenario(Figure 5.3 and 5.4). The projected temperature in 2020s indicates that the maximum temperature will be increased by 1.13 %(0.3°C) and 0.9°C (0.25°C) for A2 and B2 respectively. In 2050s the increment will be 1.6% (0.4°C) and 1.36% (0.36°C) for A2 and B2 respectively. In 2080s the annual maximum temperature will be increased by 2.84%

(0.75°C) and 2.4% (0.63°C) for A2 and B2 respectively. The increment in maximum temperature is less than the minimum temperature. The relative increment of maximum temperature from the baseline period for both scenarios in future time horizon are shown in the Figures 5.3 and 5.4. The projected minimum and maximum temperature in all future time horizons is with the range projected by IPCC which indicates the average temperature that will be risen by 1.4 to 4 towards end of this century.

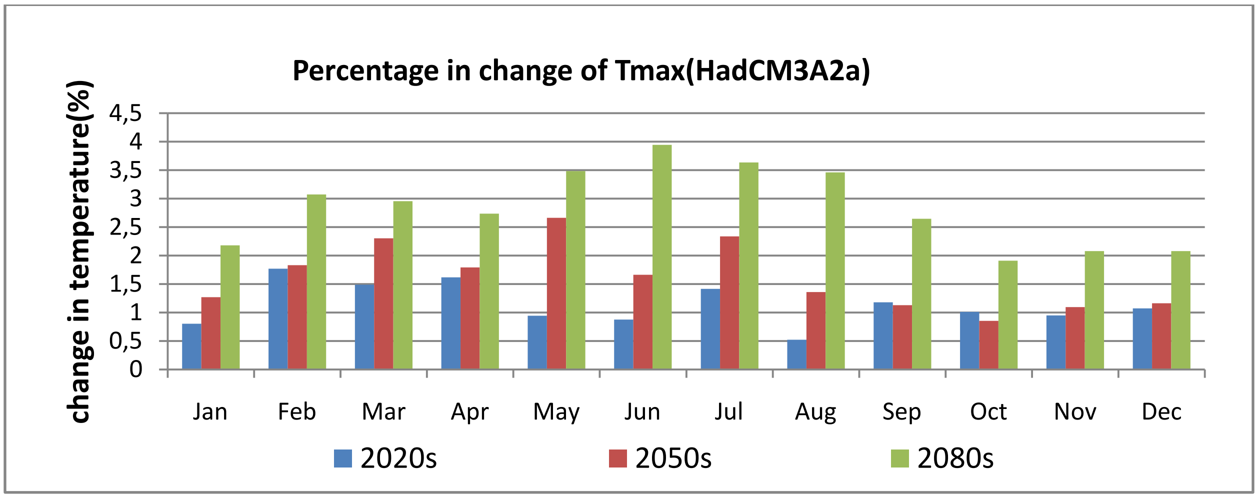

Figure5.3Change of downscaled monthly maximum temperature from baseline period for HadCM3A2a

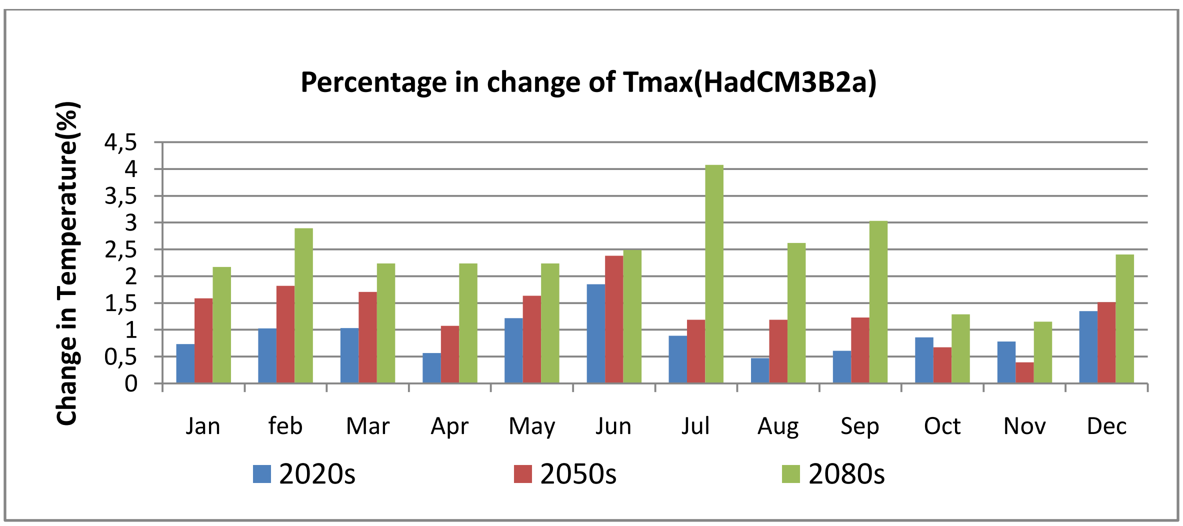

Figure 5.4 Change of Downscaled monthly maximum temperature from baseline period for HadCM3B2a

- **Precipitation**

Delta factors as percentage differences are estimated by obtaining the differences of present and future climate change model outputs, respectively. Then the Delta factor is applied to observed rainfall and temperature time series for subsequent use. The Figure 5.5 and 5.6 show percentage differences of specific periods 2011-2040, 2041-2070 and 2071-2099 in proportion to 1961-1990 as the baseline from projected scenarios using A2 and B2.

The results imply that 30.2% (for 2020s) and 41.1% (for 2070s) maximum increase in quantity of rainfall in June and in September for A2 and B2emission scenario respectively are expectable. Under A2 we expect to have a decline in average daily precipitation in compare to the present days (1961-1990). In general, total annual rainfall decrease of 0.2% and 5.9 % are expectable for 2020s for A2 and B2 respectively. A decrease of 4.4% and increase of 1.08% are likely to happen for s for A2 and B2 respectively. İn 2080s the Annual rainfall will be increase by 4.51% and 7% for A2 and B2 respectively.

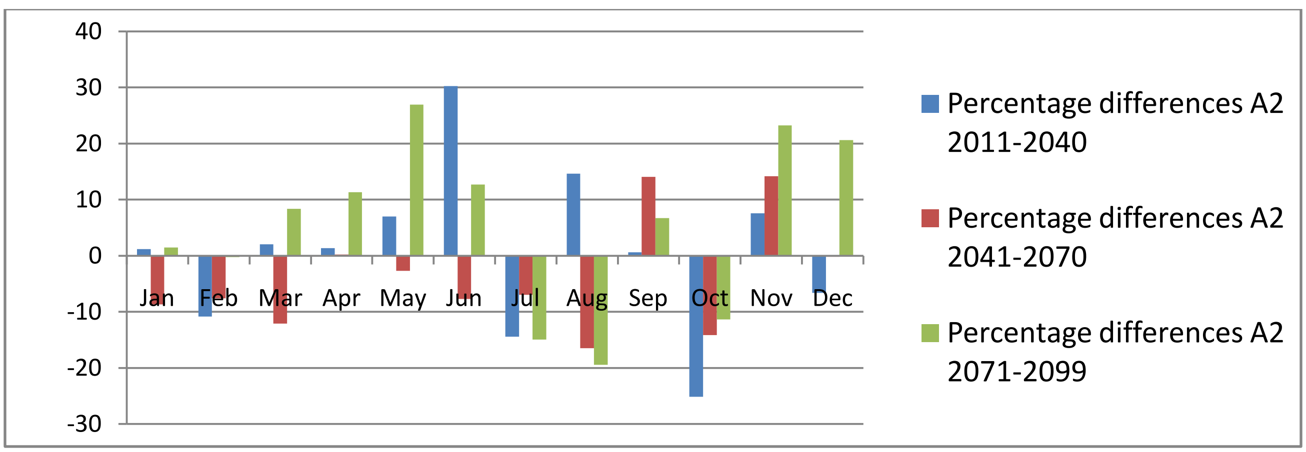

Figure 5.5 Delta factors as percentage differences to 1961-1990 (A2 Scenario)

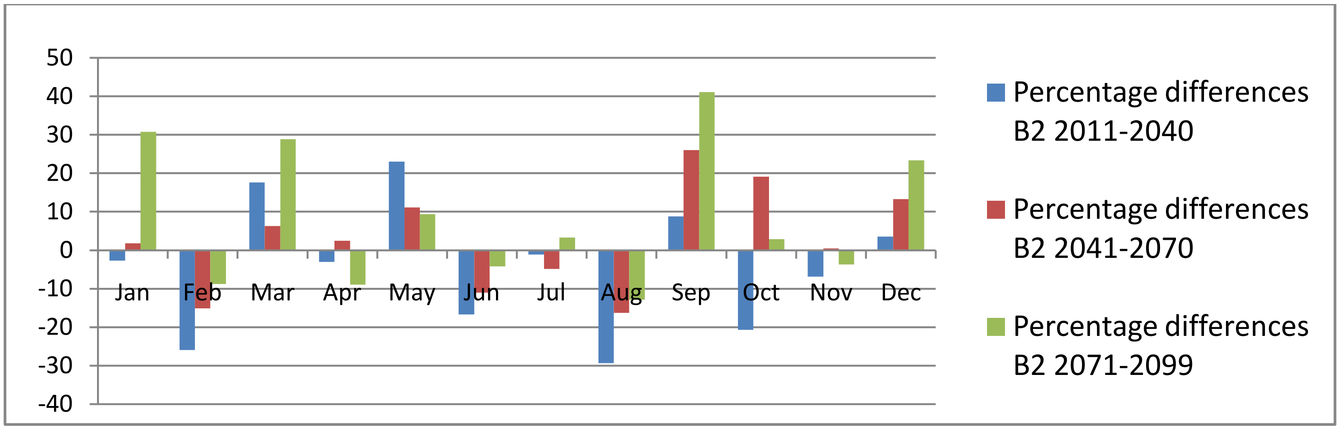

Figure 5.6 Delta factors as percentage differences to 19961-1990 (B2 Scenario)

The projection of rainfall did not manifest a systematic increase or decrease in all future time horizon. Unlike that of maximum and minimum temperature which exhibits an increasing trend for both A2 and B2 scenarios.

5.1.2 Rainfall Frequency Analysis

The cumulative distribution has been used for determining the return periods of extreme events (maximum rainfalls). From Figure 5.7; increasing in return periods for daily maximum rainfall values from 1961-1990 to 2011-2040 is obvious. No considerable change was observed for 2041-2070 and 2071-2099 comparing to the baseline period for HasCM3A2 model.

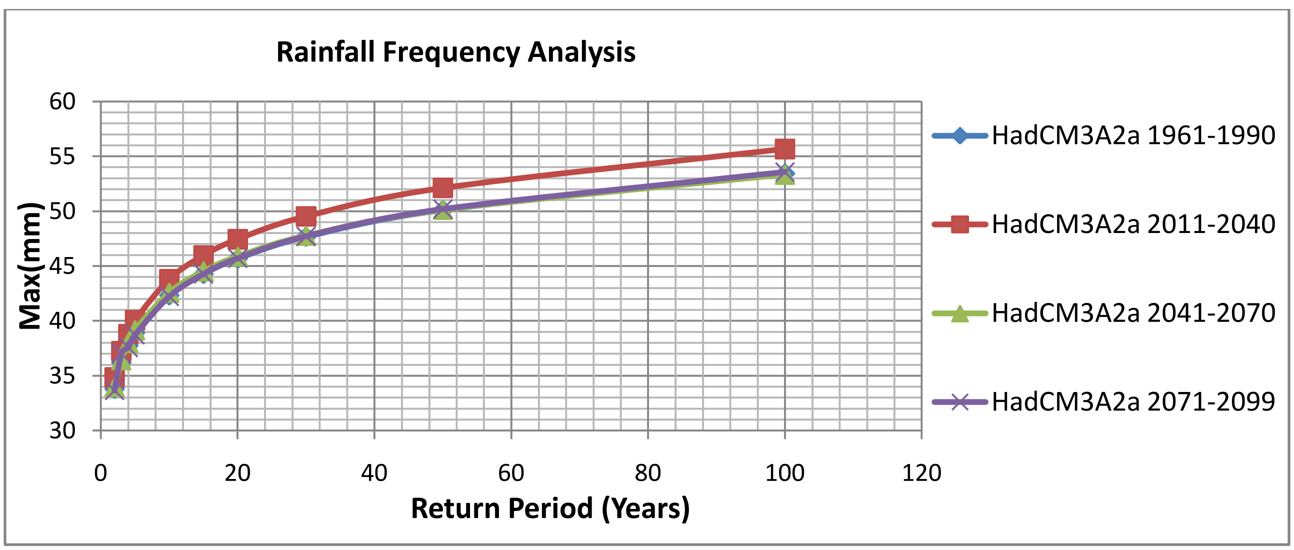

Figure 5.7 Cumulative distributions of maximum values for HadCM3A2

Development according B2 pattern in Figure 5.8 implies a considerable increase in maximum daily events. The considerable change in return periods can be observed for 2011-2040 where the maximum value becomes 56.58 mm/day is projected. Like A2 emission scenarios, B2 projects a temporary increase in maximum daily events for period of 2011-2040 and a dramatic decline for period of 2041-2070 and increase again for 2071-2099. Based on B2 emission scenarios we will project more flash rainfall in 100 years.

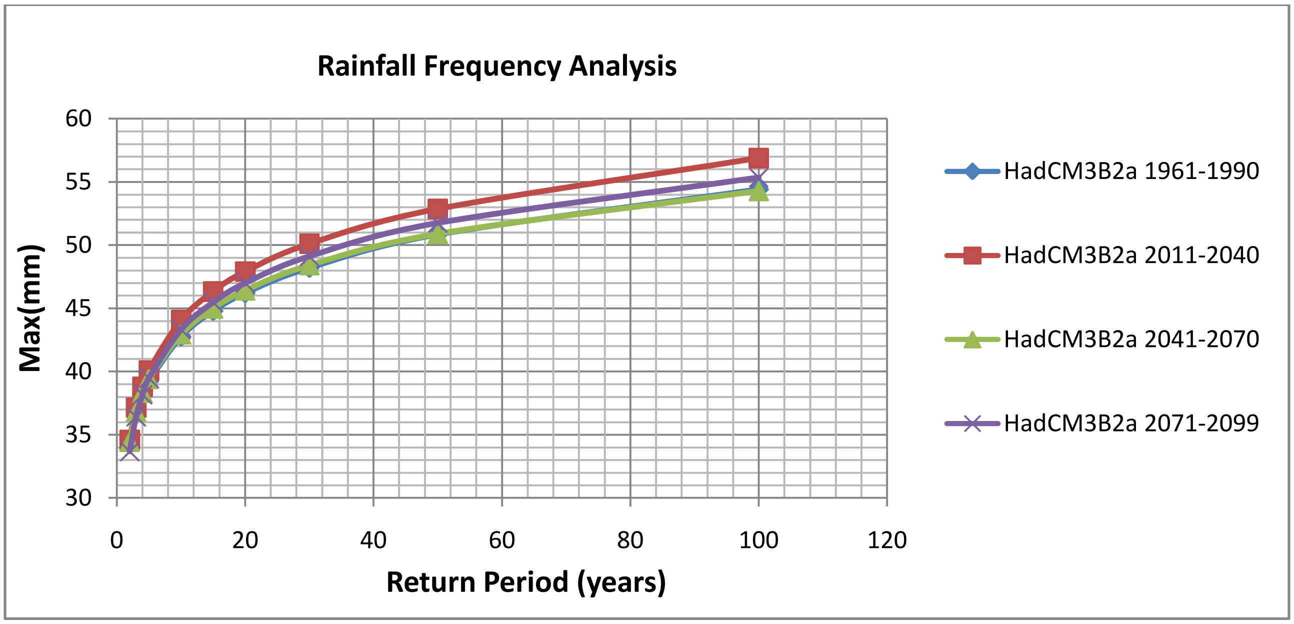

Figure 5.8 Cumulative distributions of maximum values for HadCM3B2

5.2 Hydrological Model Results

In this study the validity of the hydrologic modeling results is evaluated, by analyzing the models loss and transform calculations as well as by discussing the appropriateness of the applied design storms. The hydrographs resulting from hydrologic modeling of the 2hr frequency based design storms are discussed in this section.

5.2.1 Flood Hydrographs without Considering Climate and Land Use Change Impact

The Figure 5.9 is showing the flood hydrographs that the HEC HMS predicted for the Nyabugogo watershed at the flooded area for return periods ranging from 2 to 100 years without considering climate and land use change impact.

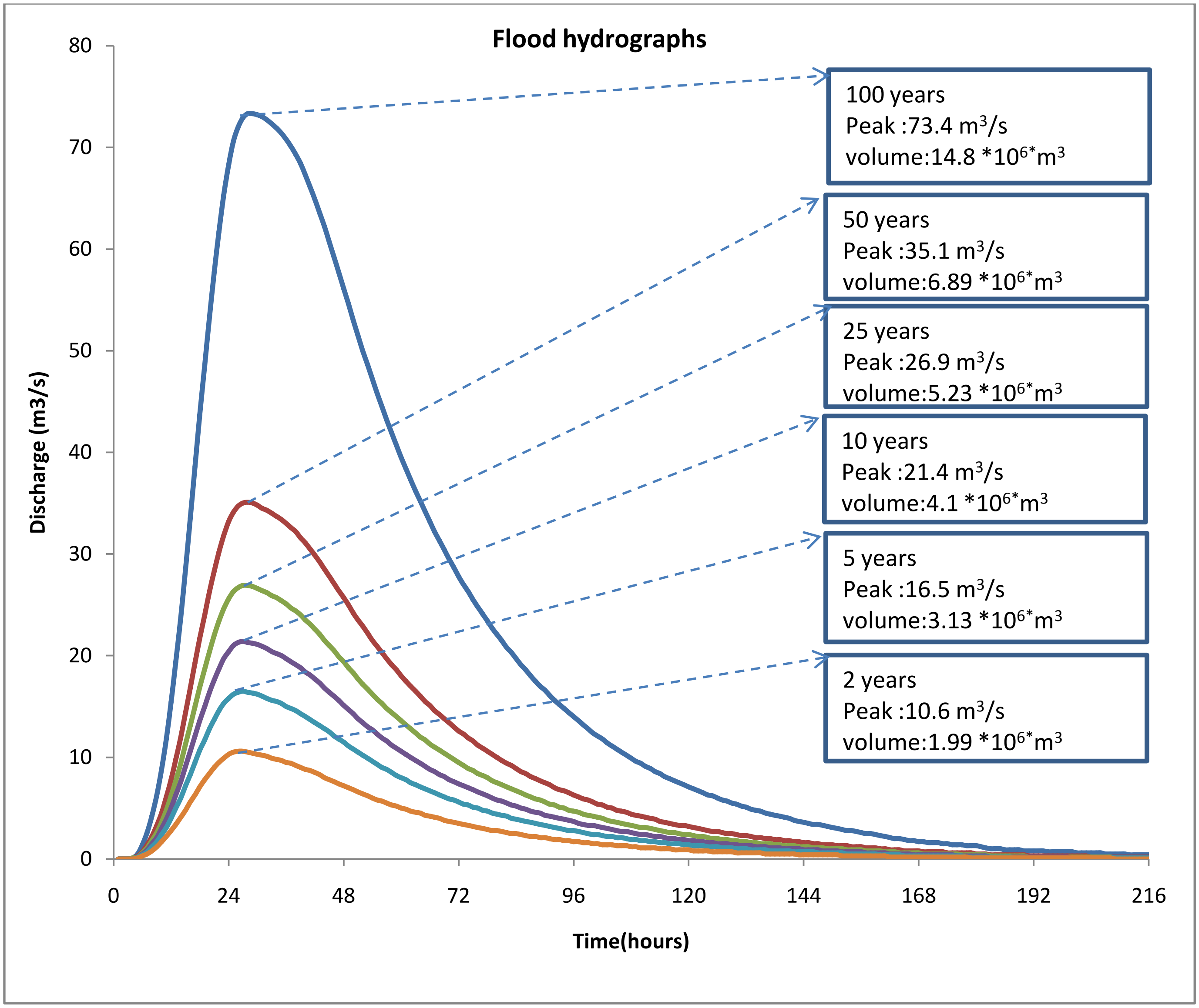

Figure 5.9 Flood hydrographs without considering climate change impact

From the Figure 5.9, it can be seen that the 2 years storm leads to a peak discharge of 10.6 m^3/s whereas a 5 years storm comes to a peak discharge of 16.5 m^3/s. The peak discharge continues to increase with the return period of 10, 25 and 50 years with respectively values of 21.4, 26.9 and 35.1 m^3/s. the biggest Peak flowis observed at 100 years storm with peak value of 73.4 m^3/s.

5.2.2 Flood Hydrographs with Consideration of Climate Change

Considering the impact of climate change on daily rainfall by using HadCM3 model (A2 and B2 emission scenarios), we come out by modeling the output of this model in HEC-HMS to create the flood hydrographs for different return period. The Figure 5.10reveals the hydrographs obtained from HEC-HMS model simulations using frequency storm Method.

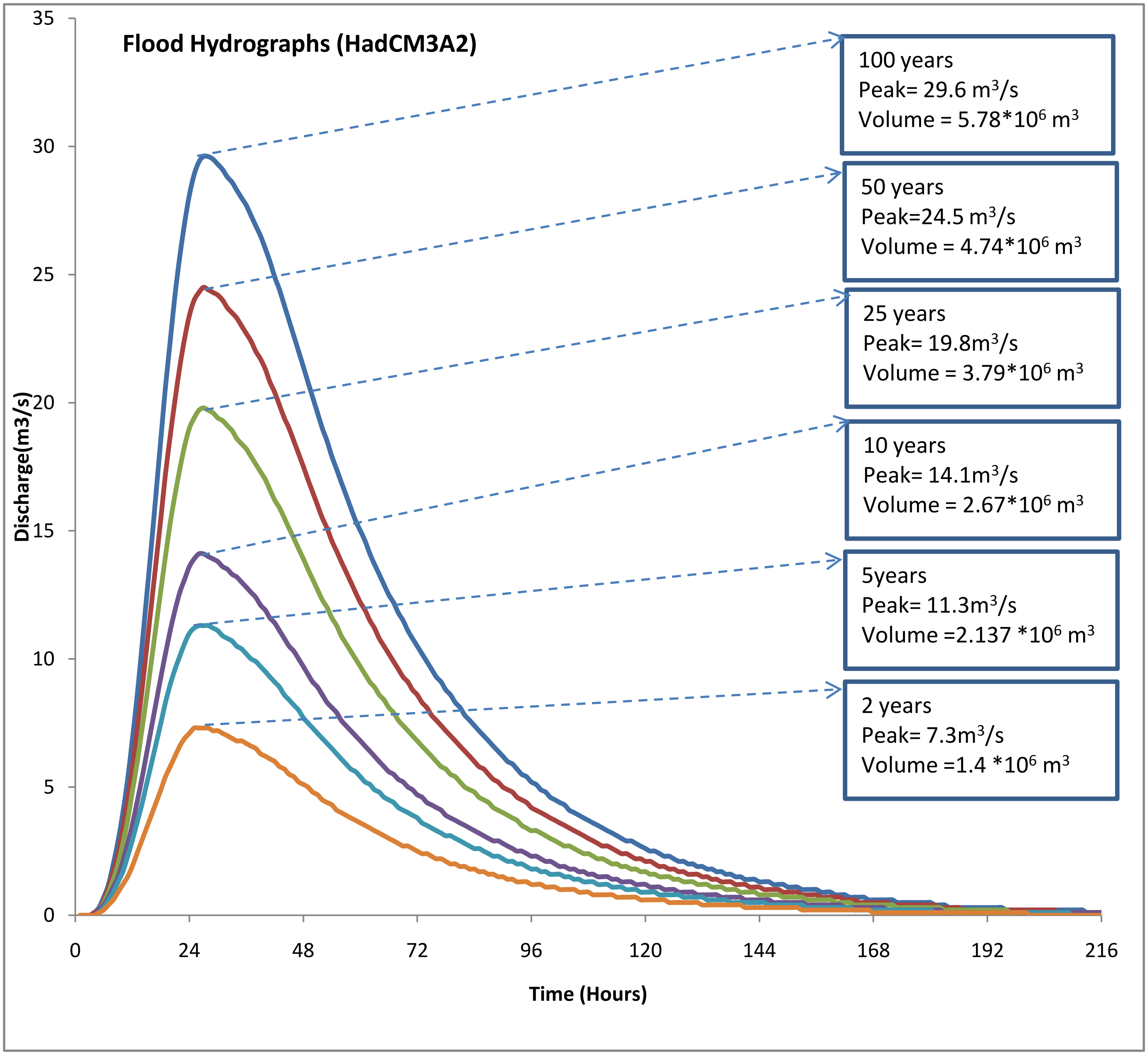

Figure 5.10 Flood hydrographs considering climate change impact (Emission A2)

As It can be observed from the figure 5.10, the 2 years storm leads to the peak discharge of 7.3 m^3/s in, 5 years storm leads to a peak discharge of 11.3 m^3/s whereas the peak discharge for 10, 25 and 50 years storms reach respectively 14.1, 19.8 and 24.5 m^3/s. The highest Peak discharge value can be seen at 100 years storm with peak discharge of 29.6 m^3/s.

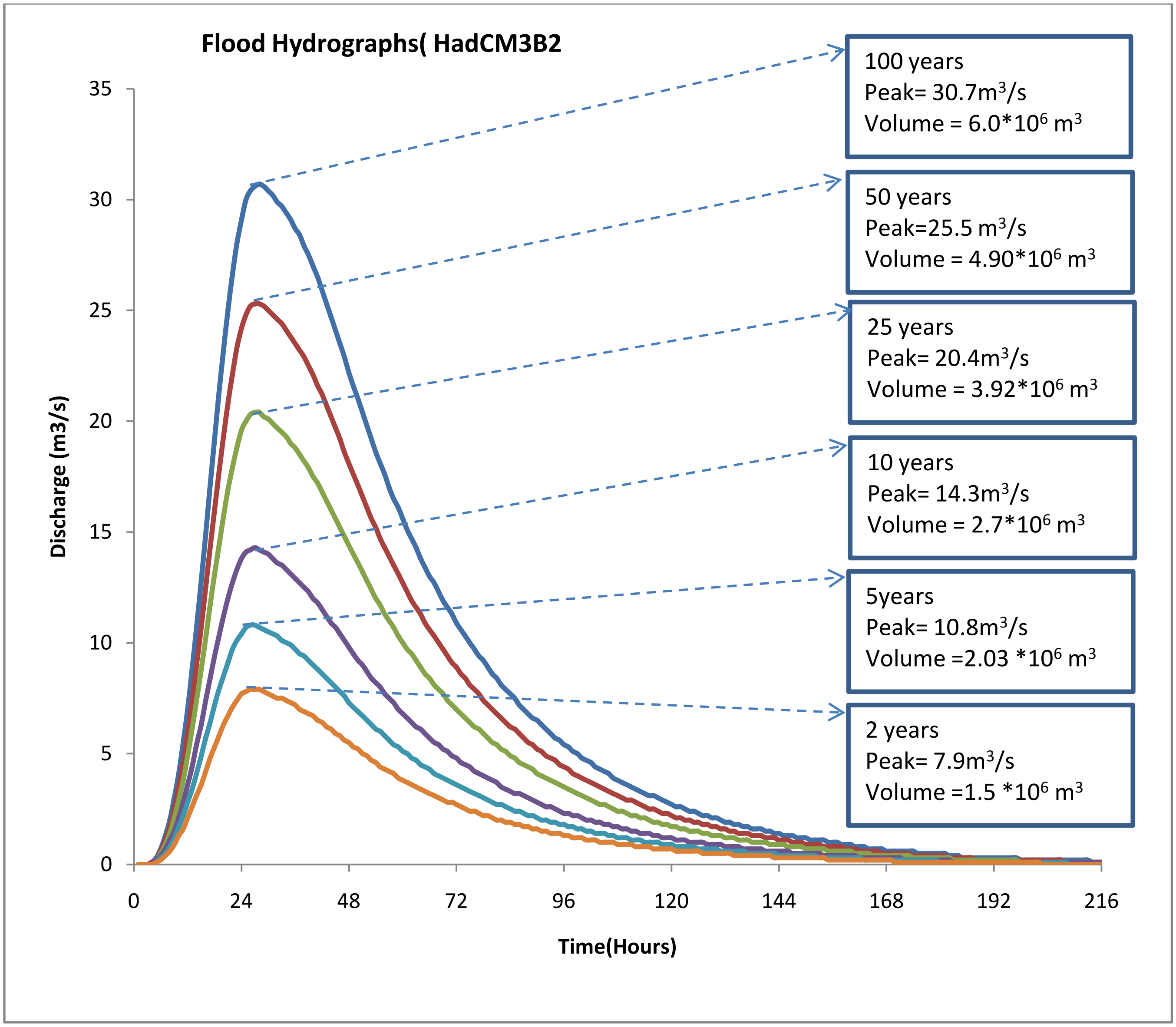

Figure5.11Flood hydrographs considering climate change impact (Emission B2)

After modeling the output of HadCM3 model for Emission scenario B2 in HEC-HMS, the results show that the 2 year storm leads to a peak discharge of 7.9 m^3/s, 5 year storm leads to a peak discharge of 10.8 m^3/s whereas the peak discharge for 10, 25 and 50 years storms reach respectively 14.3, 20.4 and 25.4 m^3/s. the biggest Peak discharge can be seen at 100 years storm with peak value of 30.7 m^3/s. The climate change show a decreasing of daily rainfall therefore it leads to the significant impact in decreasing flood discharge in Nyabugogo catchment.

5.2.3 Flood Hydrographs Considering Land Use Change

The Figure 5.12 is comparing the flood hydrographs given by HEC-HMS modeling for the Nyabugogo basin by considering land use change impact for return periods ranging from 2 to 100years.

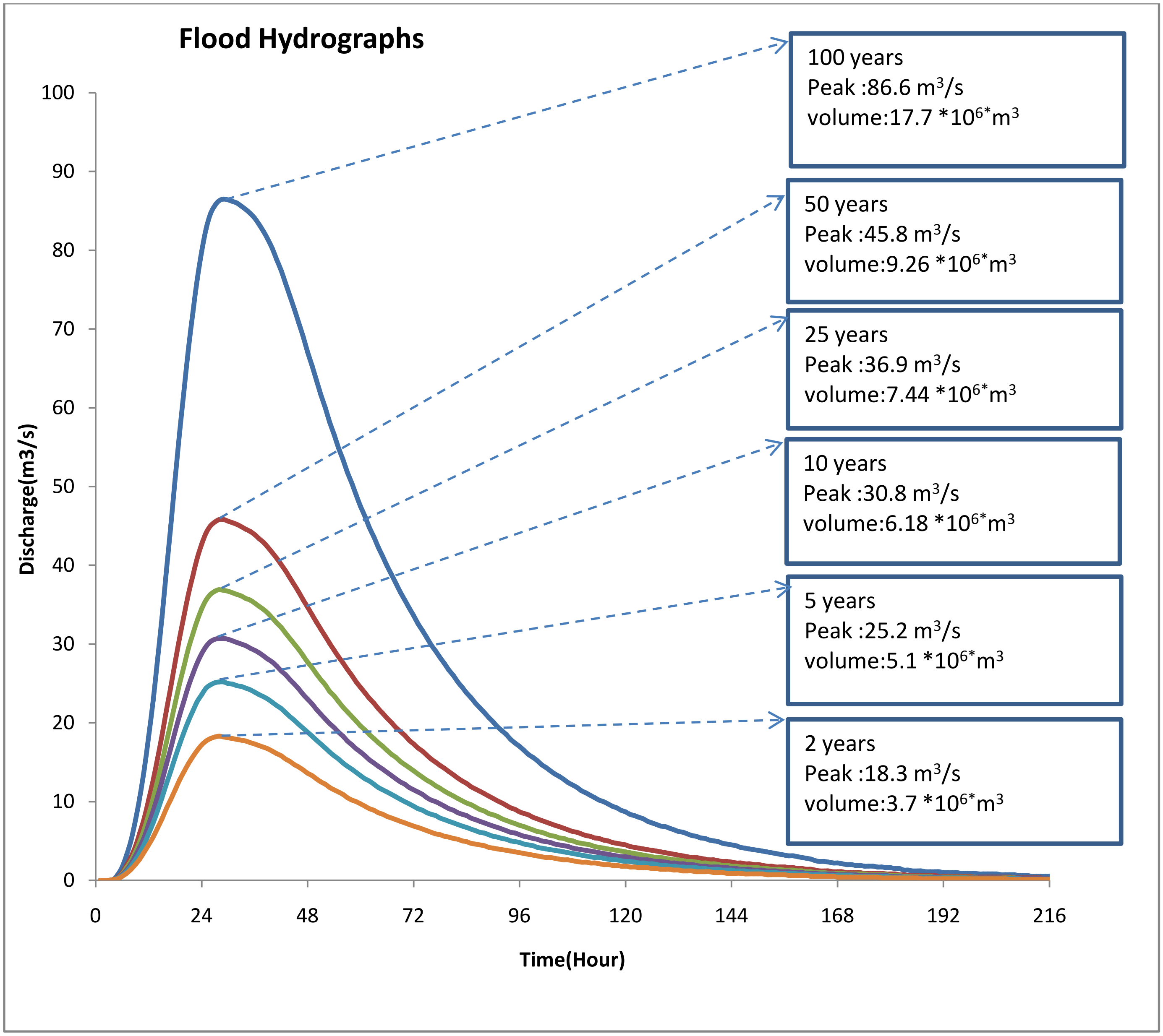

Figure5.12Flood hydrographs without considering climate change impact

It can be clearly seen that the 2 years storm leads to a peak discharge of 18.3 m^3/s whereas a 5 year storm reach to the peak discharge of 25.2 m^3/s. The peak discharge continues to increase with the return period of 10, 25 and 50 years with respectively values of 30.8, 36.9 and 45.8 m^3/s. the biggest Peak flow can be observed at 100 years storm with peak value of 86.6 m^3/s.

5.2.4 Flood Hydrographs Considering Climate and Land use change

The Figure 5.13 shows the hydrographs obtained from HEC-HMS model simulations using frequency storm Method for combination of climate and land use change impact on Nyabugogo watershed.

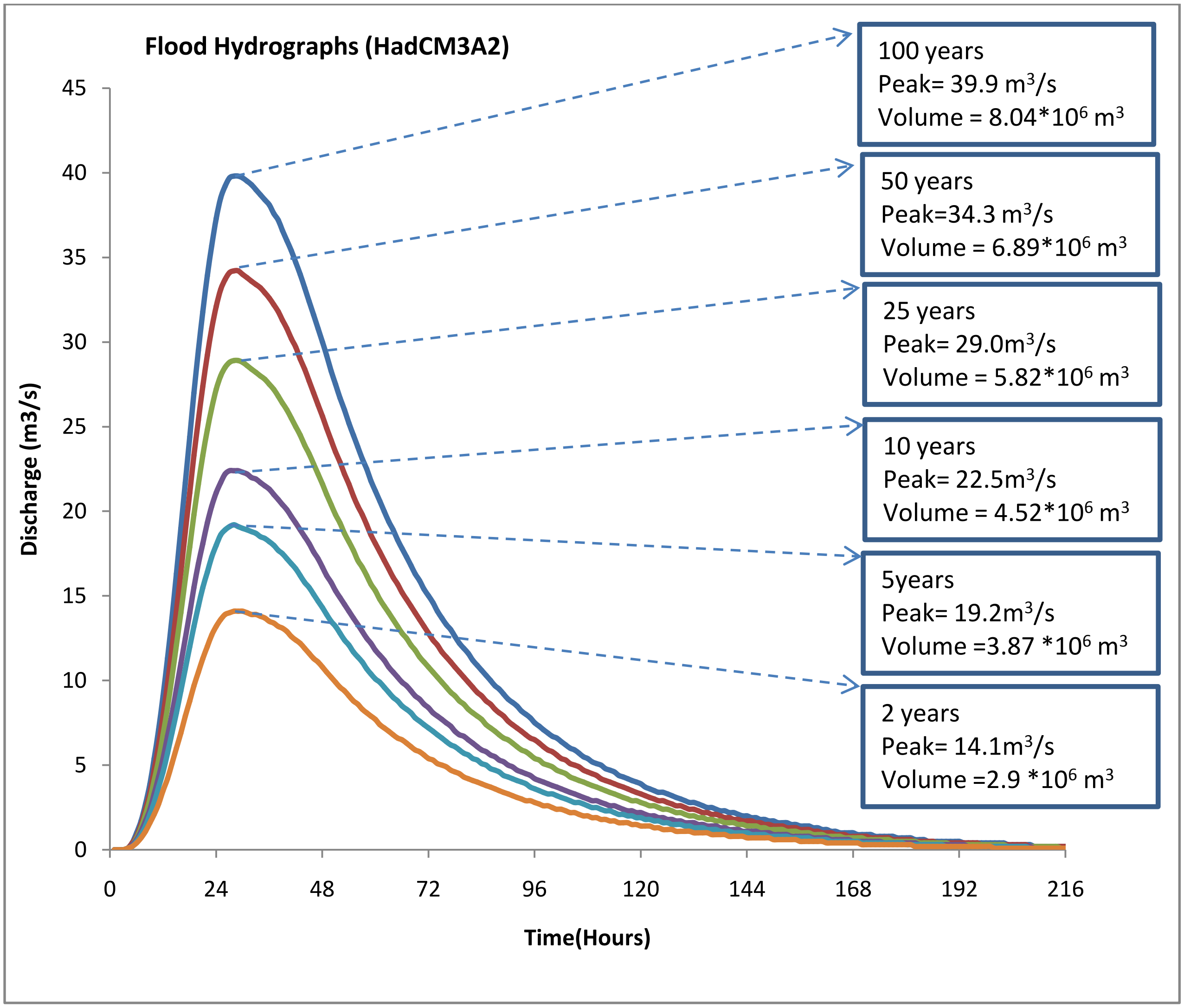

Figure5.13 Flood hydrographs considering climate and land use change impact (Emission A2)

The graph 5.13 shows the corresponding peak values and volumes of each hydrograph. As It can be observed from the figure 5.13, the 2 years storm leads to the peak discharge of 14.1 m^3/s in, 5 year storm leads to a peak discharge of 19.2 m^3/s whereas the peak discharge for 10, 25 and 50 years storms reach respectively 22.5, 29.0 and 34.3 m^3/s. the highest Peak discharge value can be seen at 100 years storm with peak discharge of 39.9 m^3/s.

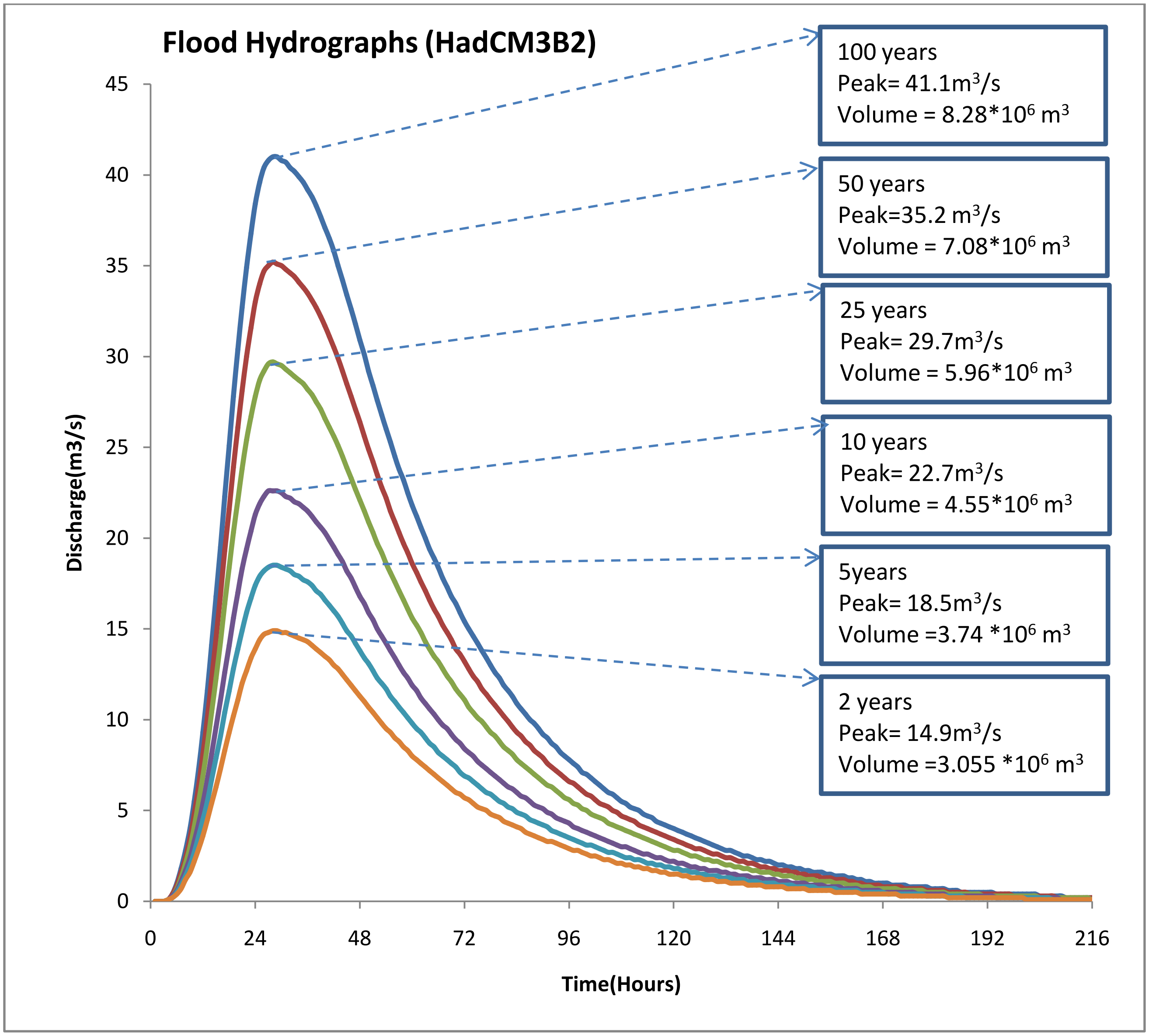

Figure5.14 Flood hydrographs considering climate and land use change impact (Emission B2)

After modeling the output of HadCM3 model for Emission scenario B2 in HEC-HMS, the results show that the 2 years storm leads to a peak discharge of 14.9 m^3/s, 5 years storm leads to a peak discharge of 18.5 m^3/s whereas the peak discharge for 10, 25 and 50 years storms reach respectively 22.7, 29.7 and 35.2m^3/s. the biggest Peak flow can be seen at 100 years storm with peak value of 41.1 m^3/s.

5.2.3 Comparison of Hydrographs Results

After generating the floods hydrographs for different return periodsof storm, we compared the results to detect which factor (climate or land use change) impacts most on flooding of Nyabugogo River. We considered 4 hydrographs types: (1) hydrographs without considering climate and land use change, (2) hydrographs by considering only climate change impact, (3) hydrographs by considering only land use change, (4) hydrographs by considering both climate and land use change.

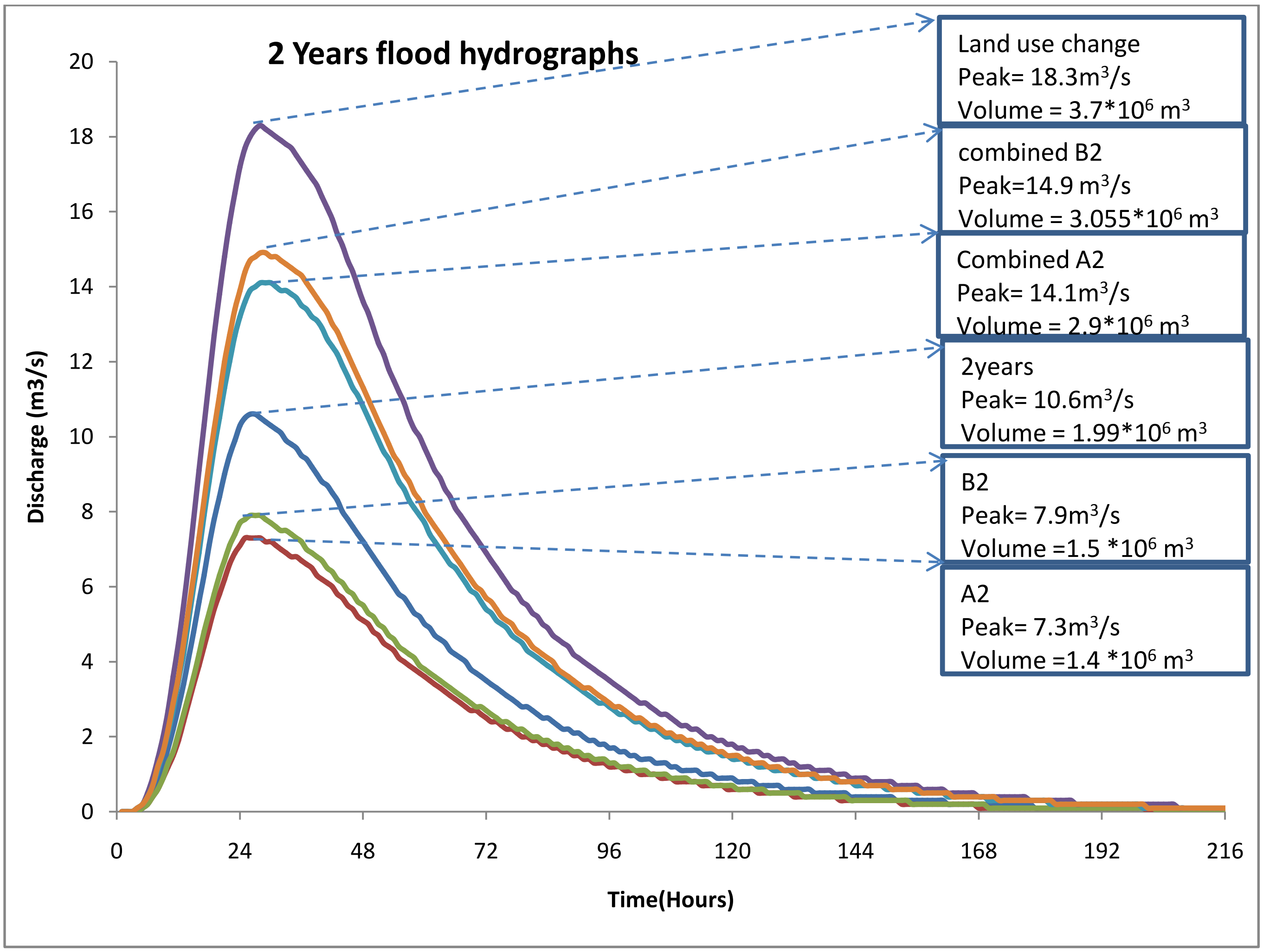

Figure5.15Twoyears hydrographs comparison

İn Figure 5.15, for two years flood hydrographs, it can be clearly seen that land use change will affect much the Nyabugogo River flooding with peak discharge of 18.3 m3/s. The combined climate and land use change come second to show impact on Nyabugogo river flooding with peak discharge of 14.9 and 14.1 m3/s for B2 and A2 emissions respectively. The hydrograph without considering climate and land use change comes third in term of peak discharge with 10.6 m3/s. Lastly, flood hydrographs by considering only climate change lead to the peak values of 7.9 and 7.3 m3/s for B2 and A2 emissions respectively.

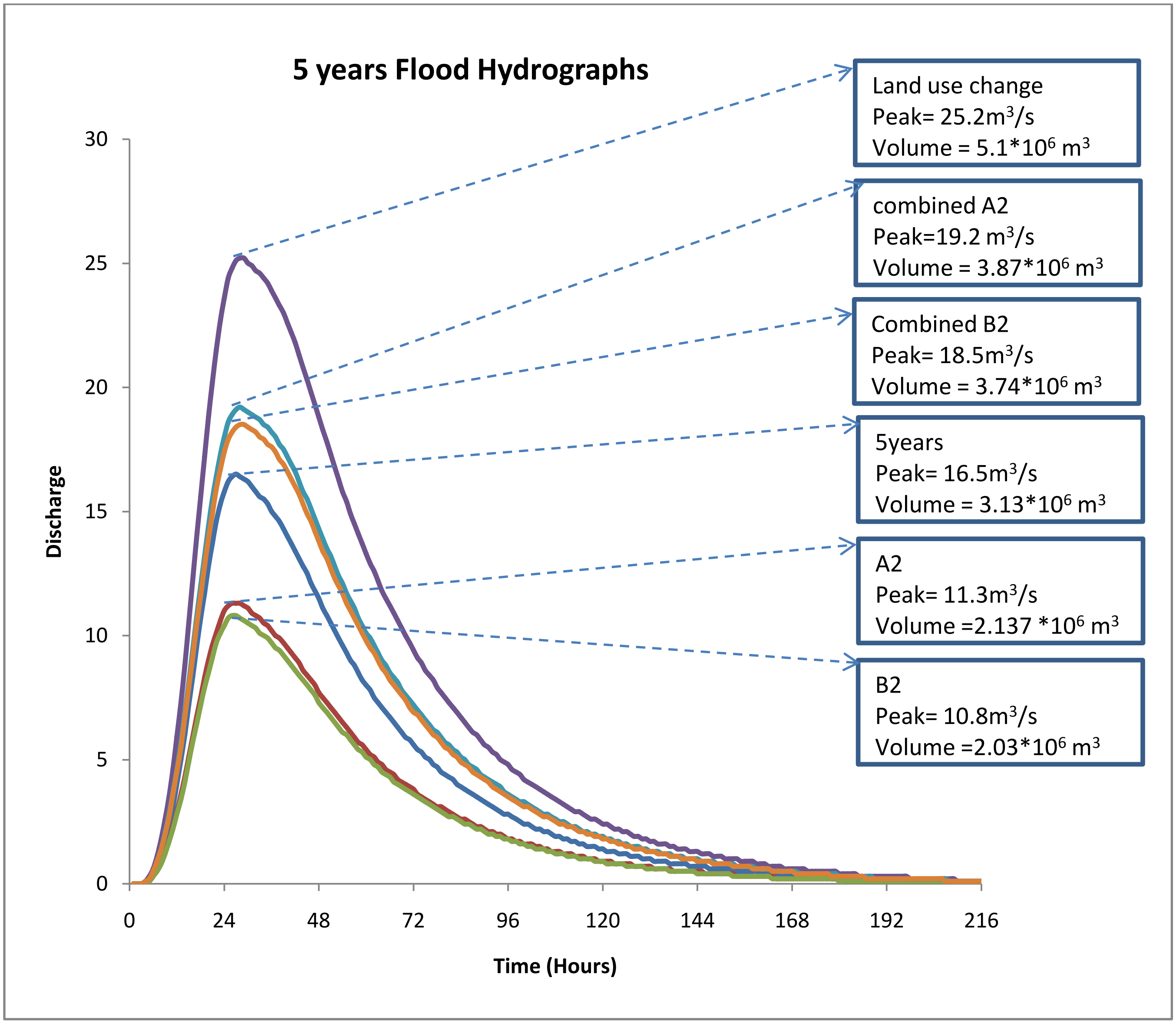

Figure 5.16 Five years hydrographs comparison

For 5 years flood hydrographs(Figure 5.16), it is observed from the graph that land use change has the biggest impact on the flooding of Nyabugogo River with peak discharge of 25.2 m3/s. The combined change of climate and land use appear second in high discharge value with peak of 19.2 and 18.5 m3/s for A2 and B2 emissions respectively. The hydrograph without considering climate and land use change comes third in term of peak discharge with 16.5 m3/s.

Lastly, flood hydrographs by considering only climate change lead to the peak values of 11.3 and 10.8 m3/s for A2 and B2 emissions respectively.

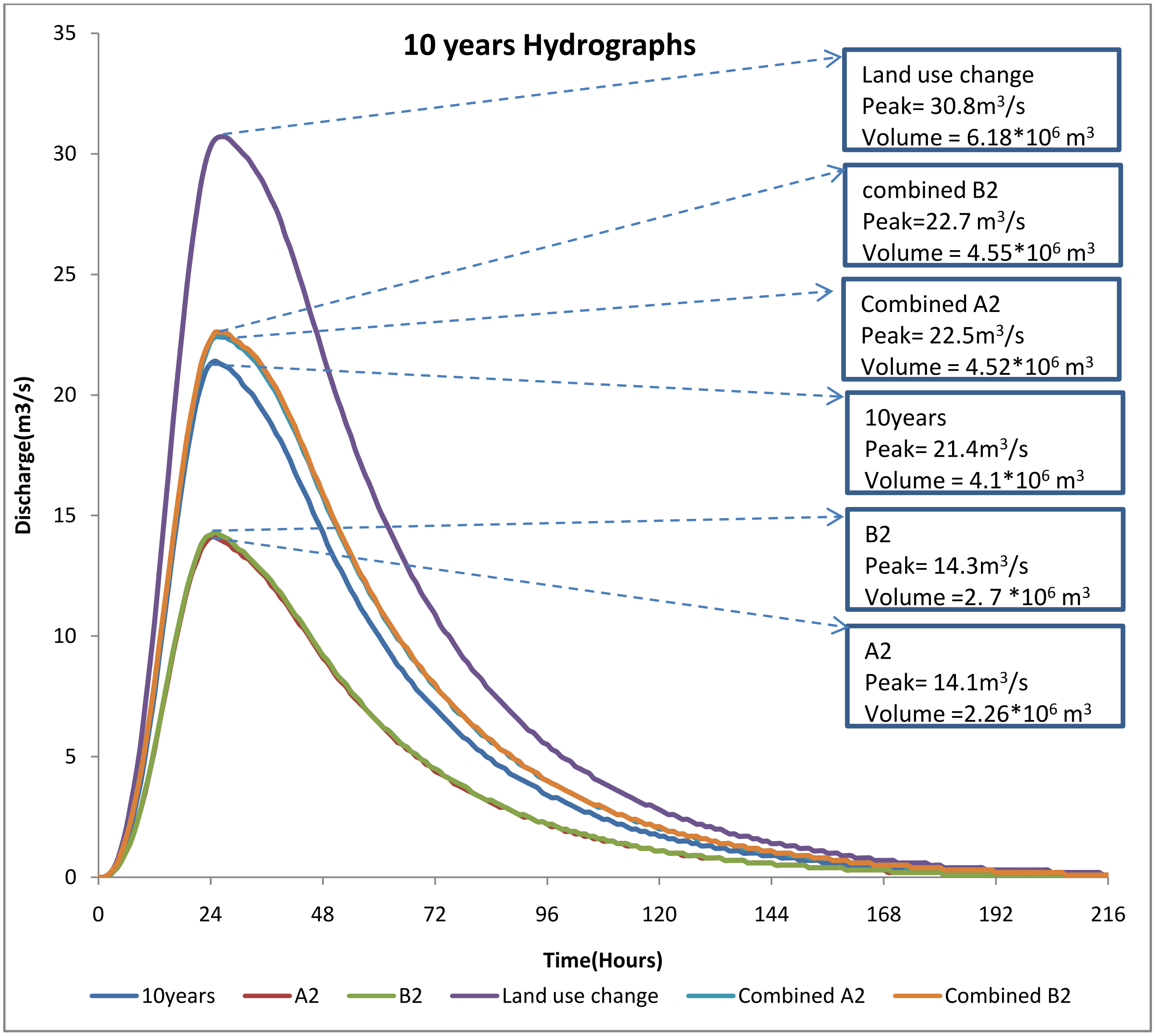

Figure5.17Ten years hydrographs comparison

For ten years flood hydrographs(Figure 5.17), it can be seen that again land use change show high peak discharge among other hydrographs with peak discharge of 30.8 m3/s. The combined climate and land use change come second to show impact on Nyabugogo river flooding with peak discharge of 22.7 and 22.5 m3/s for B2 and A2 emissions respectively. The hydrograph without considering climate and land use change comes third with peak discharge with 21.4

m3/s. Lastly, flood hydrographs by considering only climate change come with to the peak values of 14.3 and 14.1 m3/s for B2 and A2 emissions respectively.

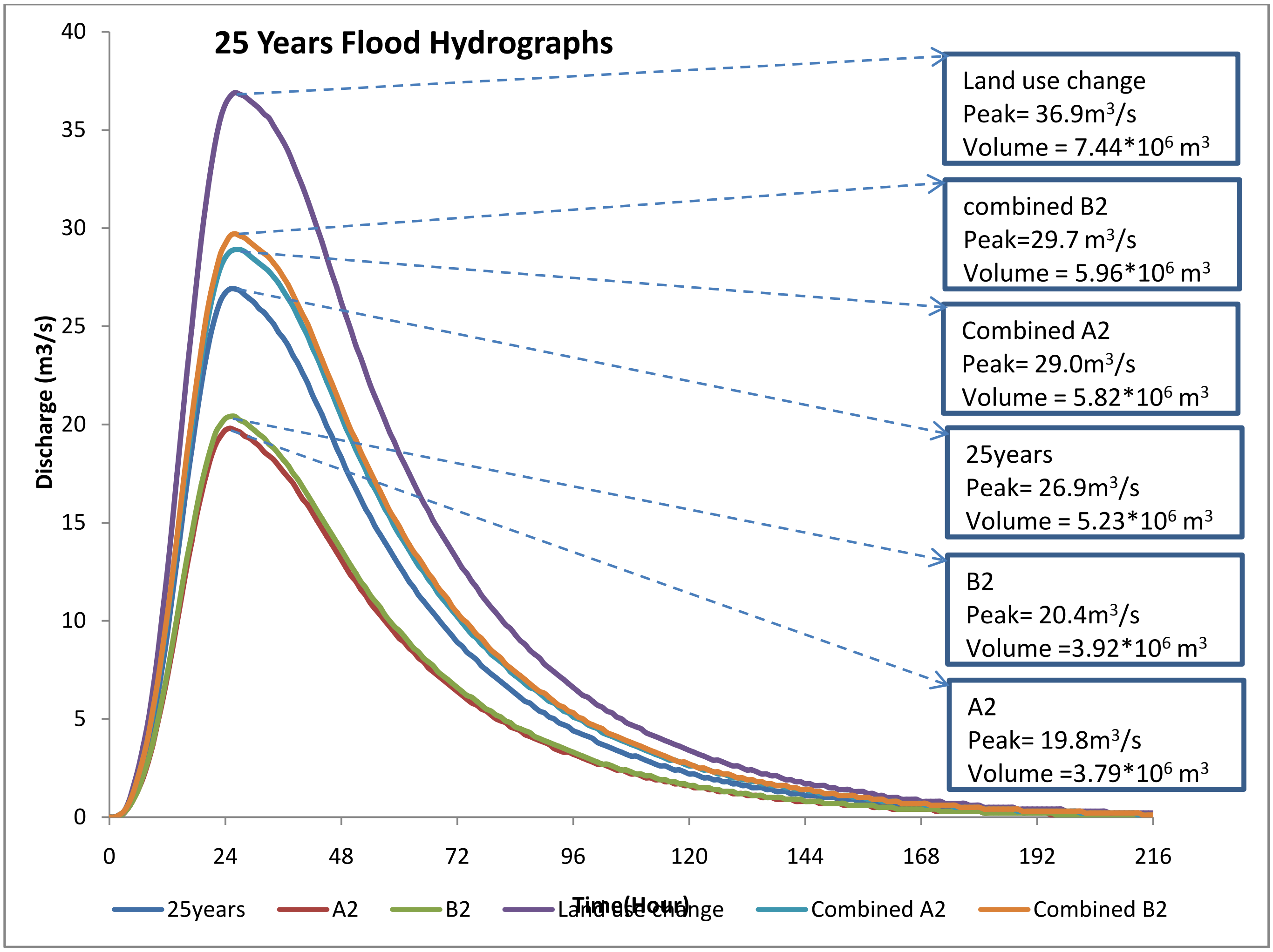

Figure5.18 25 Years hydrographs comparison

From 25years flood hydrographs(Figure 5.18), it can be observed that land use change will affect much the Nyabugogo River flooding with peak discharge of 36.9 m^3/s. The climate and land use change combination come second to show impact on Nyabugogo river flooding with peak discharge of 29.7 and 29.0 m^3/s for B2 and A2 emissions respectively. The hydrograph without considering climate and land use change comes third with peak discharge of 26.9 m^3/s. Lastly, flood hydrographs by considering only climate change lead to the peak values of 20.4 and 19.8 m^3/sfor B2 and A2 emissions respectively.

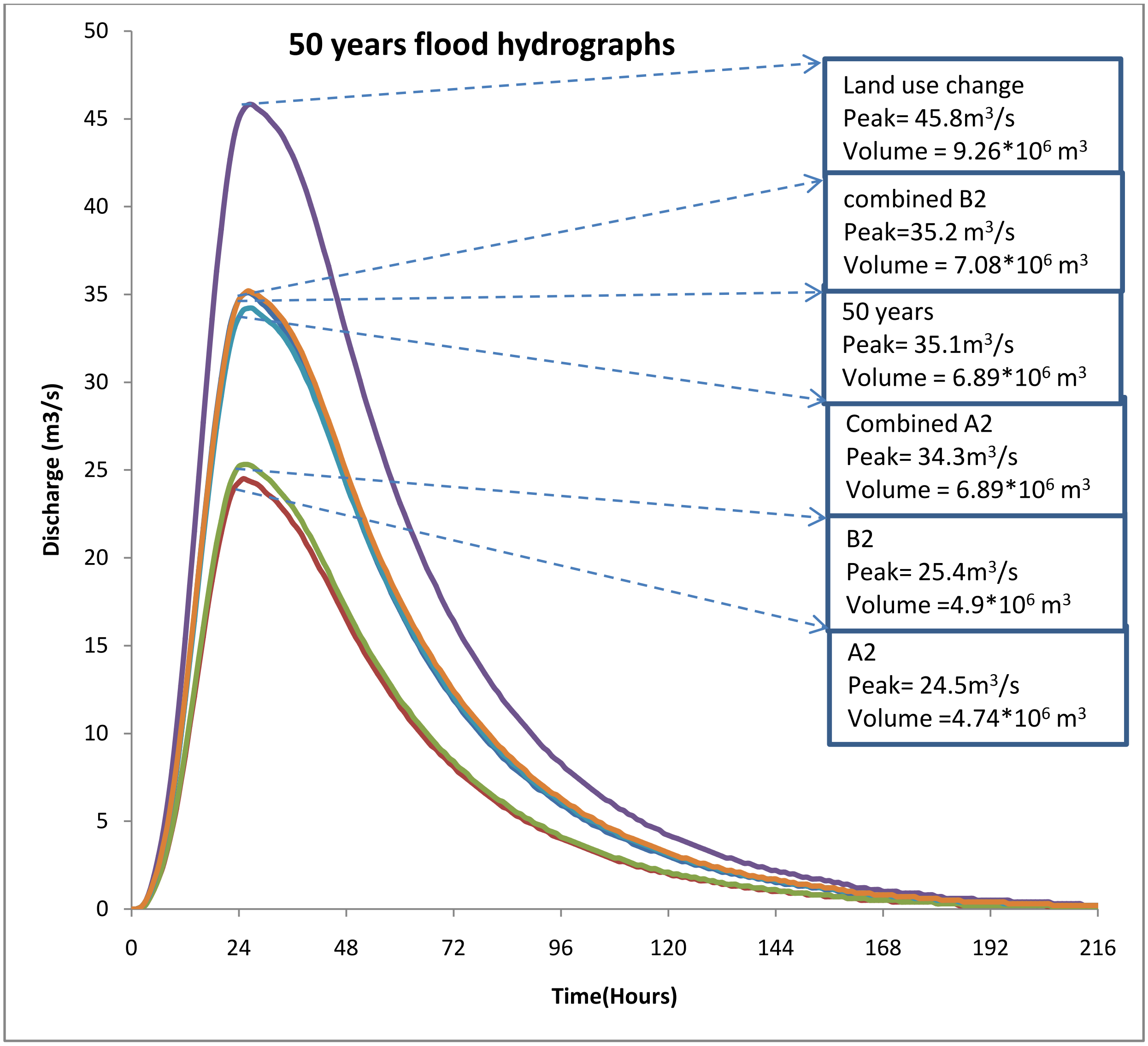

Figure5.19 50 Years Flood Hydrographs Comparison

For 50 years flood hydrographs, it is observed that land use change show highest peak discharge among other hydrographs with peak discharge of 45.8 m^3/s. The combined (climate and land use change) and hydrograph (without considering climate and land use change) has almost equal peak discharge with peak discharge of 35.2 , 35.1 and34.3 $m^3/s$for B2 emission, hydrograph without considering climate and land use change and A2 emission respectively. Lastly, flood hydrographs by considering only climate change come with to the peak values of 25.4 and 24.5 $m^3/s$for B2 and A2 emissions respectively.

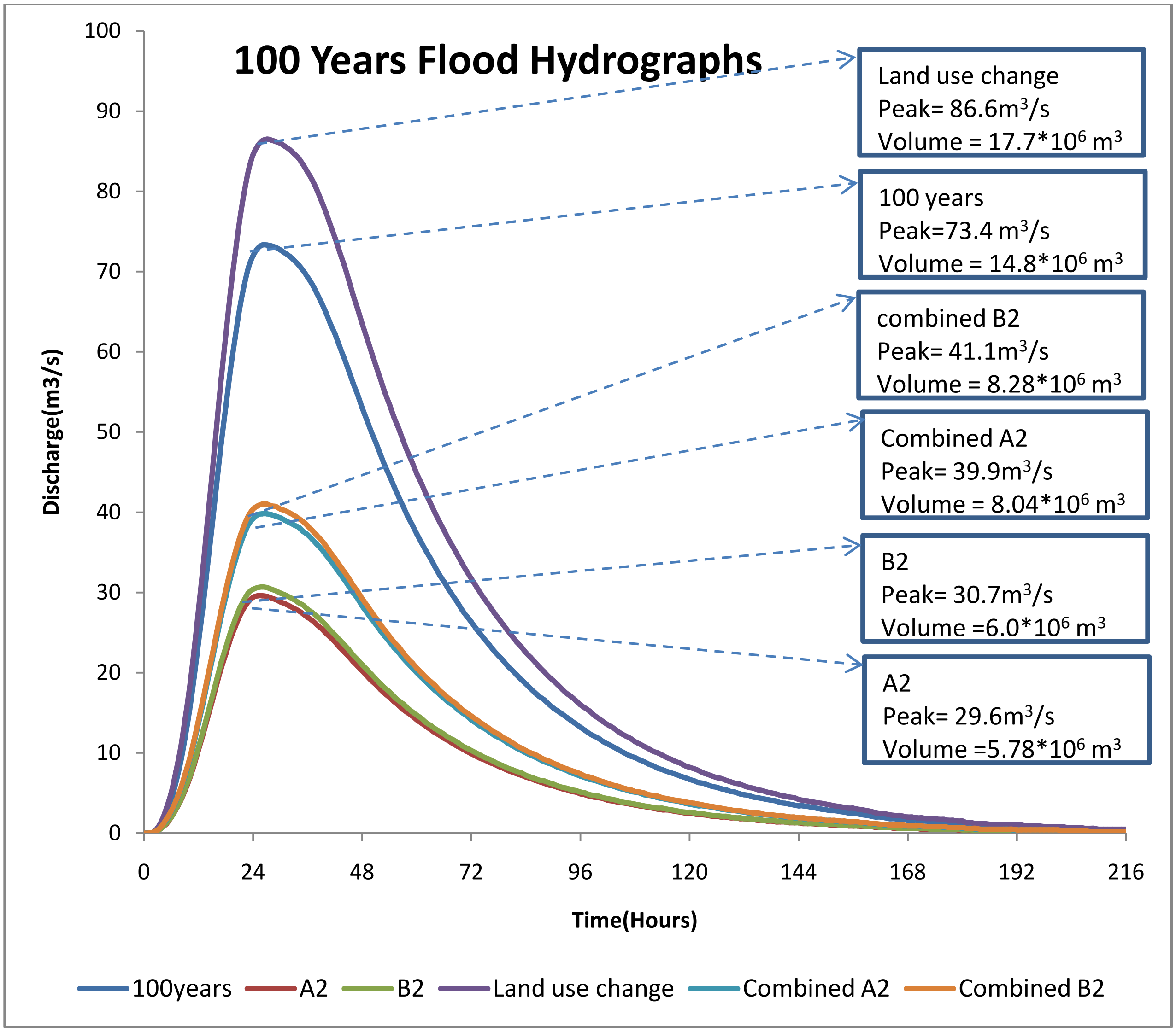

Figure 5.20 100 Years hydrographs comparison

For 100 years flood hydrographs(Figure 5.10), it is observed that land use change continues to have the biggest impact on the flooding of Nyabugogo River with peak discharge of 86.6 m^3/s. The hydrograph without considering climate and land use change comes second to show highest peak discharge of 73.4 m^3/s. The combined change of climate and land use appear follow with discharge value with peak of 41.1 and 39.9 $m^3/s$for A2 and B2 emissions respectively. Lastly, flood hydrographs by considering only climate change lead to the peak values of 30.7 and 29.6 $m^3/s$for A2 and B2 emissions respectively.

Table5.1Climate and land use impact in percentage

R.Period	**Without change**	**Land use change**		**climate change**				**combined**			
	Peak	Peak	%(+)	B2	%(-)	A2	%(-)	B2	% (+)	A2	%(+)
2 Years	10.6	18.3	72.64	7.9	25.47	7.3	31.13	14.9	40.57	14.1	33.02
5 Years	16.5	25.2	52.73	10.8	34.55	11.3	31.52	18.5	12.12	19.2	16.36
10 Years	21.4	30.8	43.93	14.3	33.18	14.1	34.11	22.7	6.07	22.5	5.14
25 Years	26.9	36.9	37.17	20.4	24.16	19.8	26.39	29.7	10.41	29	7.81
50 Years	35.1	45.8	30.48	25.4	27.64	24.5	30.20	35.1	0.00	34.3	-2.28
100 years	73.4	86.6	17.98	30.7	58.17	29.6	59.67	41.1	-44.01	39.9	-45.64

The Table 5.1 describes factor that affect much the normal condition (no climate and land use change taken into account) in percentage. It can be seen that land use is highly impacting floodsin kigali city by increasing the expected peak discharge (in normal condition). The climate change decrease the expected peak value for different return period of storm while the combined climate change and land use change increase the expected peak for 2 years to 25 years return period and decreases the expected peak discharge for 50 and 100 years of storm return period.

CHAPTER 6

CONCLUSION

The main goal of this research was to assessthe climate and land use change impact on urban flooding firstlyby developing future climate scenarios on extremes temperature and rainfall based on a general circulation Models and Statistical Downscaling Model(GCM and SDSM),secondary byestimating flood volumes and peak discharge values considering the climate scenarios results and land use change projections in future by using HEC-HMS model. This study has been done to support decision-makers in Kigali city capital of Rwanda when dealing with floofing events undber climate and land use change.

In this research, Statistical Downscaling model, a widely used support tool, was successfully calibrated for period of 1961-1990 to explore the future changes in temperatures extremes (Tmin, Tmax) and rainfall data in Nyabugogo watershed for the future periods of 2011-2040, 2014-2070, and 2071-2099 under A2 and B2 scenarios relatively to the baseline period of 1961-1990 recommended by IPCC.

The results from applied statistical downscaling model (SDSM) indicate that temperature extremes (both maximum and minimum) show an increasing trend for the future periods for both A2 and B2 emission scenarios. The average annual minimum temperature will be increased by 1.4 °C and 1.2 °C forB2 scenario respectively and the average maximum temperature will be increased by 2.84 °C for A2 and 2.4 °C for B2 towards the end of century. Climate change scenarios for Africa, based on the results from several General Circulation Models using the data collated by intergovernmental panel on climate change data distribution center (IPCC-DDC) indicate that the future warming across Africa with ranges from 2°C(low scenario) to 5°C (high Scenario) by 2100. Therefore the results obtained from SDSM lies within the range of IPCC.

The result of downscaled rainfall does not manifest a systematic increase or decrease in all future time horizons for both A2 and B2 scenarios unlike that of temperature. The total annual rainfall decrease of 0.2% and 5.9 % are expectable for 2020s for A2 and B2 respectively. A decrease of 4.4% and increase of 1.08% are likely to happen for 2050s for A2 and B2 respectively and also for 2080s the Annual rainfall will be increase by 4.51% and 7% for A2 and B2 respectively.

In this research, the model HEC-HMS version 4.0, a hydrologic modeling software was applied to the Nyabugogo watershed and the model parameters (infiltration and baseflow) were calibrated using the observed stream flows. The model performed reasonably well over the calibration period by reproducing the observed flow volumes and simulating the observed peaks in terms of timing and quantity. The results reveal that the only climate change has a significant impact in decreasing of peak discharge of expected hydrographs in normal condition (without climate and land use change) for all return periods of storm whereas the land use change has shown the considerable increase of expected discharge peak without considering the climate and land use change. The combination of climate and land use change has show also increase of flood peak discharge of expected hydrographs for 2, 5, 10, 25 years of return period whereas there is a decrease for 50 and 100 years of return period.

Runoffs generated from frequency storm method will be extremely useful for future flood hazard and risk assessment studies in the nyabugogo catchment. Evapotranspiration is not included in the model calibrations. In future, if it is possible, evaporation measurements with different land use characteristics should be performed in the basin, and evapotranspiration component should be added to the model to see how it affects on flood volume of Nyabugogo River.

For this study, the results reveal that land use change inKigali city will considerably affect the hydrologiy processes of the watershed by increasing the amount of surface runoff which will lead to the considerable flooding in kigali city. Therefore it is highly recommended to the province of kigali city to increase pervious areas in the city such as forest and grass cover for reducing the runoff in city and to apply the Nyabarongo River restorationaccodingly to land use change for reducing the damages that can be caused by the River flooding.

The implications of this study results need to be taken into consideration and integrated into policies and planningfor adaptation strategies, including measures to incorporate climate and land use change into engineering infrastructure design standards and disaster risk reduction measures in kigali City District.

REFERENCE

[1] IPCC, (2013). Summary for Policymakers. Contribution of Working Group I to the Fifth Assessment Report of the Intergovernmental Panel on Climate Change. Cambridge University Press, Cambridge, United Kingdom and New York, NY, USA.

[2] Milly, P.C.D., Betancourt, J., Falkenmark, M., Hirsch, R.M,, Kundzewicz, Z.W., Lettenmaier, D.P.and Stouffer, R.J., (2008). ``Stationarity is dead: Whither water management?´´ 319(5863): 573-574.

[3]IPCC, (2001).``Third Assessment Report, Intergovernmental Panel on Climate Change´´. Available at http://www.ipcc.ch/.

[4]IPCC, (2007). ``Fourth Assessment Report, Intergovernmental Panel on Climate Change´´. Available at http://www.ipcc.ch/.

[5]Huong, H. T. L. and Pathirana, A., (2013). ``Urbanization and climate change impacts on future urban flooding in Can Tho city, Vietnam´´. Hydrol. Earth Syst. 17: 379-394.

[6] Blöschl, G., Ardoin, B.S., Bonell, M., Dorninger, M., Goodrich, D., Gutknecht, D., Bouabid, R. and Elalaoui, C. A., (2010). `` Impact of climate change on water resources.

[7] Mailhot, A. and Duchesne, S., (2010). ``Design criteria of urban drainage infrastructures under climate change´´. Journal of Water Resources Planning and Management 136: 201-208.

[8] Karamouz, M., Hosseinpour, A. and Nazif, S., (2010). ``Improvement of urban drainage system performance under climate change´´. Journal of Hydrologic Engineering.

[9] REMA, (2009). Economic impact of climate change in Rwanda. Report. Kigali, Rwanda.

[10] Rajib,S. and Anshu,S., (2011). Climate and disaster Resilience in cities. Community, Envoronment and disaster Risk Management, UK.

[11] Munyaneza,O., Nzeyimana K. and Wali, G., (2013). Hydraulic structures Design for Flood Control in the Nyabugogo wetland. Rwanda.

[12] Zilberman, D., Liu, X. Roland, D.H. and Sunding, D., (2004). ``The economics of climate change in agriculture´´. Strategies for global change, 9:365-382.

[13] Forster, P., Ramaswamy, V., Artaxo, P., Berntsen, T., Betts, R., Fahey, D.W., Haywood, J., Lean, J. , Lowe, D.C., Myhre, G., Nganga, J., Prinn, R., Raga, G., Schulz, M. and Van Dorland, R., (2007). ``Changes in Atmospheric Constituents and in Radiative Forcing´´. In: Climate Change 2007: The Physical Science Basis. Contribution of Working Group I to the Fourth Assessment Report of the Intergovernmental Panel on Climate Change. Cambridge University Press, Cambridge, United Kingdom and New York, NY, USA.

[14] Ashiq, M., Zhao, C., Ni, J.and Akhtar, M., (2010). ``GIS-based high-resolution spatial interpolation of precipitation in mountain–plain areas of Upper Pakistan for regional climate change impact studies´´. Theor Appl. Climatol. 99 (3):239–253.

[15] Dibike, Y.B. and Coulibaly, P., (2004). ``Downscaling of Global Climate model Output for Flood Frequency Analysis in Saguenay River System´´. Project no.S02-15-01, Departement of civil Engineering, McMaster University, Canada.

[16] Flato, G., Marotzke, J., Abiodun, J., Braconnot, P., Chou, S.C., Collins, W., Cox, P., Driouech, F., Emori, S., Eyring, V., Forest, C., Gleckler, P., Guilyardi, E., Jakob, C., Kattsov, V. and Rummukainen, M., (2013). ``Evaluation of Climate Models´´. In Climate Change 2013: The Physical Science Basis. Contribution of Working Group I to the Fifth Assessment Report of the Intergovernmental Panel on Climate Change.

Cambridge University Press, Cambridge, United Kingdom and New York, NY, USA.

[17] Goosse H., Barriat, P.Y., Lefebvre, W., Loutre, M.F. and Zunz, V. (2010). ``Introduction to Climate Dynamics and Climate Modeling´´. Online textbook available at http://www.climate.be/textbook.

[18] Karamouz, M., Nasif, S. and Fallahi, M., (2010). `` Rainfall Downscaling using Statistical Downscaling and Canonical Correlation Analysis: a case study in Palmer´´. R.N.(Ed) World Environmental and water resources congress: challenges on change-proceedings of the world environmental and water resources congress 2010 American Society of Civil Engineers, Reston, Va., 4579-4587.

[19] Karsh, P.,Yash,S., Himanshu, A.and Rounak,J., (2015). "Role of satellites in climate prediction using computer models", International journal of engineering Research and Technology, 4(3):151-160.

[20] Houghton, J.T., (2001). Climate change 2001: the scientific basis: contribution of working group I to the third assessment report of the intergovernmental panel on climate change. Cambridge University Press.

[21] William, B., (2003). Climate into 21st Century, Cambridge university press., Cambridge, United Kingdom.

[22] George, Z., (2012). Dynamical downscaling of climate in the Eastern Mediterranean and the Middle East. Young scholars Forum/the Cyprus Institute.

[23] Beniston, M., (2002). Climate modeling at various spatial and temporal scales: where can dendrochronology help?, Switzerland.

[24] Hay, L.E. and Clark, M.P., (2003). ´´Use of statistically and dynamically downscaled atmospheric model output for hydrologic simulations in three mountainous basins in the western United States´´. Journal of Hydrology (282):56-75.

[25] Dibike, Y.B. and Coulibaly, P., (2006). ``Hydrologic impact of climate change in the Saguenay watershed: comparison of downscaling methods and hydrologic models´´.

Journal of hydrology, 307(1-4):145-163.

[26] Coulibaly,P. and Debike, Y.B, (2004). Downscaling of global climate model outputs for flood frequency analysis in the Saguenay River System. Hamilton.

[27] Mearns, L.O., Giorgi, F., Whetton, P., Pabon, D., Hulme,M. and Lal, M., (2003). Guidelines for use of climate scenarios developed from Regional climate Model experiments, DDC of IPCC TGCIA.

[28] Wilby, L.R., Zorita, E., Timbal, B.,Whetton, P., Mearns, L.O. and Charles, S.P., (2004). Guidelines for use of climate scenario Developed from statistical Downscaling Methods Environmental Agency of England and wales, UK.

[29] Mikhail, A. and Elaine, M., (2002). LARS-WG a stochastic weather generator for use in climate impact studies. User manual, version 3.0. UK.

[30] Dawson, C.W. and Wilby, R.L., (2007). Statistical Downscaling Model SDSM, version 4.1. Department of Geography, Lancaster University, UK.

[31] Van Vuuren, D.P., Eickhout, B., Lucas, P.L. and den Elzen, M.G.J., (2006). ``Long-term multi-gas scenarios to stabilise radiative forcing—exploring costs and benefits within an integrated assessment framework´´. Energ J (27):201–233.

[32] Smith, S.J.and Wigley, T.M.L., (2006). ``MultiGas forcing stabilization with minicam´´. The Energy Journal Special issue (3):373–392.

[33] Van Vuuren, D.P., Den Elzen, M.G.J., Lucas, P.L., Eickhout, B., Strengers, B.J., Van Ruijven, B., Wonink, S. and Van Houdt, R., (2007a). ``Stabilizing greenhouse gas concentrations at low levels: an assessment of reduction strategies and costs´´. Clim Chang (81):119–159.

[34] John, A., (2003). Mathematical models and reality. Trinity western university. Canada V2Y1Y1.

[35] Halwatura, D. and Najim, M., (2013). ``Application of the HEC-HMS model for runoff simulation in a tropical catchment´´. Environmental Modeling & Software, (46):155–162.

[36] Sardoii, E. R., Rostami, N., Sigaroudi, S. K., and Taheri, S., (2012). ``Calibration of loss estimation methods in HEC-HMS for simulation of surface runoff (Case Study: Amirkabir Dam Watershed, Iran)´´. Adv. Environ. Biol., (6): 343–348.

[37] Christopher, A. J. and Yung, C. A., (2001). ``The use of HEC-HMS and HECGeoHMS to perform Grid-based Hydrologic Analysis of a watershed´´. ASFPM Conference, USA, 4 pp.

[38] Fleming, M, and Neary, V., (2004). ``Continuous Hydrologic Modeling Study with the Hydrologic Modeling System´´. J. Hydrol. Eng.-ASCE, (9): 175–183.

[39] Neary, V. S., Habib, E. and Fleming, M., (2004). `` Hydrologic Modeling with NEXRAD Precipitation in Middle Tennessee´´. J. Hydrol. Eng.-ASCE, (9): 339–349.

[40] Cunderlik, J. M. and Simonovic, S. P., (2005). `` Hydrological extremes in a southwestern Ontario river basin under future climate conditions´´. Hydrolog. Sci. J., (50): 631–654.

[41] Chu, X. and Steinman, A. D., (2009). ``Event and Continuous Hydrologic Modeling with HEC-HMS´´. J. Irrig. Drain. Eng.-ASCE, (135):119–124.

[42] Bouabid, R. and Elalaoui, C. A., (2010). ``Impact of climate change on water resources in Morocco``. The case of Sebou Basin, Séminaires Méditerranéens, (9): 57–62.

[43] Boyogueno, S. H., Mbessa, M., and Tatietse, T. T., (2012). ``Prediction of Flow-Rate of Sanaga Basin in Cameroon Using HEC-HMS Hydrological System´´. Application to the Djerem Sub-Basin at Mbakaou, Energy Environ. Res.

[44] HEC (Hydrologic Engineering Center), (2000). HEC-HMS Technical Reference Manual. U.S. Army Corps of Engineers Hydrologic Engineering Center, Davis, CA.

[45] Valentin. H., (2013). Master's thesis: GIS based flood modeling as part of integrated development strategy for Informal settlements. Haiti.

[46] Munyaneza, O., (2008). Space-time patterns of hydrological processes and water resources in Rwanda, with special focus on the meso-scale Migina catchment. PhD Proposal approved by Academic Board of UNESCO-IHE, Delft, Netherlands.

[47] FAO, (2005). Système d'information de la FAO sur l'eau et l'agriculture (in French), Information system for water and agriculture. Food and Agriculture Organization (FAO) of the UnitedNation.

[48] Nhapi, I., Wali, U.G., Uwonkunda, B.K., Nsengimana.H., Banadda.N. and Kimwaga.R, (2011). Assessment of Water Pollution Levels in the Nyabugogo Catchment,Rwanda.

[49] Surbana, (2012).Detailed Kigali City Master Plan. Vision Report. Rwanda

[50] SHER, (2013). Technical Note on a Nyabugogo Flood Risk Mitigation Strategy and Action Plan Proposal for a Flood Risk Mitigation Strategy. Final Version, Kigali, Rwanda.

[51] Nduwayezu,G., (2015). Modeling Urban Growth in Kigali city Rwanda. Master's thesis, Netherland.

[52] Christensen, J.H. and Solomon, S., (2007). ``Climate change 2007: The physical science Basis contribution of working Group, to the Fourth Assessment Report of Intergovernmental Panel on climate change´´. Cambridge University Press, New York, NY, PP.847-940.

[53] Wilby, R.L., Dawson, C.W and Barrow, E.M., (2002). ``SDSM- a decision support tool for the assessment of regional climate impacts´´. Environ Model, Softw.17 (2): 147-159.

[54] Prudhomme, C. and Davies, H., (2009). ``Assessing uncertainties in climate change impact analysis on the river flow Regimes in the UK``. Part 1: baseline climate. Clim. Chang. 93(1-2): 177-195.

[55] Scharffenber, W. A. and Fleming, M. J., (2010). Hydrological Modeling System HEC-HMSUser's Manual. Davis: United States Army Corps of Engineers.

[56] Khan, M.S., Coulibaly, P. and Dibike, Y., (2006a). ``Uncertainty analysis of statistical Downscaling Methods´´. J. Hydrol. 319(1-4): 357-382.

[57] Wilby, R.L. and Dawson, C.W., (2004). ``Using SDSM Version 3.1—A Decision Support Tool for the Assessment of Regional Climate Change Impacts´´. User Manual. United Nations Framework Convention on Climate Change, Bonn, Germany.

[58] Fleming, M. J. And Doan, J. H., (2010). ``HEC-GeoRMS Geospatial Hydrologic ModleingExtension´´. Davis: United States Army Corps of Engineering.

[59] Claire, A.J., Scott J.G. and Mary K. S., (2003). ``Using the SLEUTH urban growth model to simulate the impacts of future policy scenarios on urban land use in the Baltimore Washington metropolitan area´´. Environment and planning, 251-27.

CURRICULUM VITAE

PERSONAL INFORMATION

Name Surname : Emmanuel RUKUNDO

Date of birth and place :23 July 1984, Rwanda

Foreign Languages : French, English, Kinyarwanda

E-mail :emmyruk7bc@gmail.com

EDUCATION

Degree	**Department**	**University**	**Date of Graduation**
Master	Civil engineering	Yildiz Technical University	2015
Undergraduate	Civil Engineering	National university of Rwanda	2012
High School	Mathematics and physics	Byimana High School	2005

PUBLICATIONS

Conference Papers

1. A. Doğan, V. Mohsen, E. Rukundo, (2014).” Emergency action plan for dam’s safety application for Seyhan dam in Adana”, presented in Fourthnational conference of dam safety held from 09-11, October 2014 at Fırat University, Elazığ.
2. A. Doğan, V. Mohsen, E. Rukundo, (2014). ‘’Role of Flood Warning System on reduction loss of life in dam break scenarios’’, presented in Fourth International conference of dam safety from 09-11, October 2014 at Fırat University, Elazığ.